Contributions of Global and Regional Sources to Mercury Deposition in New York State

Final Report 02-09

June 2002

New York State
Energy Research and
Development Authority

NYSERDA

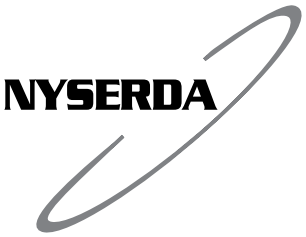

The New York State Energy Research and Development Authority (NYSERDA) is a public benefit corporation created in 1975 by the New York State Legislature. NYSERDA's responsibilities include:

- Conducting a multifaceted energy and environmental research and development program to meet New York State's diverse economic needs.
- Administering the **New York Energy $mart**[SM] program, a Statewide public benefit R&D, energy efficiency, and environmental protection program.
- Making energy more affordable for residential and low-income households.
- Helping industries, schools, hospitals, municipalities, not-for-profits, and the residential sector, including low-income residents, implement energy-efficiency measures.
- Providing objective, credible, and useful energy analysis and planning to guide decisions made by major energy stakeholders in the private and public sectors.
- Managing the Western New York Nuclear Service Center at West Valley, including: (1) overseeing the State's interests and share of costs at the West Valley Demonstration Project, a federal/State radioactive waste clean-up effort, and (2) managing wastes and maintaining facilities at the shut-down State-Licensed Disposal Area.
- Coordinating the State's activities on energy emergencies and nuclear regulatory matters, and monitoring low-level radioactive waste generation and management in the State.
- Financing energy-related projects, reducing costs for ratepayers.

NYSERDA administers the **New York Energy $mart**[SM] program, which is designed to support certain public benefit programs during the transition to a more competitive electricity market. Some 1,100 projects in more than 30 programs are funded by a charge on the electricity transmitted and distributed by the State's investor-owned utilities. The **New York Energy $mart**[SM] program provides energy efficiency services, including those directed at the low-income sector, research and development, and environmental protection activities.

NYSERDA derives its basic research revenues from an assessment on the intrastate sales of New York State's investor-owned electric and gas utilities, and voluntary annual contributions by the New York Power Authority and the Long Island Power Authority. Additional research dollars come from limited corporate funds. Some 400 NYSERDA research projects help the State's businesses and municipalities with their energy and environmental problems. Since 1990, NYSERDA has successfully developed and brought into use more than 141 innovative, energy-efficient, and environmentally beneficial products, processes, and services. These contributions to the State's economic growth and environmental protection are made at a cost of about $.70 per New York resident per year.

Federally funded, the Energy Efficiency Services program is working with more than 540 businesses, schools, and municipalities to identify existing technologies and equipment to reduce their energy costs.

For more information, contact the Communications unit, NYSERDA, 17 Columbia Circle, Albany, New York 12203-6399; toll-free 1-866-NYSERDA, locally (518) 862-1090, ext. 3250; or on the web at www.nyserda.org

Contributions of Global and Regional Sources to Mercury Deposition in New York State

Final Report

Prepared for the

New York State
Energy Research and
Development Authority

Albany, NY
www.nyserda.org

Mark R. Watson
Project Manager

and

Electric Power Research Institute

Palo Alto, CA

Prepared by

Atmospheric and Environmental Research, Inc.

San Ramon, CA

Christian Seigneur
Kristen Lohman
Krish Vijayaraghavan
Run-Lie Shia
Project Managers

NYSERDA
Report 02-09

NYSERDA 6485

July 2002

NOTICE

This report was prepared by Atmospheric and Environmental Research, Inc., in the course of performing work contracted for and sponsored by the New York State Energy Research and Development Authority and the Electric Power Research Institute (hereafter the "Sponsors"). The opinions expressed in this report do not necessarily reflect those of the Sponsors or the State of New York, and reference to any specific product, service, process, or method does not constitute an implied or expressed recommendation or endorsement of it. Further, the Sponsors and the State of New York make no warranties or representations, expressed or implied, as to the fitness for particular purpose or merchantability of any product, apparatus, or service, or the usefulness, completeness, or accuracy of any processes, methods, or other information contained, described, disclosed, or referred to in this report. The Sponsors, the State of New York, and the contractor make no representation that the use of any product, apparatus, process, method, or other information will not infringe privately owned rights and will assume no liability for any loss, injury, or damage resulting from, or occurring in connection with, the use of information contained, described, disclosed, or referred to in this report.

ACKNOWLEDGMENTS

This work was co-funded by EPRI under Contracts WO3218-08 and WO3508-03. The nominal base case simulations with the global model and the continental model were conducted under the EPRI contracts, Dr. Leonard Levin, Project Manager.

NYSERDA appreciates the input of project reviewers, especially Dr. Praveen Amar, Director, Science and Policy, NESCAUM, and Dr. Daniel Jacob, Professor of Atmospheric Chemistry & Environmental Engineering, Division of Engineering & Applied Science, Harvard University.

PREFACE

The New York State Energy Research and Development Authority (NYSERDA) is pleased to publish "Contributions of Global and Regional Sources to Mercury Deposition in New York State." The report was prepared by Atmospheric and Environmental Research, Inc., with cofunding support from the Electric Power Research Institute (EPRI). This report represents a preliminary assessment of mercury fate and transport into New York State. Although significant uncertainty in mercury modeling remains, the report represents the state-of-science and begins to elucidate the relative contributions of global and regional sources of mercury into critical New York State ecosystems. It is our hope that such an analysis will be useful as policies to control mercury across a variety of geographical scales are being discussed and developed. Equally important, the analysis conducted here identifies critical data gaps in our understanding of mercury which will need to be addressed if we are to are to evaluate the effectiveness of mercury control strategies.

This project was funded as part of the New York State Energy $mart^{SM} Environmental Monitoring and Evaluation Program and represents one of several mercury modeling and monitoring studies underway in New York State.

TABLE OF CONTENTS

TABLE OF CONTENTS (continued)

LIST OF TABLES

LIST OF FIGURES

LIST OF FIGURES (continued)

LIST OF FIGURES (continued)

LIST OF FIGURES (continued)

EXECUTIVE SUMMARY

Mercury is a naturally-occurring, inorganic element present in coal and of value in numerous industrial processes. At high concentrations, it can be a potent neurotoxin, capable of impairing neurological development in fetuses and young children and damaging the central nervous system of adults. Mercury cycles in the environment as a result of natural and human (anthropogenic) activities. Recent emission inventories developed by the U.S. Environmental Protection Agency (EPA) and Atmospheric & Environmental Research, Inc./Electric Power Research Institute are in general agreement and indicate that 158 tons and 139 tons, respectively, of mercury are emitted from U.S. manmade sources every year. The human activities that are most responsible for causing mercury to enter the environment are the burning of mercury-containing fuels and materials, and some industrial processes. Based on these emission inventories, the highest emitters of mercury to the air include coal burning electric utilities, municipal waste combustors, commercial and industrial boilers, medical waste incinerators, chlor-alkali plants, hazardous waste combustors, lamp breakage activities, mining and cement manufacturers. Mercury is transported through the air and deposited to water and land where humans and wildlife may be exposed. Even in small quantities, mercury bioaccumulates, and may reach levels of concern in fish at the top of the aquatic food chain. Thirty-seven states have issued fish consumption advisories due to mercury contamination.

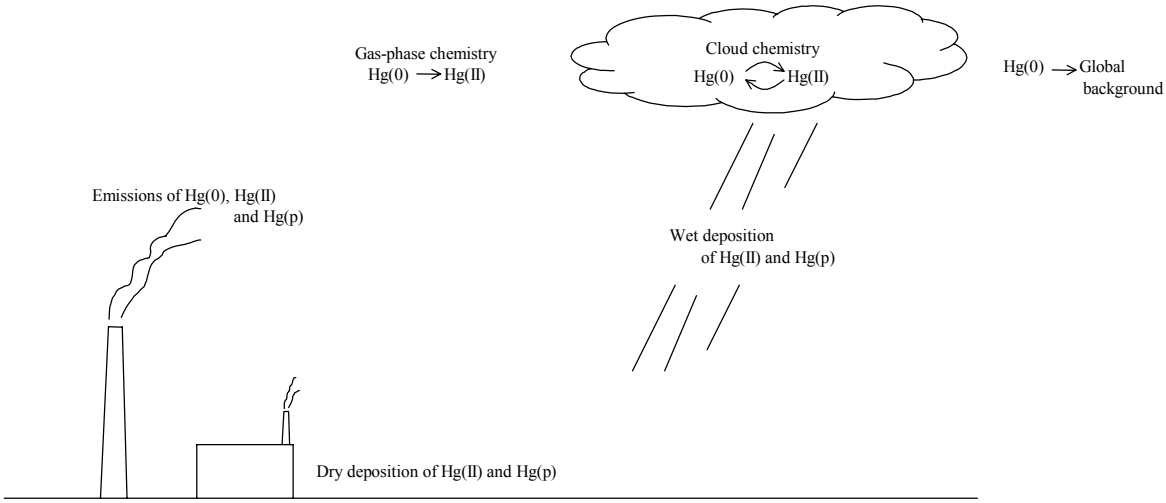

Schematic description of the atmospheric fate and transport of Hg species

An important policy question is whether controlling mercury emissions within a given region, (e.g., state, U.S.) will lead to significant reductions in mercury deposition within that region. The sources that contribute most to mercury deposition in a region must be identified in order to develop effective regional, national and international policies necessary to reduce the emissions from the sources that are the main contributors. The goals of this project were to assess the contributions of local, regional and global mercury sources to mercury deposition in New York State, and identify critical data gaps needed to refine these estimates.

Project Background

Mercury is present in the atmosphere as gaseous elemental mercury, gaseous divalent mercury and particulate divalent mercury. Gaseous elemental mercury has an atmospheric lifetime of about one year whereas gaseous divalent mercury and particulate divalent mercury tend to be removed more rapidly with lifetimes on the order of one day and one week, respectively. Consequently, gaseous divalent mercury species tend to deposit near their source of emissions. Conversion between the forms of mercury occurs in the atmosphere, particularly in the presence of clouds. Therefore, the potential impacts of mercury emissions to the atmosphere depend on the speciation of the mercury emissions, meteorological processes such as transport and precipitation, and chemical transformations, which may range from local to global scales.

A modeling system was used to simulate the atmospheric transport, transformations and deposition of mercury. Three scenarios were used that differ in the values of some key model inputs: (1) a nominal or baseline scenario, (2) a scenario conducive to local deposition and (3) a scenario conducive to long-range transport. Deposition fluxes of mercury were analyzed at three receptor locations in New York State: the Adirondack Mountains, the Finger Lakes District and the Catskill Mountains.

Results

The modeling results can be summarized as follows for the baseline scenario. Eleven to twenty one percent of total Hg deposited in New York State originates from within New York State. The balance is transported into the State, with 25-49% coming from the contiguous U.S., 13-19% from Asia, 5-7% from Europe, 2-5% from Canada, 2-3% each from Africa and South America, and 0-1% each from Mexico and Oceania. Natural sources from the oceans and land contributed 16 to 24%. The results from the local deposition and long-range transport scenarios varied only slightly from these results.

Baseline Scenario: Regional and global contributions to total Hg deposition at three New York State receptor sites:

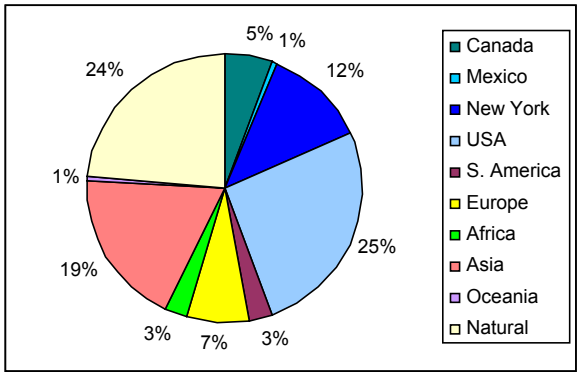

Adirondacks receptor

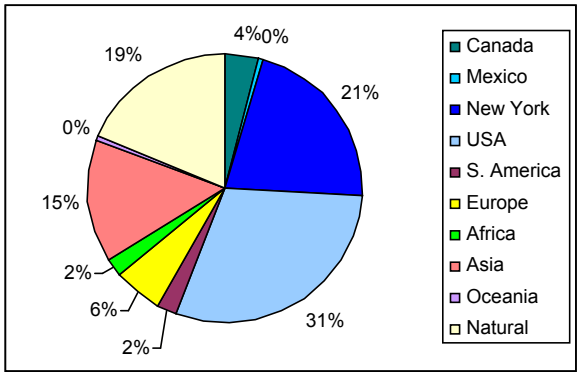

Finger Lakes receptor

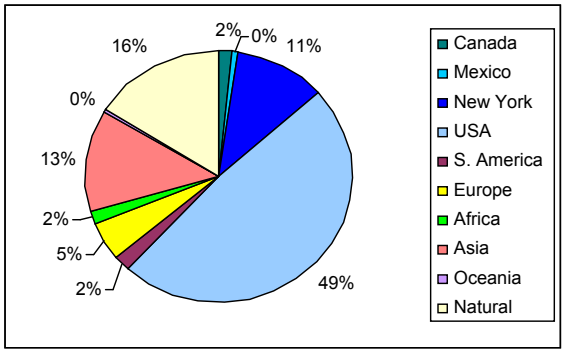

Catskills receptor

These source attribution results must be seen as preliminary because the model performance evaluation showed that mercury wet deposition in the northeastern United States tends to be overpredicted by as much as 50% at some sites. Clearly, uncertainties still remain in our understanding of the atmospheric fate and transport of mercury and the source contributions presented here are likely to change, as some of those uncertainties are resolved.

Major sources of uncertainties that have been identified include the mercury emissions (including mercury speciation), the dry deposition of divalent mercury and, for lake mercury cycling models, the sediment burial rate. In addition, our knowledge of the atmospheric chemistry of mercury is still incomplete and laboratory experiments are needed to identify and characterize the most important reactions. Finally, there is a dire need for mercury measurements to evaluate models, including ambient atmospheric concentrations of gaseous elemental mercury, gaseous divalent mercury and particulate divalent mercury; mercury wet deposition fluxes and mercury dry deposition fluxes.

Notwithstanding the uncertainties, the analysis conducted here represents the state of the science understanding of mercury fate and transport, and provides an indication of the relative contributions of local, regional and global sources of mercury to mercury deposition in New York State.

1. INTRODUCTION

Mercury (Hg) is present in the atmosphere as gaseous elemental Hg (Hg(0)), gaseous divalent Hg (Hg(II)) and particulate divalent Hg (Hg(p)). Hg(0) is not readily soluble and is not removed rapidly from the atmosphere; it has an atmospheric lifetime on the order of 1 year. On the other hand, Hg(II) species are very soluble and Hg(II) is removed rapidly from the atmosphere via dry and wet deposition processes. Hg(p) is present mainly in fine particles (i.e., particles less than 2.5 μm in diameter, $PM_{2.5}$); as a result, it is not removed as fast as Hg(II) but its atmospheric lifetime is considerably shorter than that of Hg(0). Therefore, the potential impacts of atmospheric Hg emissions may range from local impacts due primarily to the wet deposition of Hg(II) and Hg(p) and dry deposition of Hg(II) to global impacts due to the long-range transport of Hg(0) and, under dry conditions, Hg(p) (see Figure 1-1). It is, therefore, essential to assess the relative importance of local, regional, continental and global sources of Hg to deposition in sensitive watersheds in order to develop effective emission control strategies. However, significant uncertainties still remain in our understanding of the fate and transport of Hg in the environment. Therefore, the attribution of Hg deposition to various sources must be qualified by the associated uncertainties.

The objectives of this work are twofold:

(1) to provide quantitative estimates of the relative contributions of local emissions versus long-range transport to Hg deposition in New York State (hereafter referred to as New York).
(2) to identify the critical data gaps that should be addressed to refine those estimates.

The first objective is addressed here by applying a multi-scale modeling system for the atmospheric fate and transport of Hg. This modeling system comprises a global model of the atmospheric cycle of Hg with a horizontal resolution of about 1000 km at mid-latitudes and a continental model that covers North America with a horizontal resolution of 100 km. The source areas being considered include New York, the other

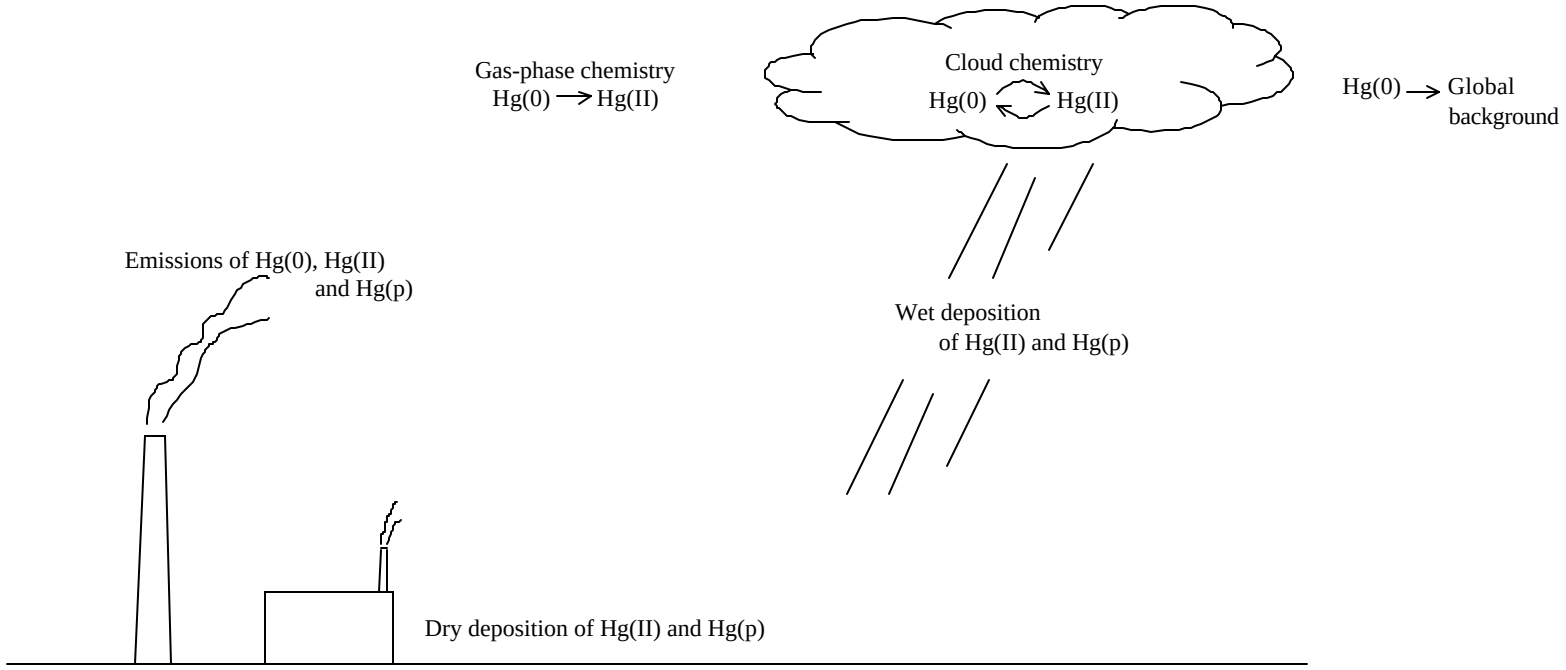

Figure 1-1. Schematic description of the atmospheric fate and transport of Hg species.

contiguous United States, Canada, Mexico and the other five continents (i.e., Europe, Asia, South America, Africa and Oceania). We selected three potentially sensitive areas in New York: the Adirondacks, the Finger Lakes area and the Catskill Mountains. In order to account for some of the uncertainties associated with the major model inputs, three sets of simulations are conducted:

- one set with nominal values of the model input parameters
- one set of model input parameters within their plausible range that is conducive to local deposition of Hg
- one set of model input parameters within their plausible range conducive to long-range transport of Hg

The two sensitivity simulations (i.e., local deposition scenario and long-range transport scenario) were designed to provide plausible results when compared to observations. Therefore, they are useful to indicate how the system responds to changes in some model inputs but they do not constitute a rigorous uncertainty analysis.

The second objective is addressed by conducting a sensitivity/uncertainty analysis that provides quantitative information on the major sources of uncertainties in model predictions of (1) Hg deposition to watersheds in New York and (2) Hg bioaccumulation in the aquatic food chain. As part of this effort, we reviewed existing data bases for atmospheric Hg concentrations and deposition, Hg fish concentrations and lake/watershed data. Then, we provide recommendations on which additional data need to be collected in the atmosphere and in lakes/watersheds to reduce in the most effective manner the uncertainties associated with the origin and fate of Hg as they affect model predictions in New York.

We present in Section 2 the results of our global modeling of atmospheric Hg. In Section 3, we present the results of our continental modeling of atmospheric Hg and combine the global and continental modeling results to attribute Hg deposition in New York to the various source areas enunciated above. We present our sensitivity/uncertainty analysis of the fate and transport of Hg in Section 4. Concluding remarks are provided in Section 5.

2. GLOBAL ATMOSPHERIC MODELING OF MERCURY

2.1 Description of the Global Atmospheric Mercury Model

The formulation of the global Hg model has been described in detail by Shia et al. (1999) and Seigneur et al. (2001a). We present here an overview of the model formulation.

The global Hg model is based on the three-dimensional (3-D) chemical transport model (CTM) developed at the Goddard Institute for Space Studies (GISS), Harvard University, and the University of California at Irvine. The 3-D model provides a horizontal resolution of 8 degrees latitude and 10 degrees longitude (about 1000 km at mid-latitudes) and a vertical resolution of nine layers ranging from the Earth's surface to the lower stratosphere. Seven layers are in the troposphere (between the surface and ~12 km altitude), and two layers are in the stratosphere (between ~12 km and 30 km altitude).

Transport processes are driven by the wind fields and convection statistics calculated every 4 hours (for 1 year) by the GISS general circulation model (Hansen et al., 1983). This 1-year data set is used repeatedly for multiyear simulations until steady state is achieved. The interhemispheric transport and vertical transport have been previously evaluated through comparisons with measurements (Prather et al., 1987; Jacob et al., 1987; Jacob and Prather, 1990). Other recent applications of the model are described by Kotamarthi et al. (1998) and Jacob et al. (1999).

The Hg transformation processes include gas-phase transformations, gas/droplet equilibria, ionic equilibria, solution/particle adsorption equilibrium, and aqueous-phase transformations. Table 2-1 lists these transformation processes. The gas-phase transformations include the oxidation of Hg(0) to Hg(II) by ozone (O_3), hydrogen chloride (HCl), hydrogen peroxide (H_2O_2) and molecular chlorine (Cl_2). Among those, the reaction with O_3 is dominant with a Hg(0) half-life of 9 months for O_3 = 40 ppb. The aqueous-phase chemistry includes the reduction of Hg(II) to Hg(0) via reaction with hydroperoxy radicals (HO_2) and by the formation of the sulfite complexes (at low HCl concentrations), as well as the oxidation of Hg(0) to Hg(II) by dissolved O_3, hydroxyl radicals (OH), and Cl_2. The kinetics of the reduction of $Hg(SO_3)$ to Hg(0) was updated

Table 2-1. Equilibria and reactions of atmospheric Hg.

Equilibrium Process or Chemical Reaction	Equilibrium or Rate Parameter[a]	Reference
$Hg(0)\ (g) \rightleftharpoons Hg(0)\ (aq)$	0.11 M atm^{-1}	Sanemasa, 1975; Clever et al., 1985
$HgCl_2\ (g) \rightleftharpoons HgCl_2\ (aq)$	1.4×10^{6} M atm^{-1}	Lindqvist and Rohde, 1985
$Hg(OH)_2\ (g) \rightleftharpoons Hg(OH)_2\ (aq)$	1.2×10^{4} M atm^{-1}	Lindqvist and Rohde, 1985
$O_3\ (g) \rightleftharpoons O_3(aq)$	1.13×10^{-2} M atm^{-1}	Kosak-Channing and Helz, 1983
$HCl\ (g) \rightleftharpoons HCl\ (aq)$	1.1 M atm^{-1}	Marsh and McElroy, 1985
$SO_2\ (g) \rightleftharpoons SO_2\ (aq)$	1.23 M atm^{-1}	Smith and Martrell, 1976
$Cl_2\ (g) \rightleftharpoons Cl_2\ (aq)$	0.076 M atm^{-1}	Lin and Pehkonen, 1998
$H_2O_2\ (g) \rightleftharpoons H_2O_2\ (aq)$	7.4×10^{4} M atm^{-1}	Lind and Kok, 1986
$HgCl_2\ (aq) \rightleftharpoons Hg^{2+} + 2\ Cl^-$	10^{-14} M^2	Sillen and Martell, 1964
$Hg(OH)_2\ (aq) \rightleftharpoons Hg^{2+} + 2\ OH^-$	10^{-22} M^2	Sillen and Martell, 1964
$HCl\ (aq) \rightleftharpoons H^+ + Cl^-$	1.7×10^{6} M	Marsh and McElroy, 1985
$Cl_2\ (aq) \longleftrightarrow HOCl + Cl^- + H^+$	5.0×10^{-4} M^2	Lin and Pehkonen, 1998
$HOCl \longleftrightarrow OCl^- + H^+$	3.2×10^{-8} M	Lin and Pehkonen, 1998
$SO_2\ (aq) + H_2O_2\ (aq) \longrightarrow SO_4^{2-} + 2\ H^+$	instantaneous[b]	McArdle and Hoffman, 1983
$SO_2\ (aq) + H_2O\ (l) \rightleftharpoons HSO_3^- + H^+$	1.23×10^{-2} M	Smith and Martell, 1976
$HSO_3^- \rightleftharpoons SO_3^{2-} + H^+$	6.6×10^{-8} M	Smith and Martell, 1976
$Hg^{2+} + SO_3^{2-} \rightleftharpoons HgSO_3$	5×10^{12} M^{-1}	Munthe et al., 1991
$HgSO_3 + SO_3^{2-} \rightleftharpoons Hg(SO_3)_2^{2-}$	2.5×10^{11} M^{-1}	Munthe et al., 1991
$Hg(II)\ (aq) \rightleftharpoons Hg(II)\ (p)$	34 l/g	Seigneur et al., 1998
$Hg(0)\ (g) + O_3\ (g) \longrightarrow Hg(II)\ (g)$	3×10^{-20} cm^3 $molec^{-1}$ s^{-1}	Hall, 1995
$Hg(0)\ (g) + HCl(g) \xrightarrow{(HCl)} HgCl_2(g)$	10^{-19} cm^3 $molec^{-1}$ s^{-1}	Hall and Bloom, 1993
$Hg(0)\ (g) + H_2O_2\ (g) \longrightarrow Hg\ (OH)_2\ (g)$	8.5×10^{-19} cm^3 $molec^{-1}s^{-1}$	Tokos et al., 1998

Table 2-1. Equilibria and reactions of atmospheric Hg (continued).

Equilibrium Process or Chemical Reaction	Equilibrium or Rate Parameter[a]	Reference
$Hg(0)\ (g) + Cl_2(g) \longrightarrow HgCl_2(g)$	$4.0 \times 10^{-18}\ cm^3\ molec^{-1} s^{-1}$	Calhoun and Prestbo, 1998
$Hg(0)\ (aq) + O_3\ (aq) \longrightarrow Hg^{2+}$	$4.7 \times 10^7\ M^{-1}\ s^{-1}$	Munthe, 1992
$Hg(0)\ (aq) + OH\ (aq) \longrightarrow Hg^{2+}$	$2.0 \times 10^9\ M^{-1}\ s^{-1}$	Lin and Pehkonen, 1997
$HgSO_3\ (aq) \longrightarrow Hg(0)\ (aq)$	$0.0106\ s^{-1}$	van Loon et al., 2000
$Hg(II)\ (aq) + HO_2\ (aq) \longrightarrow Hg(0)\ (aq)$	$1.7 \times 10^4\ M^{-1}\ s^{-1}$	Pehkonen and Lin, 1998
$Hg(0)\ (aq) + HOCl\ (aq) \longrightarrow Hg^{2+}$	$2.09 \times 10^6\ M^{-1}\ s^{-1}$	Lin and Pehkonen, 1998
$Hg(0)\ (aq) + OCl^- \longrightarrow Hg^{2+}$	$1.99 \times 10^6\ M^{-1}\ s^{-1}$	Lin and Pehkonen, 1998

Hg(II) refers to all divalent Hg species

[a] The parameters are for temperatures in the range of 20 to 25°C, see references for exact temperature; temperature dependence is included in the model for the Henry's law parameters of Hg(0) (Clever et al., 1985), O_3, HCl, SO_2 (Liu et al., 1997; Seigneur and Saxena, 1988), and Cl_2 (Lin and Pehkonen, 1998), and for the kinetics of the $HgSO_3$ decomposition (van Loon et al., 2000).

[b] This reaction between HSO_3^- and H_2O_2 is fast and is treated as an instantaneous titration between SO_2 and H_2O_2. Since H_2SO_4 is a strong acid, the effect of this reaction on pH is taken into account.

(k = 0.0106 s^{-1} at 25° C) to reflect recent laboratory data that include temperature dependence (van Loon et al., 2000). The reaction of Hg(II) with HO_2 typically governs Hg(II) reduction. Over the oceans, the aqueous oxidation of Hg(0) is dominated by the nighttime reaction with Cl_2; over land, it is governed primarily by reaction with O_3. Adsorption of Hg(II) species on atmospheric particulate matter (PM) is simulated using an adsorption coefficient based on experimental data (K = 34 l/g as recommended by Seigneur et al., 1998). Adsorption is assumed to be reversible and results in a slight decrease in the rate of Hg(II) reduction.

The chemical species reacting with Hg were input to the model as follows. The concentrations of O_3, sulfur dioxide (SO_2), and OH were obtained from Wang et al. (1998), Chin et al. (1996) and Spivakovsky et al. (1990; 2000), respectively. The 3-D concentrations of HO_2 and H_2O_2 were obtained from Spivakovsky (2001). These concentration fields are spatially and temporally varying. The spatial resolution is 8° latitude and 10° longitude (about 1000 km at mid latitudes). The temporal resolution is monthly. The aqueous concentrations of OH and HO_2 were calculated from the gas-phase concentrations using their temperature-dependent Henry's law constants (Jacobson, 1999). The gas-phase concentrations of OH and HO_2 were also reduced by factors of 2 and 10, respectively, to account for reduced photochemical activity and heterogeneous chemistry within clouds (Jacob, 2000; Jaegle et al., 2001). The aqueous concentration of HO_2 was further assumed to have a maximum value of 2 x 10^{-9} M. The OH and HO_2 concentrations were assumed to be zero at night. The HCl concentration was assumed to be 1.2 x 10^{10} molecules cm^{-3} at the surface decreasing to 10^8 molecules cm^{-3} at 10 km altitude (Graedel and Keene, 1995); these values are constant in time and in the horizontal directions. The Cl_2 concentration was assumed to be zero over land, 100 ppt at the surface and 50 ppt aloft at night, and 10 ppt during the day over the oceans (Spicer et al., 1998). The particulate matter concentration in cloud droplets was assumed to be temporally and spatially constant with a value of 0.02 g/l (Seigneur et al., 1998).

The dry deposition velocities were selected to be spatially and temporally constant with values of 0.25 and 0.01 cm s^{-1} for Hg(II) and Hg(0), respectively. The Hg(p) deposition velocity was selected to be 0.1 cm/s over land and 0.01 cm/s over water; these values are typical for fine particles (e.g., Zannetti, 1990). Therefore, Hg(II)

is assumed to deposit 25 times faster than Hg(0) and Hg(p) is assumed to deposit over land 10 times faster than Hg(0). Wet deposition is calculated using the cloud droplet chemical concentrations and the precipitation patterns. For below-cloud scavenging, we assumed no scavenging of Hg(0), 100% scavenging of Hg(II) and 50% scavenging of Hg(p).

The Hg emissions consisted of Hg(0), Hg(II) and Hg(p) gridded emissions for anthropogenic and background sources. Background emissions are defined here to include natural sources (e.g., from the oceans and terrestrial Hg deposits) and re-emission of anthropogenic Hg previously deposited on soils. The development of this emission inventory is described by Seigneur et al. (2001a).

2.2 Base Simulations

We conducted three base simulations.

- A nominal base simulation that corresponds to that conducted under the EPRI project and reported by Seigneur et al. (2001a). This nominal base simulation uses the model inputs described above.
- A base simulation conducive to local Hg deposition (hereafter referred to as local deposition base simulation).
- A base simulation conducive to long-range transport of Hg (hereafter referred to as long-range transport base simulation).

As mentioned in Section 1, the latter two simulations were designed to provide useful indication of the sensitivity of the model outputs to changes in some model inputs. However, they are not intended to be a rigorous uncertainty analysis (see for example Lohman et al., 2000a, 2000b for comprehensive sensitivity/uncertainty analyses).

The inputs used for the local deposition and long-range transport base simulations are presented in Table 2-2. A perturbation of 5% was assigned to those model inputs that were obtained from data bases (i.e., speciation of Hg emissions), model simulations (i.e., concentrations of HO_2, OH, O_3, H_2O_2 and SO_2), or measured concentrations (i.e.,

Table 2-2. Global model inputs used in the local deposition and long-range transport simulations.

Model input	Change from nominal value	
	Local deposition simulation	**Long-range transport simulation**
Hg speciation of anthropogenic emissions	+5% Hg(II), -5% Hg(0)	-5% Hg(II), +5% Hg(0)
HO_2 concentrations	x 0.95	x 1.05
Cl_2 concentrations	x 1.05	x 0.95
OH concentrations	x 1.05	x 0.95
O_3 concentrations	x 1.05	x 0.95
H_2O_2 concentrations	x 1.05	x 0.95
SO_2 concentrations	x 0.95	x 1.05
HCl concentrations	x 1.25	x 0.8
PM concentrations	x 1.25	x 0.8
Adsorption coefficient of Hg on PM	x 1.25	x 0.8
Dry deposition velocity of Hg(II)	x 1.25	x 0.8
Dry deposition velocity of Hg(p)	x 1.25	x 0.8
Scavenging coefficient of Hg(p)	x 1.25	x 0.8

concentrations of Cl_2). A perturbation factor of 1.25 was assigned to inputs that were assumed based on professional judgment (i.e., concentrations of HCl and PM; dry deposition velocities of Hg(II) and Hg(p); and scavenging coefficient of Hg(p)).

The concentrations of Hg(0), Hg(II) and Hg(p) simulated with these three base scenarios are compared to concentrations measured at Mace Head, Ireland in September 1995 (Ebinghaus et al., 1999) in Table 2-3. That location represents a global background site. The Hg(0) concentration shows a significant variation among the three base simulations (-13% for the local deposition simulation and +11% for the long-range transport simulation with respect to the nominal simulation). The lower Hg(0) concentration obtained in the local deposition simulation results from lower Hg(0) emissions, faster oxidation of Hg(0) to Hg(II) and greater deposition of Hg. All these processes lead to a shorter average atmospheric lifetime of Hg and, therefore, lower Hg(0) concentrations. The reverse is true for the long-range transport simulation. The Hg(0) concentration simulated in the local deposition scenario is slightly lower than the range of measured values; the Hg(0) concentrations simulated in the nominal and long-range transport scenarios are within the range of the measurements. The variation in the Hg(II) concentration is about 7% for both the local deposition simulation and the long-range transport simulation with respect to the nominal simulation. The lower Hg(II) concentration in the local deposition simulation results from faster removal of Hg(II), which is compensated to some extent by greater Hg(II) emissions and faster oxidation of Hg(0) to Hg(II). The reverse is true for the long-range transport simulation. The results obtained for Hg(p) reflect the changes in the dry deposition and wet deposition rates, i.e., lower concentration for the local deposition simulation which has greater deposition rates and greater concentration for the long-range transport simulation which has lower deposition rates.

The Hg deposition rates in the grid cell that includes New York are presented in Table 2-4. The dry deposition fluxes of Hg(0) and Hg(II) are commensurate because, although Hg(0) has a much lower deposition velocity than Hg(II), its ambient concentration is about two orders of magnitude greater than that of Hg(II). However, one must note that a significant fraction of deposited Hg(0) is expected to be re-emitted to the atmosphere. The Hg(0) dry deposition flux decreases for the local deposition scenario

Table 2-3. Comparison of simulated and measured concentrations of Hg species at Mace Head, Ireland.

Mercury species	**Nominal base simulation[(a)]**	**Local deposition base simulation**	**Long-range transport base simulation**	**Measurements[(b)]**
Hg(0) (ng/m^3)	1.63	1.41	1.81	1.44 to 3.0
Hg(II) (pg/m^3)	14	13	15	14 to 94
Hg(p) (pg/m^3)	4	3	5	5 to 115

(a) monthly average value

(b) range represents variability over several days and uncertainty among several laboratories, sampling times ranged from one to several hours from 11 to 15 September 1995 (Ebinghaus et al., 1999).

Table 2-4. Hg deposition fluxes simulated with the global model for the New York grid cell.

Deposition process	Deposition flux (μg/m^2-yr)		
	Nominal base simulation	**Local deposition base simulation**	**Long-range transport base simulation**
Dry deposition of Hg(0)	5.3	4.6	5.9
Dry deposition of Hg(II)	4.7	5.5	4.3
Dry deposition of Hg(p)	0.2	0.2	0.2
Wet deposition of Hg(II) and Hg(p)[(a)]	10.1	11.2	9.1
Total deposition of Hg(II) and Hg(p)	15.0	16.9	13.6
Total deposition of Hg(0), Hg(II) and Hg(p)	20.3	21.5	19.5

(a) Wet deposition of Hg(0) is negligible because of its very low solubility.

and increases for the long-range transport scenario with respect to the nominal scenario. These results are consistent with the change in the global background Hg(0) concentrations (see Table 2-3), the decrease in Hg(0) emissions and increase in Hg(0) conversion to Hg(II) for the local deposition scenario (and vice-versa for the long-range transport scenario). The dry deposition flux of Hg(II) increases in the local deposition scenario and decreases in the long-range transport scenario with respect to the nominal scenario. These results are consistent with the changes in Hg(II) emissions, formation and removal that, for example, favor Hg(II) local deposition in the local deposition scenario. There is little change in the dry deposition flux of Hg(p). The wet deposition flux increases in the local deposition scenario and decreases in the long-range transport scenario with respect to the nominal scenario.

2.3 Contributions of Global Source Areas

The global Hg model was used to investigate the effects of global Hg cycling on Hg deposition in New York. In the global model, New York is entirely contained within one of the model's grid cells. Also located in this grid cell are Connecticut, Rhode Island, Vermont, New Hampshire, Massachusetts, and parts of Pennsylvania, New Jersey, Maine, Quebec, and Ontario.

Several simulations were conducted to determine the contributions of different source regions of Hg emissions to deposition to the New York grid cell. The contribution of a given source region was calculated by conducting a simulation with only that source region (this approach is feasible because the Hg atmospheric system is linear; i.e., a perturbation in Hg emissions results in a proportionate change in Hg concentrations and deposition fluxes). The source regions for anthropogenic emissions are North America, South America, Europe, Asia, Africa, and Oceania. The contribution of background emissions is also taken into account. Background emissions are comprised of (1) natural emissions of Hg due to outgassing from the oceans and naturally Hg enriched soils as well as (2) re-emissions of previously deposited anthropogenic Hg emissions.

As described in Section 2.2, three different scenarios (nominal, local deposition, and long-range transport scenarios) were modeled. The local deposition and long-range

transport scenarios were used to bound the results from the nominal case. The deposition fluxes to the New York grid cell for each of these scenarios were presented in Table 2-4.

2.3.1 Nominal scenario

Figure 2-1 presents the contributions of the various continents and background emissions to Hg deposition in the New York grid cell. We only considered deposition of Hg(II) and Hg(p) since Hg(0) deposition is typically not taken as an input to watershed/lake models (e.g., Harris et al., 1996). As shown in Figure 2-1c, 25% of the deposition of Hg(II) and Hg(p) in the New York grid cell is attributed to North American anthropogenic emissions. Asian anthropogenic emissions contribute 15%, while Europe (7%), South America (2%), Africa (1%), and Oceania (<1%) contribute small amounts. The rest of the deposition (50%) is due to background emissions.

Figures 2-1a and 2-1b present the results for the dry and wet deposition fluxes, respectively. Local sources tend to have a larger impact on dry deposition because this process depends directly on the atmospheric concentration of Hg. As the air parcel moves away from the source, the Hg concentration decreases due to deposition and dispersion and the Hg dry deposition flux decreases accordingly. Nearly half the dry deposition (47%) in the New York grid cell is attributed to North American sources, with most of the rest attributed to background emissions (38%).

For wet deposition, background emissions contribute over half of the deposition in New York. Asia (18%), North America (14%) and Europe (8%) contribute most of the balance. The source areas with the greatest impact on wet deposition tend to be farther away from the receptor than in the case of dry deposition because wet deposition depends on the occurrence of a precipitation event which may not occur until Hg has traveled some distance. Additionally, cloud droplets convert Hg(0) to Hg(II); Hg(II) is then available for deposition in a precipitating cloud. Since Hg(0) can travel long distances with little deposition, a distant source can easily contribute to deposition of Hg(II) as Hg(0) becomes converted to Hg(II) within a cloud.

To better understand the impact of anthropogenic emissions from each continent, the re-emissions were reapportioned to their presumed original sources. The results of

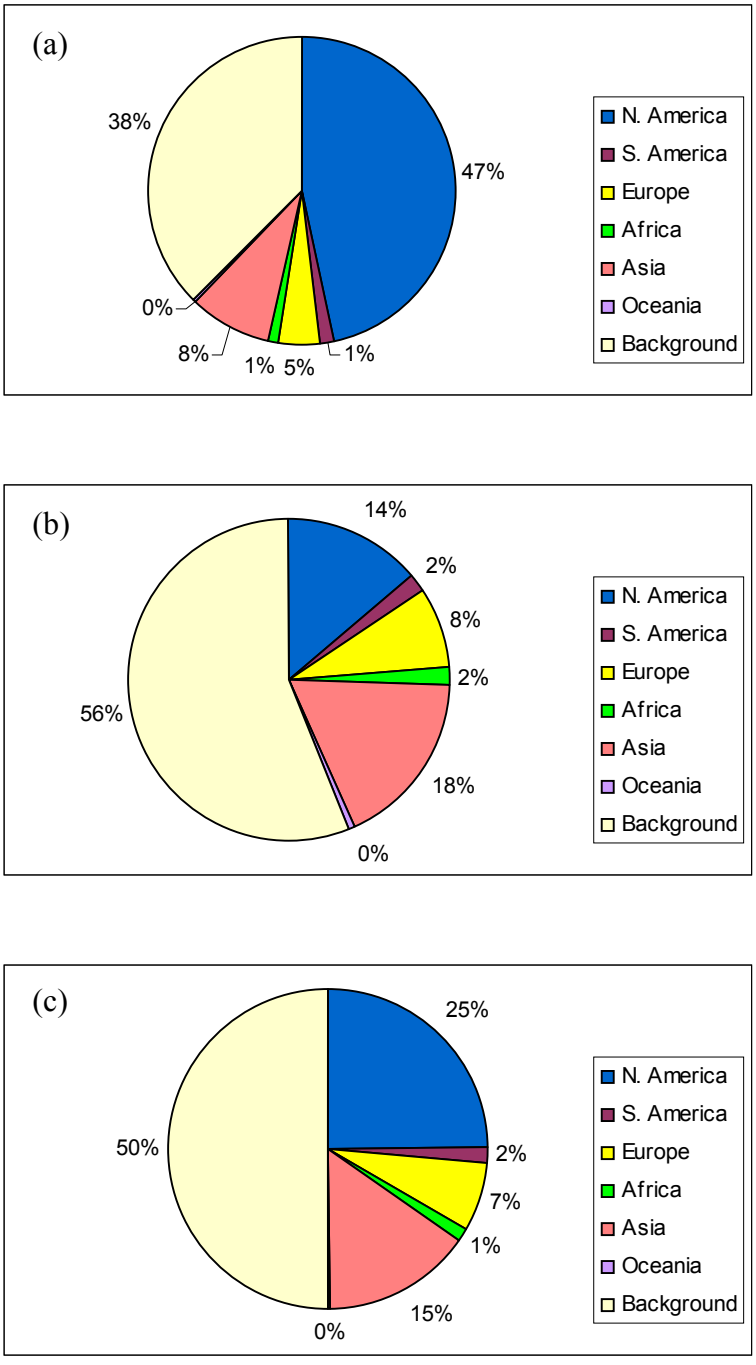

Figure 2-1. Nominal scenario: Global contributions to deposition of Hg(II) and Hg(p) in the New York grid cell (a) dry deposition, (b) wet deposition, (c) total deposition.

this reapportionment are shown in Figure 2-2. In order to reapportion the re-emissions to their original anthropogenic sources, each continent was assigned an additional Hg deposition contribution. The additional contribution was calculated by taking the fraction of background emissions (1500 Mg/y) that is attributed to re-emissions and dividing by the total background emissions (4000 Mg/y) to determine the amount of the background source contribution expected to be due to re-emissions. Next, this re-emission contribution was distributed among the continents by assigning each continent a portion of the re-emissions contribution scaled by that continent's contribution to the total global anthropogenic emission rate. According to this method, continents with higher anthropogenic emission rates would be expected to contribute more to worldwide deposition and, therefore, to worldwide re-emissions, than those continents with lower anthropogenic emissions rates. This approach may slightly overestimate the reapportionment of re-emissions to source areas located in the southern hemisphere since their emissions are more likely to impact the southern hemisphere than the northern hemisphere. However, since the contribution of these source areas to Hg deposition in New York is small (even after reapportionment), we do not anticipate the error associated with this approximation to be large.

After reapportionment, the contribution of North American emissions to total deposition of Hg(II) and Hg(p) in New York remained nearly unchanged, however, the impact of Asian emissions increased from 15 to 25%, nearly the same as the contribution from North America. Small increases were observed for the other continents as well. The impact of Asian emissions increased much more than that of other continents when re-emissions were reapportioned into continental sources, because Asia represents roughly half of all the global anthropogenic Hg emissions.

Figures 2-2a and 2-2b show the dry and wet components of total deposition of Hg(II) and Hg(p) with the reapportionment. North American emissions remained 47% of dry deposition to the New York grid cell, while Asian sources doubled to 16%. The contributions from Europe, South America, Africa, and Oceania all increased slightly. Natural emissions are estimated to be the largest source for wet deposition, contributing 35% of wet deposition in the New York grid cell. The contribution to wet deposition

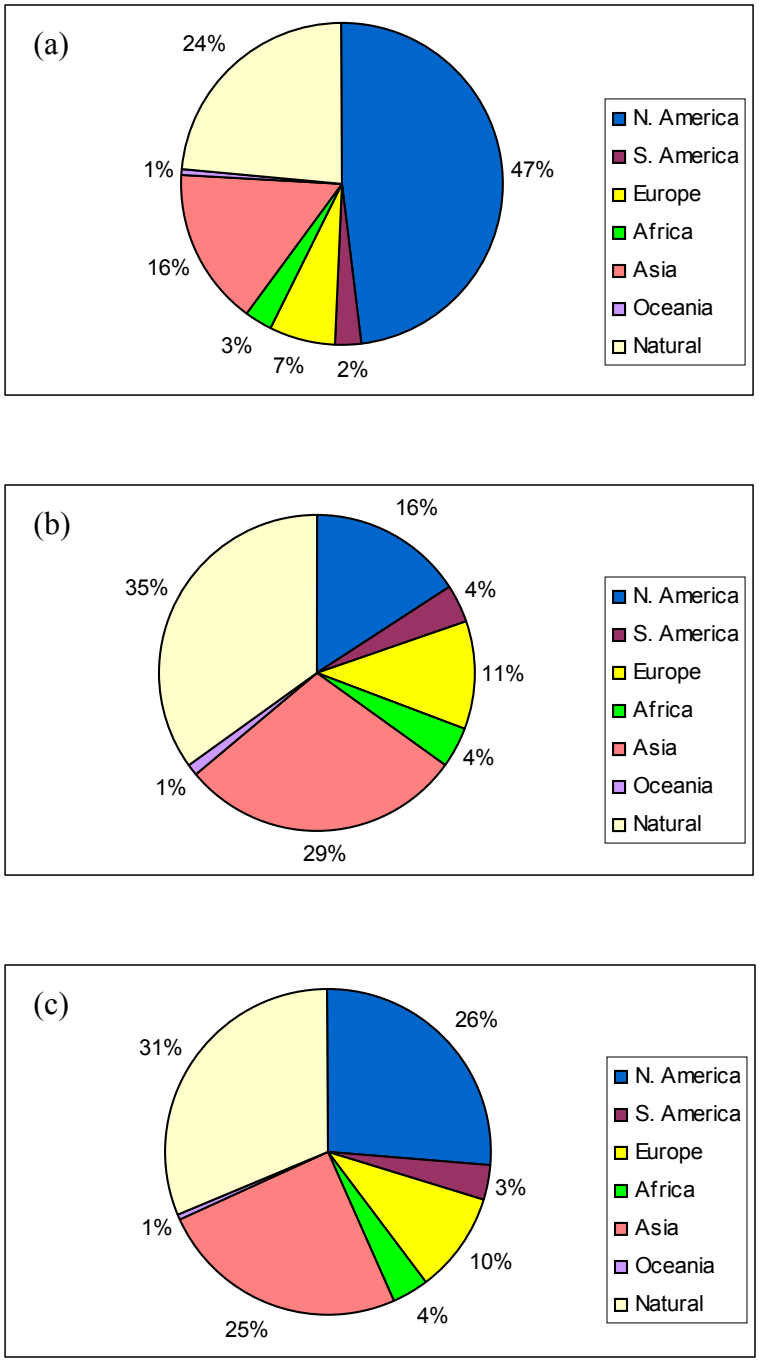

Figure 2-2. Nominal scenario: Global contributions to deposition of Hg(II) and Hg(p) in the New York grid cell with reapportionment of Hg re-emissions, (a) dry deposition, (b) wet deposition and (c) total deposition.

from Asian sources increased to 29%, while the contributions from North American (16%) and European (11%) sources increased as well.

It is interesting to note that, per unit emission, the contribution from Europe exceeds that of Asia for Hg deposition in New York. Europe contributes 0.0045 $\mu g/m^2$-yr per Mg/yr of Hg emitted whereas Asia contributes 0.0033 $\mu g/m^2$-yr per Mg/yr of Hg emitted. For comparison, North America, South America, Africa and Oceania contribute 0.021, 0.0029, 0.0022 and 0.0024 $\mu g/m^2$-yr per Mg/yr of Hg emitted. Clearly, for continents other than North America, latitude governs their contribution to deposition in New York, and as a result continents located in the southern hemisphere contribute less per unit emission than continents located in the northern hemisphere.

2.3.2 Local deposition scenario

As described in Section 2.2, the model's input parameters were altered to create a scenario that favors increased deposition from local sources.

The results of the source attribution are presented in Figures 2-3 and 2-4. In the local deposition scenario, the contributions to total deposition of Hg(II) and Hg(p) from North American and background emissions increased slightly. Contributions from the other continents were reduced.

The majority of dry deposition of Hg(II) and Hg(p) in the New York grid cell, for the local deposition scenario, is contributed by North American anthropogenic sources. This is an increase from the nominal case (from 47 to 53% without reapportionment of re-emissions and to 55% with reapportionment). Dry deposition is dominated by local deposition and North American sources were already the largest contributor in the nominal case to dry deposition in the New York grid cell. Therefore, increasing local deposition serves to increase the contribution due to North American sources at the expense of all the other source categories.

As in the nominal scenario, the largest contribution to wet deposition in the New York grid cell for the local deposition scenario is from background emissions. The contribution from background sources increased slightly (by 2%), the contribution from North American sources remained the same and the contributions from Asia and Africa

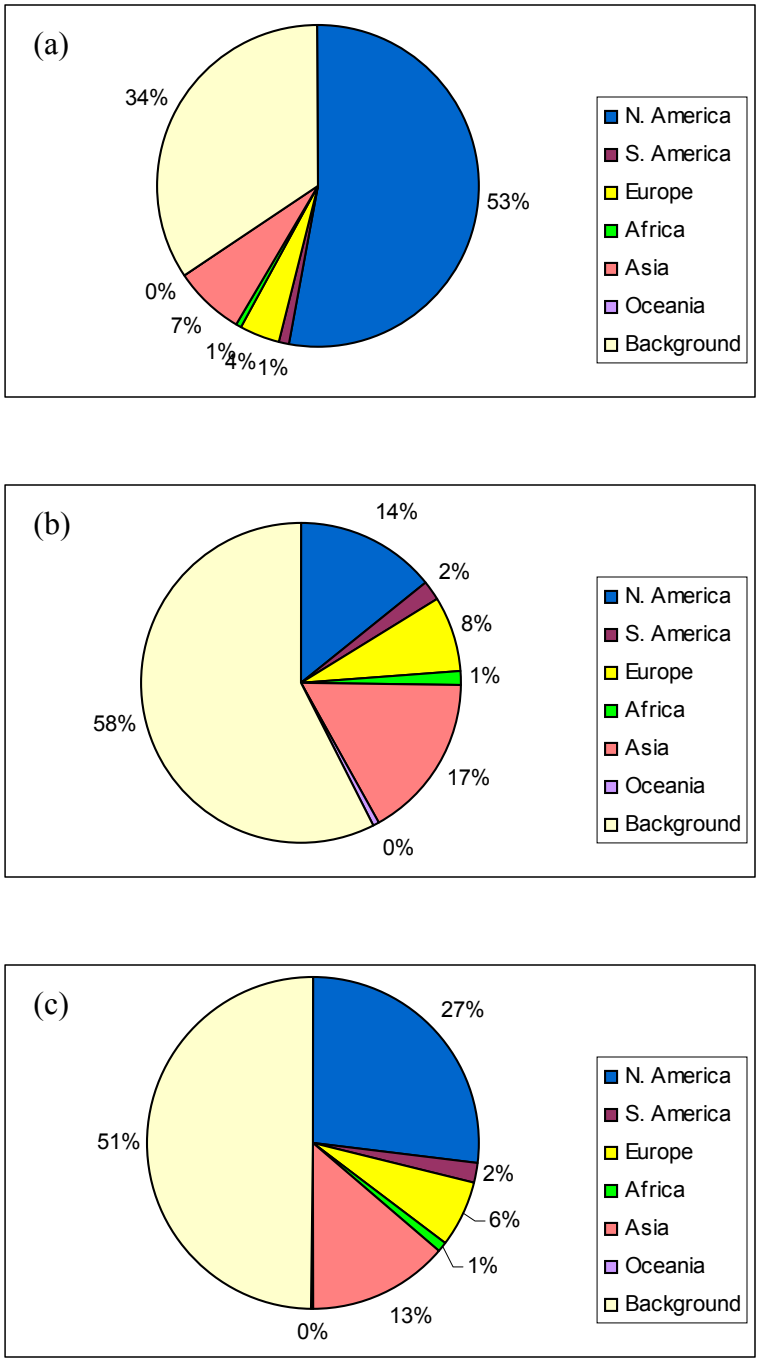

Figure 2-3. Local deposition scenario: Global contributions to deposition of Hg(II) and Hg(p) in the New York grid cell (a) dry deposition, (b) wet deposition, (c) total deposition.

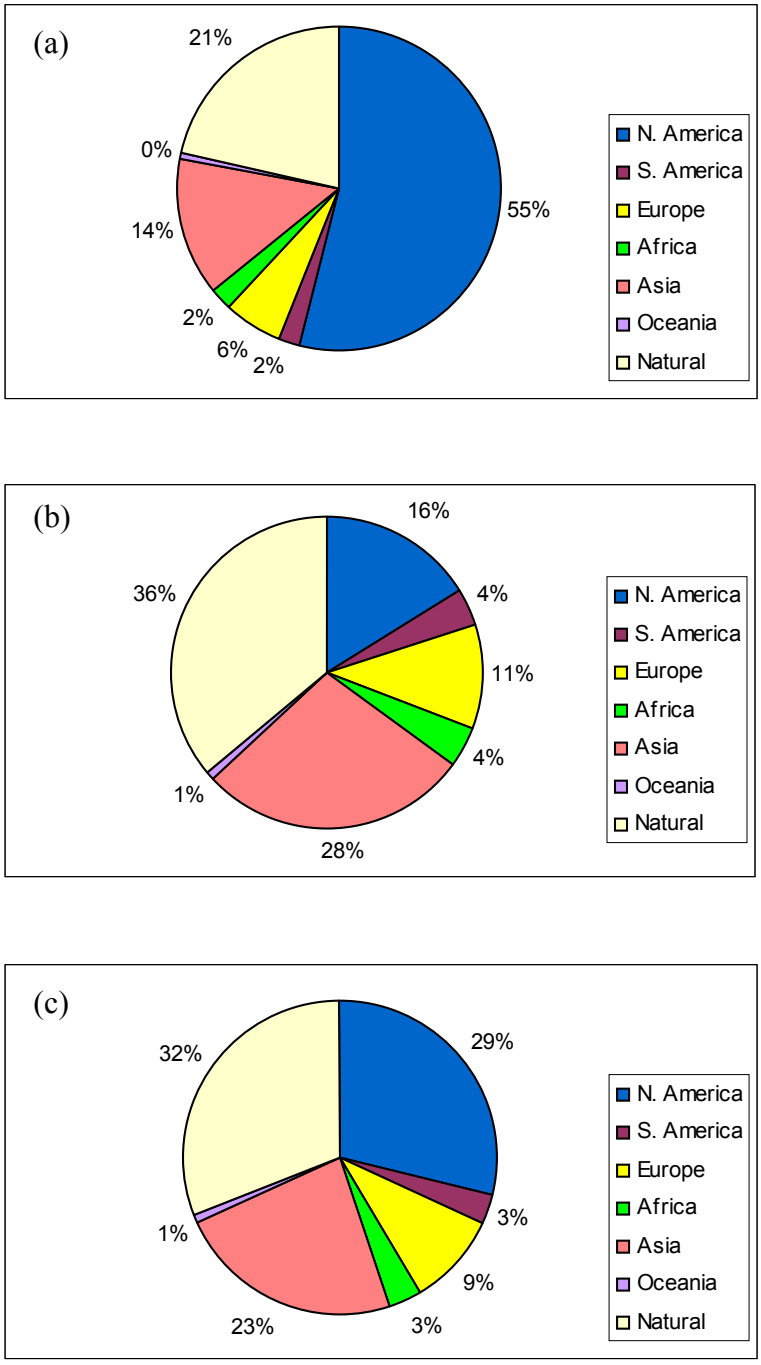

Figure 2-4. Local deposition scenario: Global contributions to deposition of Hg(II) and Hg(p) in the New York grid cell with reapportionment of Hg re-emissions, (a) dry deposition, (b) wet deposition and (c) total deposition.

decreased slightly (by 1%). The wet deposition results were little affected by the parameter changes in the local deposition scenario because some of those changes had opposing effects on wet deposition. The scavenging rate for Hg(II) and Hg(p) is increased, which increased their rate of wet deposition. This alone would have led to less deposition from distant sources as Hg would have been deposited closer to the source. However, other changes such as increased oxidant concentrations and Hg adsorption coefficient on PM, increased the rate at which Hg(0) converts to Hg(II). Since Hg(0) can travel long distances, wet deposition of Hg in New York is made up in part of Hg(II) converted from Hg(0) which originated from distant sources.

2.3.3 Long-range transport

In the long-range transport scenario, the changes to model parameters are opposite to those made for the local deposition scenario (see Table 2-2). As expected, this caused the contribution trends to move in the opposite direction as compared to the local deposition case. The results are presented in Figures 2-5 and 2-6. Total deposition of Hg(II) and Hg(p) decreased from 15 $\mu g/m^2$-yr in the nominal scenario to 13.6 $\mu g/m^2$-yr in the long-range transport scenario (see Table 2-4). However, the relative contributions of the global source areas changed little. The contribution from North American sources decreased slightly, while the contributions due to Asian and African sources increased slightly (see Figure 2-5c).

Figure 2-5a shows that contributions to dry deposition of Hg(II) and Hg(p) in the New York grid cell from Asian and background sources increased by 2% each. The contribution from North American sources decreased by 4%. European, African, South American, and Oceanian contributions were negligibly affected.

In the case of wet deposition, there was even less change. The wet deposition results for the long-range transport scenario are shown in Figure 2-5b. The contribution from Asian sources increased by 1% while the contribution from North American sources decreased by 1%. The wet deposition contributions were not much affected because wet deposition is already dominated by long-range transport as discussed in Section 2.3.1.

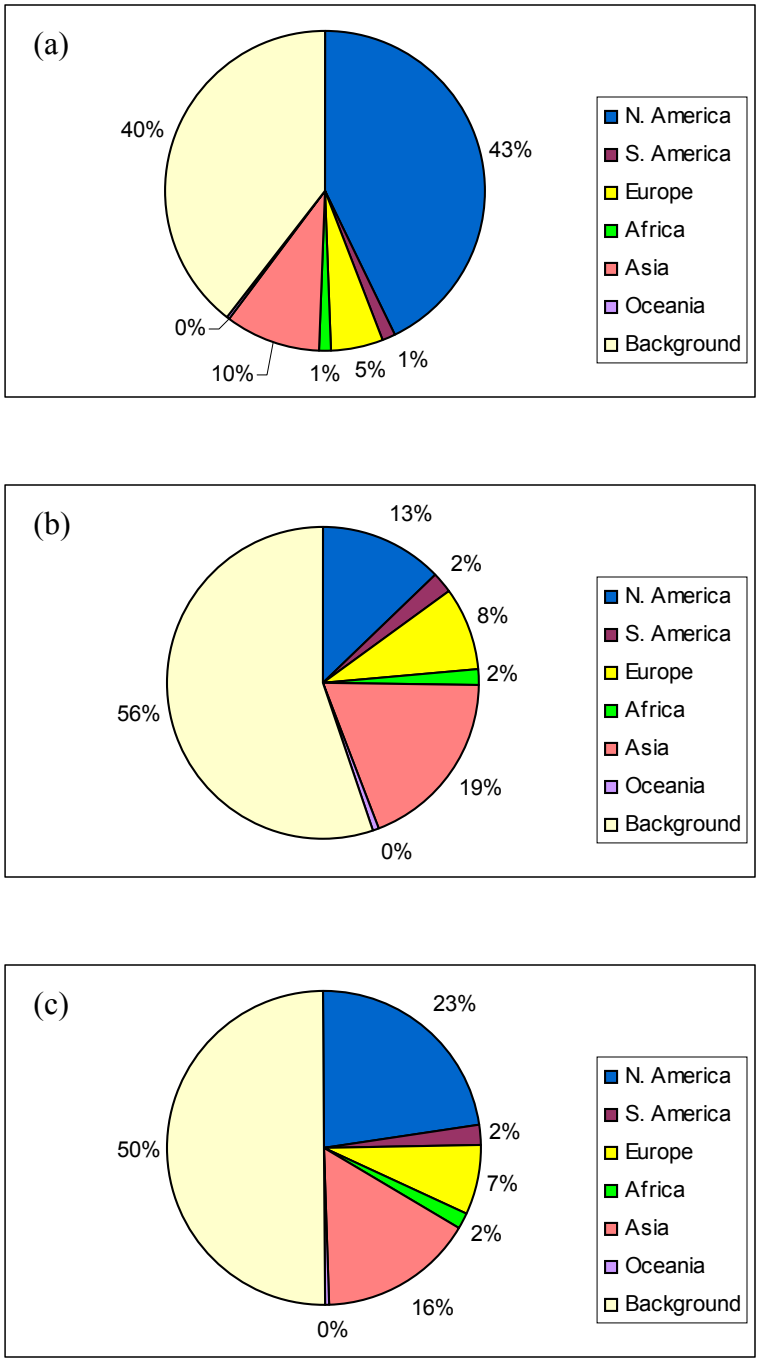

Figure 2-5. Long-range transport scenario: Global contributions to deposition of Hg(II) and Hg(p) in the New York grid cell (a) dry deposition, (b) wet deposition, (c) total deposition.

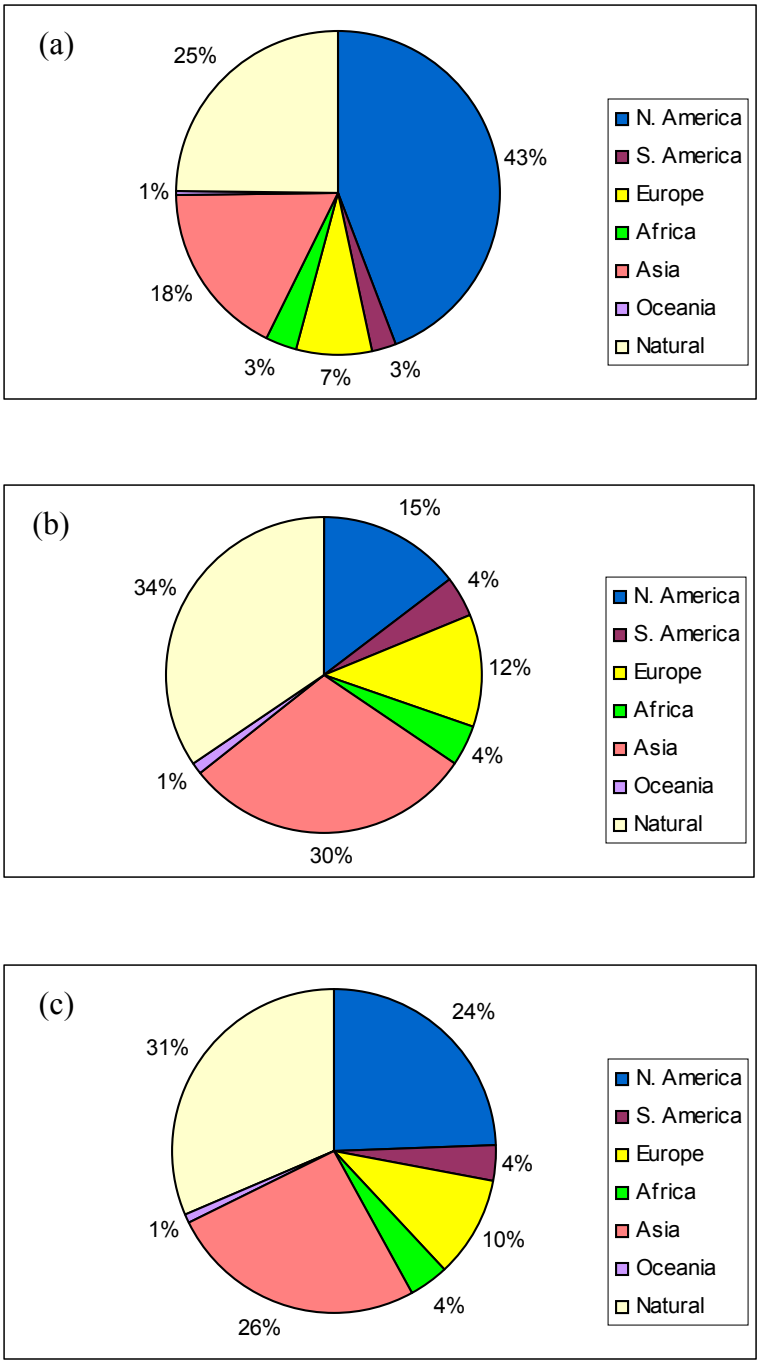

Figure 2-6. Long-range transport scenario: Global contributions to deposition of Hg(II) and Hg(p) in the New York grid cell with reapportionment of Hg re-emissions, (a) dry deposition, (b) wet deposition and (c) total deposition.

Similar results are obtained when re-emissions of Hg are reapportioned to continental source areas. For total deposition, the contribution from North America decreased from 26% in the nominal scenario to 24% in this scenario and the contribution from Asia increased from 25% in the nominal scenario to 26% in this scenario.

3. CONTINENTAL ATMOSPHERIC MODELING OF MERCURY

3.1 Description of the Continental Atmospheric Mercury Model

The formulation of the continental atmospheric model, TEAM, has been described in detail by Pai et al. (1997) and Seigneur et al. (2001a). We present here an overview of the model.

TEAM is a 3-D Eulerian model that simulates the transport, chemical and physical transformations, wet deposition and dry deposition of Hg species. In this application to North America, the horizontal grid resolution is 100 km and the vertical resolution consists of six layers from the surface to 6 km altitude with finer resolution near the surface (the layer interfaces are at 60, 150, 450, 850 and 2000 m). Transport processes include transport by the 3-D mean wind flow and dispersion by atmospheric turbulence. The module that simulates the chemical and physical transformations of Hg was updated from the original version and is the same module as that used in the global model (see Section 2). Three Hg species – Hg(0), Hg(II) and Hg(p) – are simulated. Hg(II) actually consists of several chemical species in the gas phase and in cloud droplets; Hg(II) can also adsorb to PM.

The wet deposition flux is calculated as the product of the cloud droplet concentration of the Hg species and the precipitation amount. Scavenging of these Hg species by rain below the cloud (washout) is also simulated. Scavenging is treated as a transient process using scavenging coefficients that depend on precipitation intensity.

Dry deposition is simulated using the resistance transfer approach. The deposition process is simulated as a series of three mass transfer steps: (1) turbulent transport from the bulk atmosphere to near the surface, (2) diffusion through a laminar layer near the surface and (3) uptake of the gas or particle by the surface. For Hg(0), background emissions and dry deposition are assumed to balance each other over North America. This assumption is justified by the fact that the atmospheric lifetime of Hg(0) (about 1 year) greatly exceeds its residence time (a few days) within the TEAM domain. One should note, however, that Hg(0) dry deposition was a significant component of Hg total deposition in the global simulation. For Hg(II), the dry deposition characteristics

are assumed to be similar to that of nitric acid (HNO_3) because these two gases have similar solubility. Dry deposition velocities calculated by TEAM for Hg(II) and Hg(p) over various surface types (forest, agricultural land, and water) were presented by Pai et al. (1997). The dry deposition velocities used by Pai et al. (1997) were updated for deciduous forests (median value of 2 cm/s) to reflect atmospheric measurements of Hg deposition in Tennessee and Indiana reported by Lindberg and Stratton (1998). The dry deposition of Hg(p) is treated using the characteristics of fine particles.

3.2 Base Simulations over North America for 1998

The year 1998 was selected for meteorological data. Emission inventories were developed from the years 1998 and 1999, as discussed by Seigneur et al. (2001a). We describe first the preparation of the inputs to the model. Next, we present the model simulation results and compare those with available data.

3.2.1 Model inputs

Emissions

The gridded and speciated inventory described by Seigneur et al. (2001a) was used for the anthropogenic emissions. As discussed above, background emissions are not treated in the model because the atmospheric lifetime of Hg(0) greatly exceeds its residence time within the domain.

Meteorological Inputs

The 3-D wind and temperature fields were obtained from the results of a simulation of the Nested Grid Model (NGM), a prognostic meteorological model applied by the National Oceanic and Atmospheric Administration (NOAA). The NGM data set was obtained from the National Center for Atmospheric Research (NCAR, 2000). The cloud fields were also obtained from NCAR. Daily precipitation data were obtained from NCAR for 1998 for several thousand stations in the U.S. Annual precipitation data were obtained for the same year from the National Atmospheric Deposition Program

(NADP)/Mercury Deposition Network (MDN) for about 200 stations in the U.S. Because the annual NADP/MDN data appeared more robust than the daily data, we scaled the daily data to match the annual values using a spatial interpolation algorithm ($1/r^2$ weighting with a radius of influence of 1000 km). Thus, we constructed a gridded precipitation data base with daily resolution and annual precipitation amounts consistent with MDN deposition data. Precipitation data for Canada were obtained from the Canadian Climate Network for 62 stations. These daily data were gridded using the same spatial interpolation algorithm as for the U.S. For areas over Mexico and the oceans, precipitation amounts were obtained by extrapolation from data available in the U.S. and Canada (the nearest values available were assumed to apply up to the boundary of the modeling domain).

Boundary Conditions

The results of the global model simulation are used to provide the boundary conditions for the TEAM application to North America. These boundary conditions consist of the concentrations of Hg(0), Hg(II) and Hg(p) as a function of location, height and season. The global grid cells used for these boundary conditions ranged from 20 to 68 degrees latitude north and from 45 to 145 degrees longitude west. The global model includes five layers from the surface to 6 km altitude. These layers are mapped into the six layers of TEAM. The boundary conditions vary according to season. The values simulated by the global model for January, April, July and October are used to represent winter, spring, summer and fall conditions, respectively.

Chemical Concentrations

The concentrations of O_3, OH, HO_2, H_2O_2 and SO_2 were obtained from the same 3-D fields as those used for the global simulation. The calculation of the aqueous concentrations of OH and HO_2 uses the same temperature-dependent Henry's law constants and the same scaling factors to account for the effect of clouds as used in the global model. Because SO_2 is a primary pollutant that can show strong spatial gradients in source regions, the spatial distribution of SO_2 concentrations is further refined to a finer spatial resolution using data from the CASTNet monitoring network (2001). A

uniform concentration of 1 ppb is assumed for HCl. The concentration of Cl_2 over the ocean was selected to be 150 to 50 ppt at night (decreasing with height) and 10 ppt during the day (Spicer et al., 1998). The concentration of atmospheric PM in droplets was chosen to be $5x10^{-3}$ g/l (Seigneur et al., 1998).

3.2.2 Base simulations

We conducted three base simulations.

- A nominal base simulation that corresponds to that conducted under the EPRI project (Seigneur et al., 2001a). The nominal base simulation uses the model inputs described above.
- A base simulation conducive to local Hg deposition.
- A base simulation conducive to long-range transport of Hg.

The inputs used for the local deposition and long-range transport simulations were developed in a manner similar to those used for the corresponding global simulations (see Table 2-2). In addition, the boundary conditions were modified to reflect the results of the corresponding global simulation and some anthropogenic emissions were also modified, as explained below.

For the local deposition simulations, the lower bound of Mexican emissions reported by Pai et al. (2000) was used (i.e., 17 Mg/yr). For the long-range transport simulation, the upper bound of Mexican emissions reported by Pai et al. (2000) was used (i.e., 51 Mg/yr). Also, emissions of iron ore processing that are located in Minnesota and Michigan were increased from 0.4 Mg/yr to 15 Mg/yr to reflect an earlier emission factor and emissions for chloralkali plants were increased from 6 Mg/yr to 12 Mg/yr to reflect existing uncertainties.

The simulated wet deposition fluxes of Hg are compared with available data from the Mercury Deposition Network in Figure 3-1 for the nominal base simulation. The coefficient of determination is 0.72, the average bias is –8% and the average error is 21% when deposition fluxes are compared by state or province (Figure 3-1a). When

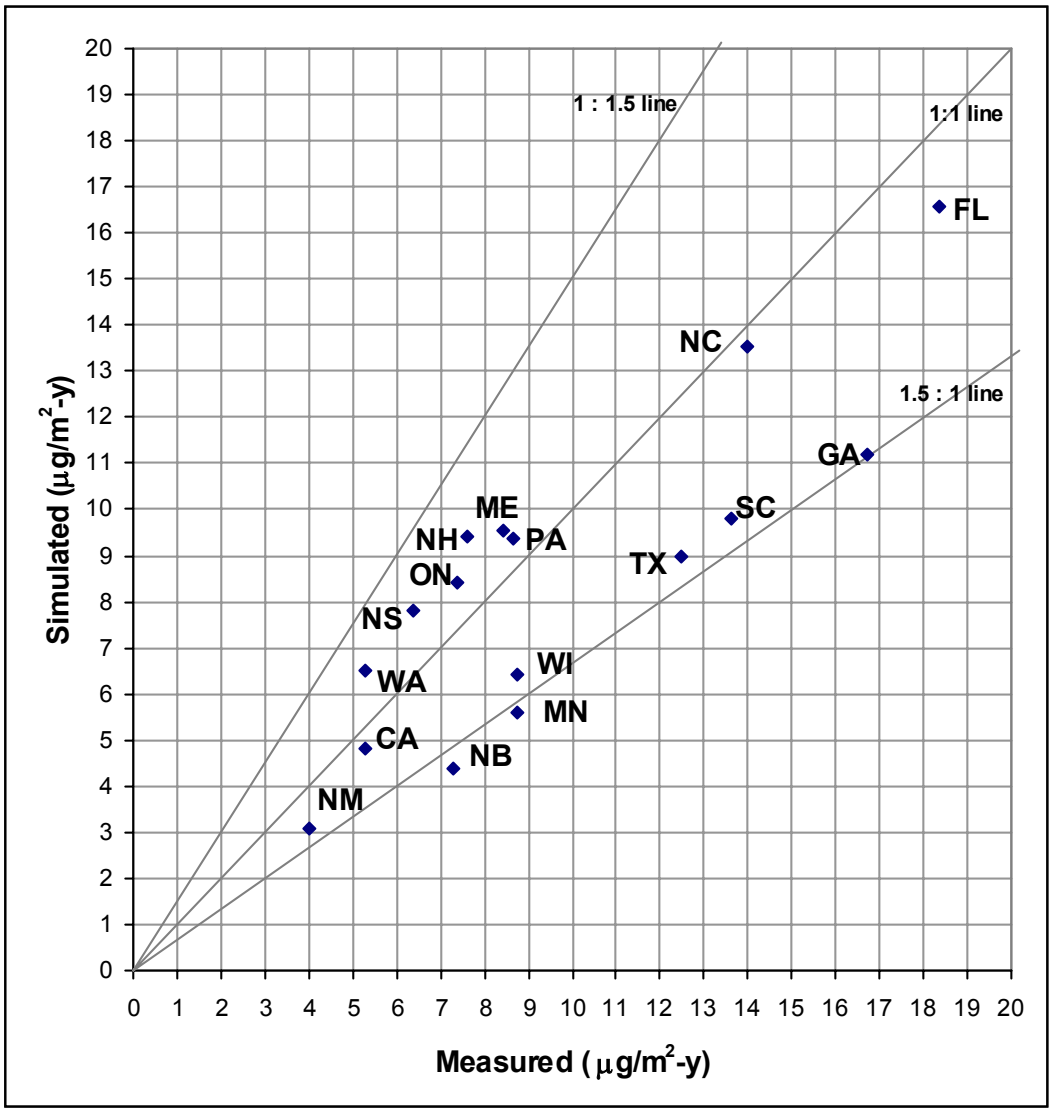

Figure 3-1a. Comparison of state- and province-averaged simulated and measured annual wet deposited fluxes of Hg ($\mu g/m^2$-y) in North America for the nominal scenario.

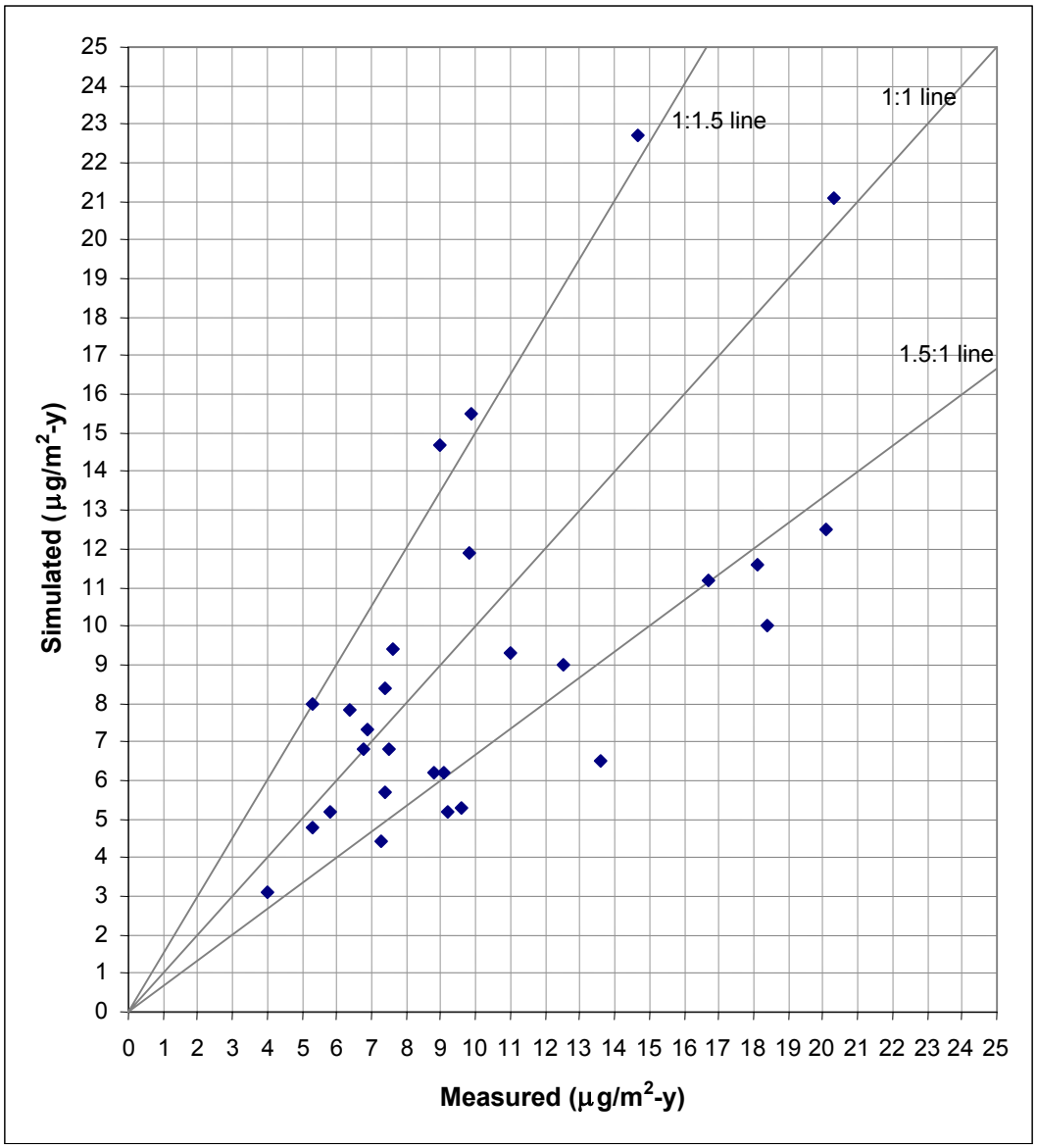

Figure 3-1b. Comparison of simulated and measured annual wet deposition fluxes of Hg (µg/m^2-y) at specific sites in North America for the nominal scenario.

deposition fluxes are compared at specific sites (Figure 3-1b), the coefficient of determination is 0.45, the average bias is –7% and the average error is 28%. The lower value of the coefficient of determination that is obtained when Hg deposition fluxes are compared at specific sites suggests that the model fails to capture the variations in Hg wet deposition fluxes at finer spatial scales (i.e., intra-state variations).

The simulated wet deposition fluxes of Hg are compared with available data from the Mercury Deposition Network in Figure 3-2 for the local deposition base simulation. The coefficient of determination is 0.69, the average bias is –9% and the average error is 22% when deposition fluxes are compared by state or province (Figure 3-2a). When deposition fluxes are compared at specific sites (Figure 3-2b), the coefficient of determination is 0.42, the average bias is –9% and the average error is 28%.

The simulated wet deposition fluxes of Hg are compared with available data from the Mercury Deposition Network in Figure 3-3 for the long-range transport base simulation. The coefficient of determination is 0.73, the average bias is –3% and the average error is 20% when deposition fluxes are compared by state or province (Figure 3-3a). When deposition fluxes are compared at specific sites (Figure 3-3b), the coefficient of determination is 0.46, the average bias is –1% and the average error is 26%.

Model performance is slightly better for the long-range transport base simulation than for the nominal base simulation. This result suggests that local deposition of Hg may be slightly overestimated in the nominal base simulation and that the long-range transport base simulation may be more representative of actual conditions.

The simulated deposition fluxes are presented in Table 3-1 for the following three sites in New York.

- Receptor 1 (Adirondack Mountains): This receptor corresponds to the Mercury Deposition Network (MDN) site of Huntington Wildlife Refuge (MDN site id NY20).
  Latitude: 43° 58’ 21’ North (43.9724)
  Longitude: 74° 13’ 15’’ West (74.2207)
  TEAM grid cell number: x = 49, y = 29

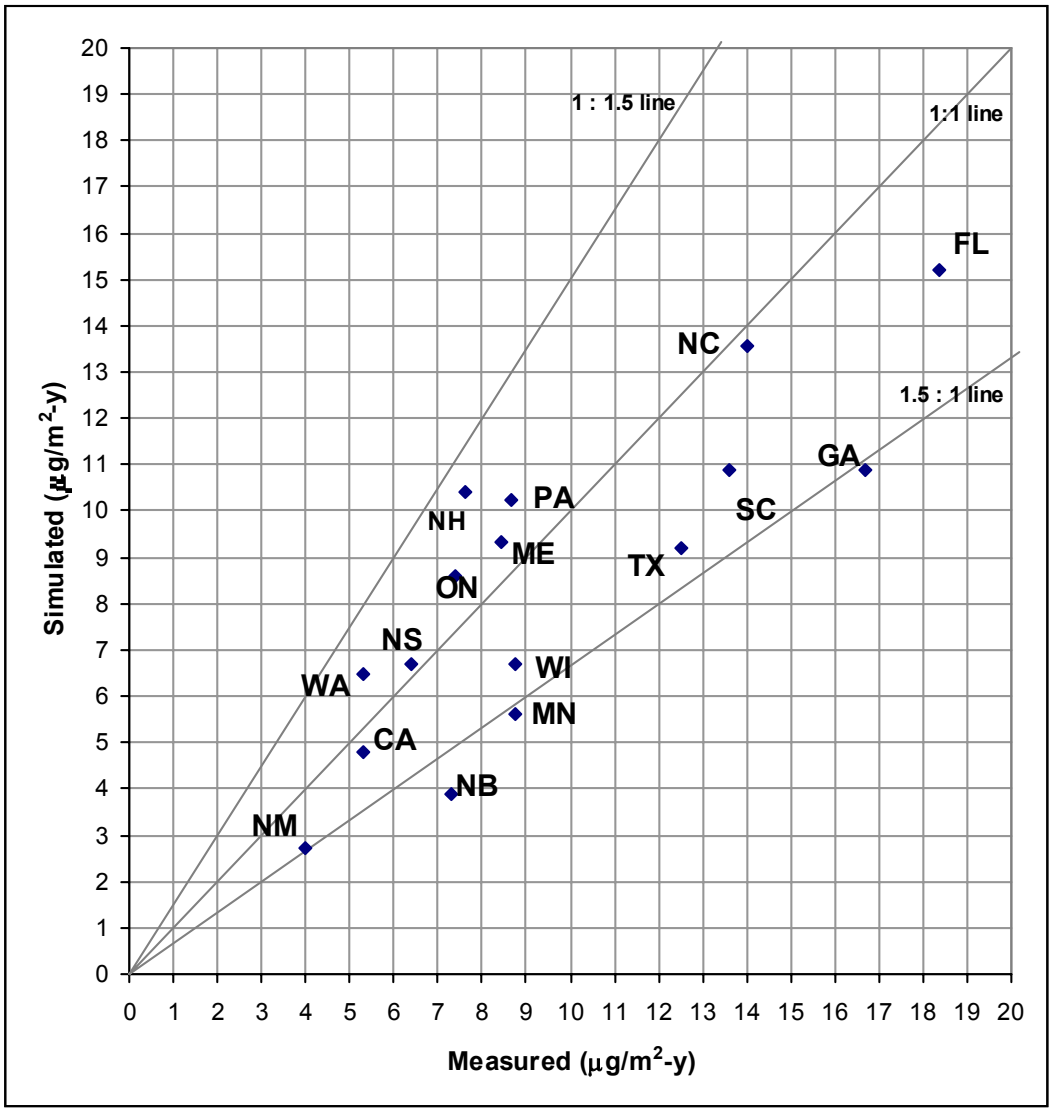

Figure 3-2a. Comparison of state- and province-averaged simulated and measured annual wet deposited fluxes of Hg (µg/m^2-y) in North America for the local deposition scenario.

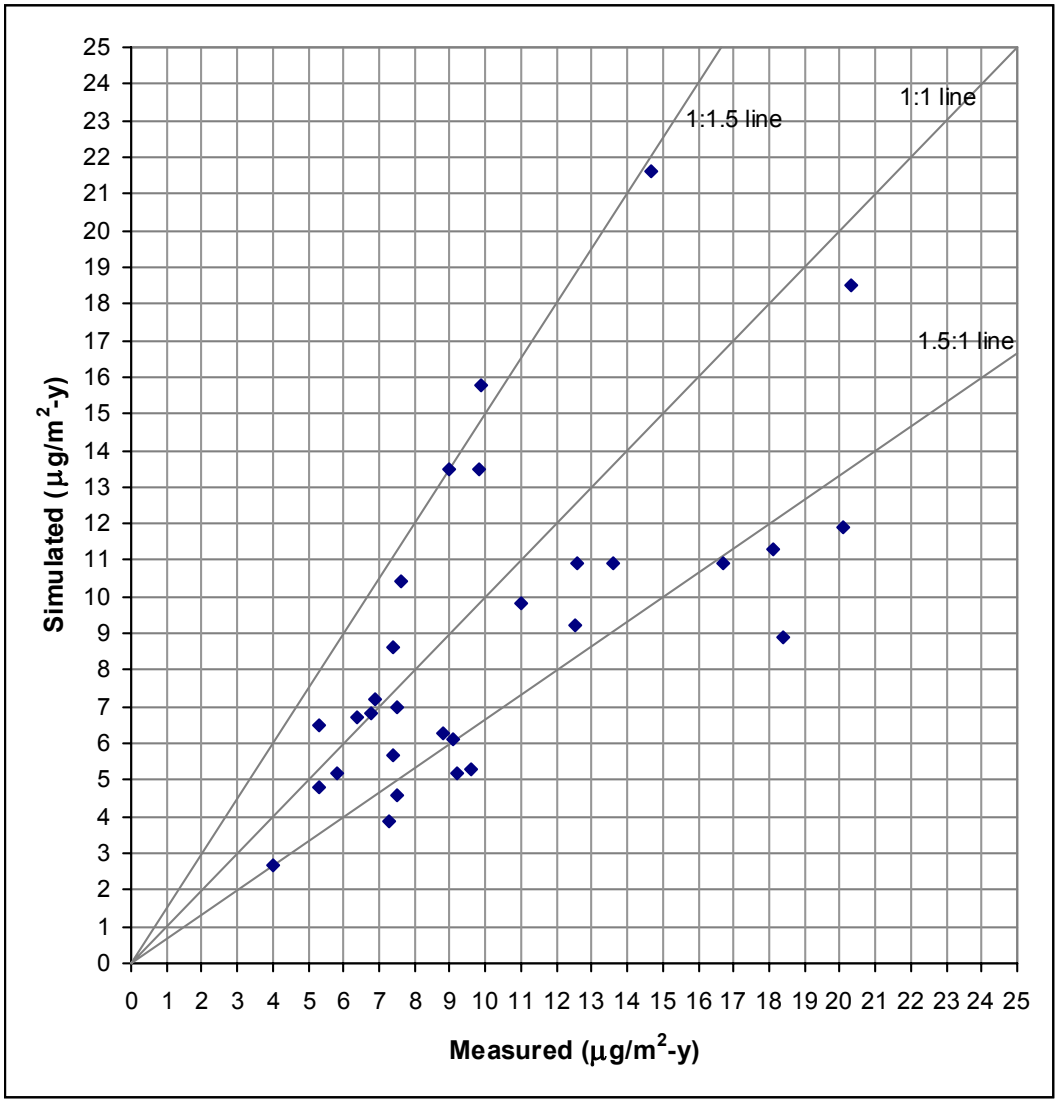

Figure 3-2b. Comparison of simulated and measured annual wet deposition fluxes of Hg (µg/m^2-y) at specific sites in North America for the local deposition scenario.

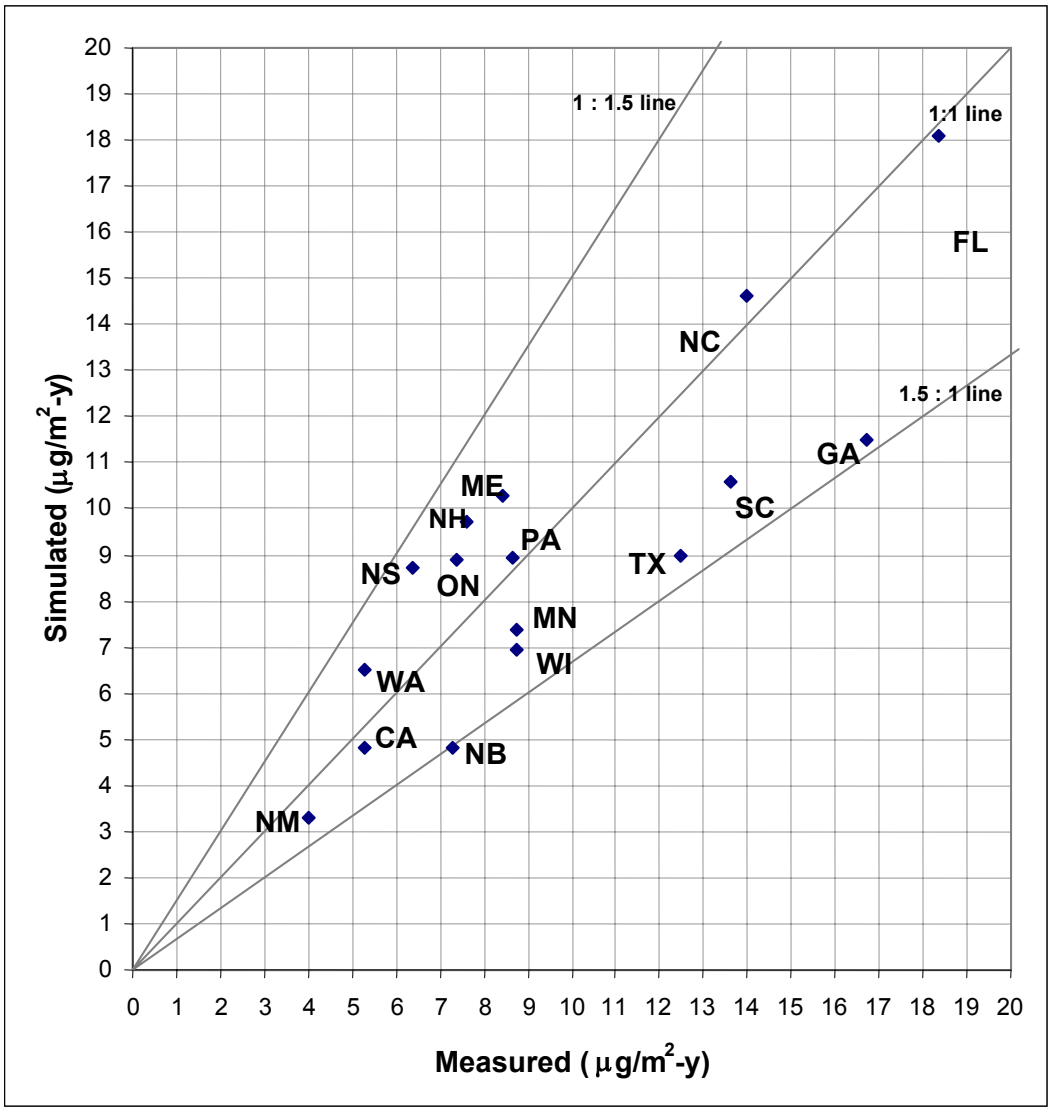

Figure 3-3a. Comparison of state- and province-averaged simulated and measured annual wet deposited fluxes of Hg (μg/m^2-y) in North America for the long-range transport scenario.

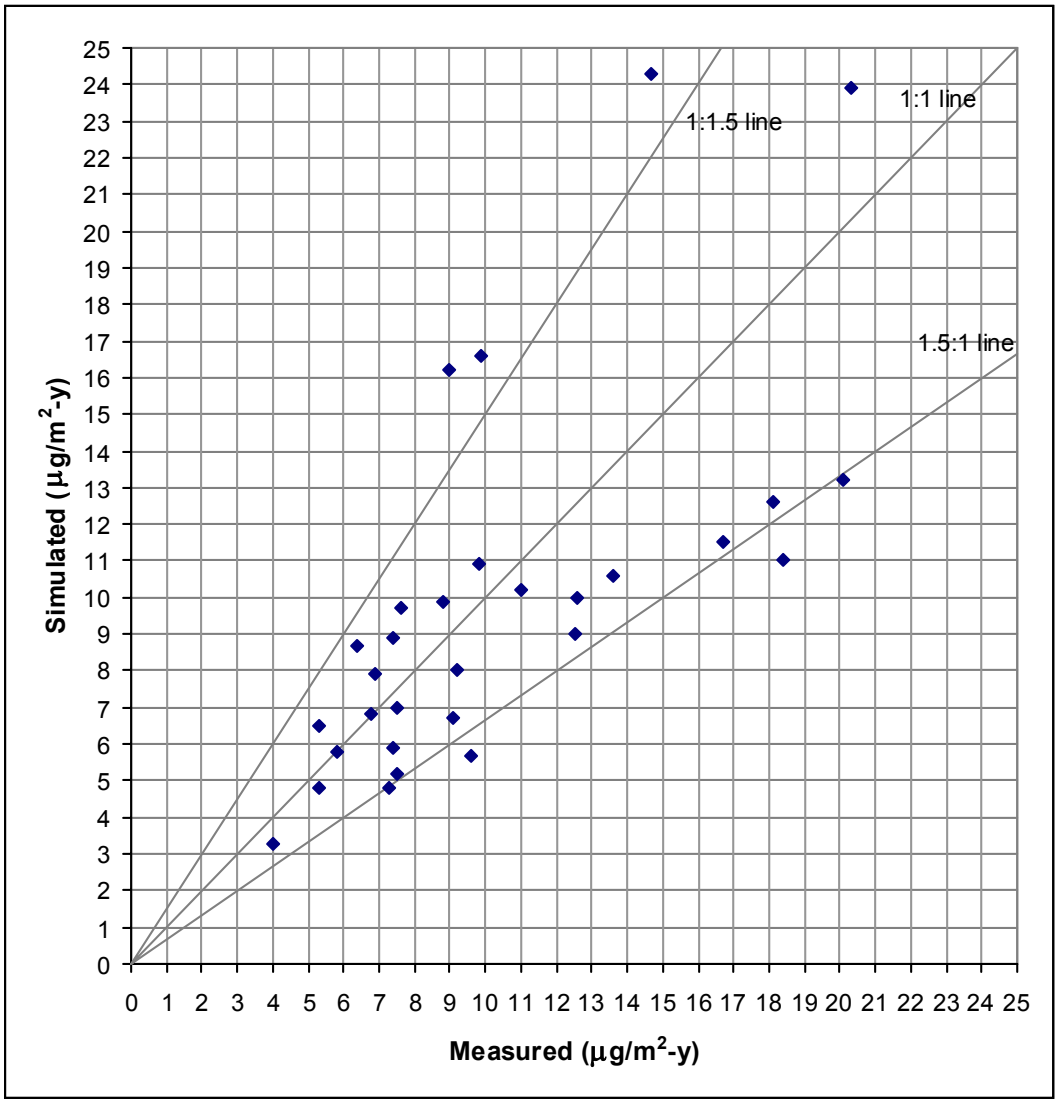

Figure 3-3b. Comparison of simulated and measured annual wet deposition fluxes of Hg (µg/m^2-y) at specific sites in North America for the long-range transport scenario.

Table 3-1. Hg deposition rates simulated with TEAM at three New York sites.

Site and deposition process[(a)]	Deposition flux (μg/m^2-yr)		
	Nominal base-simulation	**Local deposition base simulation**	**Long-range transport base simulation**
Adirondacks			
Dry deposition of Hg(II)	6.4	6.4	6.3
Dry deposition of Hg(p)	0.6	0.7	0.5
Wet deposition of total Hg	12.2	12.2	12.0
Total deposition	19.2	19.3	18.8
Finger lakes			
Dry deposition of Hg(II)	3.6	4.0	3.1
Dry deposition of Hg(p)	0.3	0.3	0.3
Wet deposition of total Hg	9.3	9.5	9.0
Total deposition	13.2	13.8	12.4
Catskills			
Dry deposition of Hg(II)	9.8	9.9	9.6
Dry deposition of Hg(p)	0.4	0.4	0.3
Wet deposition of total Hg	12.7	12.8	12.5
Total deposition	22.9	23.1	22.4

(a) Hg(0) dry deposition is not treated, see Section 3.1; Hg(0) wet deposition is negligible due to its very low solubility.

- Receptor 2 (Finger Lakes District): This receptor corresponds to the southern part of Cayuga Lake near Ithaca.
  Latitude: 42° 27’ 34’’ North (42.4594)
  Longitude: 76° 29’ 13’’ West (76.4869)
  TEAM grid cell number: x = 47, y = 26

- Receptor 3 (Catskill Mountains): This receptor corresponds to the Neversink Reservoir.
  Latitude: 41° 51’ 3’’ North (41.8509)
  Longitude: 74° 39’ 45’’ West (74.6626)
  TEAM grid cell number: x = 49, y = 26

Figure 3-4 presents the locations of these three receptors within the gridded TEAM domain.

For the nominal case, total Hg deposition ranges from 13.2 μg/m^2-yr in the Finger Lakes area, to 19.2 μg/m^2-yr in the Adirondacks and 22.9 μg/m^2-yr in the Catskills. Dry deposition ranges from 3.9 μg/m^2-yr in the Finger Lakes area to 10.2 μg/m^2-yr in the Catskills. Wet deposition shows less spatial variation; it ranges from 9.3 μg/m^2-yr in the Finger Lakes area to 12.7 μg/m^2-yr in the Catskills. In the Finger Lakes area, dry deposition accounts for 30% of total deposition. It accounts for 36% and 45% of total deposition in the Adirondacks and the Catskills, respectively. These values suggest that the Catskills are more impacted by local sources than the Adirondacks or the Finger Lakes area since Hg(II) and Hg(p) contribute to dry deposition more near their emission sources. The local deposition scenario leads to greater Hg deposition at all three sites; the increase in total deposition varies from 0.5% in the Adirondacks to 1% in the Catskills and 5% in the Finger Lakes area. The long-range transport scenario leads to less Hg deposition at all three sites; the decrease in total deposition varies from 2% in the Adirondacks and the Catskills to 6% in the Finger Lakes area.

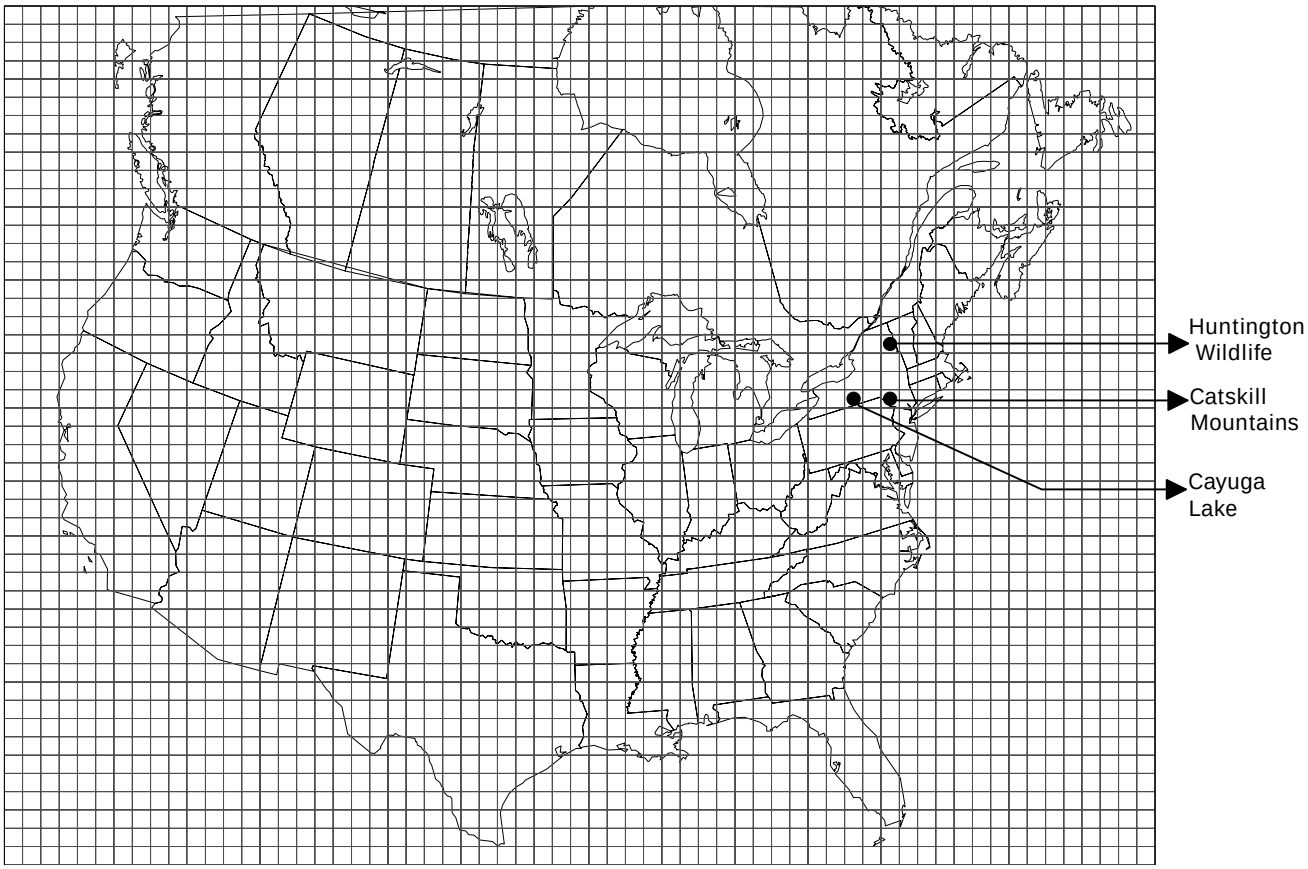

Figure 3-4. Locations of the receptor sites within the TEAM modeling grid.

These results are consistent with those obtained with the global simulation. The global simulation led to wet deposition and Hg(II) dry deposition fluxes that are within the range of values predicted in the continental simulation at the three receptors: a nominal wet deposition flux of 10.1 μg/m^2-yr in the global simulation versus a range of 9.3 to 12.7 μg/m^2-yr in the continental simulation, and a nominal dry deposition flux of Hg(II) of 4.7 μg/m^2-yr in the global simulation versus a range of 3.6 to 9.8 μg/m^2-yr in the continental simulation. The Hg(p) dry deposition flux is, however, slightly lower in the global simulation (0.2 μg/m^2-yr) than in the continental simulation (0.3 to 0.6 μg/m^2-yr) because the coarse global resolution tends to dilute the concentrations of primary species.

3.3 Contributions of North American Source Areas

Continental scale modeling was used to estimate the contributions of local (New York) and regional (the remaining 47 contiguous states, Canada, and northern Mexico) Hg emissions to Hg deposition in the three selected New York areas. We present the modeling results for the three scenarios (nominal, local deposition and long-range transport) at the three selected receptors. Hereafter, we refer to the 47 contiguous states excluding New York as the U.S. (or USA) for brevity.

3.3.1 Nominal scenario

At each receptor, the contribution from each of the four North American source areas (Canada, Mexico, New York, and the U.S.) was calculated. Contribution from the boundary inflows is also considered; it represents the contribution from sources outside North America, i.e., global and background emissions.

At the Adirondacks receptor, the majority (57%) of the total Hg deposition is from global and background sources. As shown in Figure 3-5, U.S. sources contribute 26%, New York sources 12%, Canadian sources 5%, and Mexican sources contribute less than 1%. The dry component of the Hg deposition is split mainly among global/background, U.S., and New York sources, although Canadian sources also have a

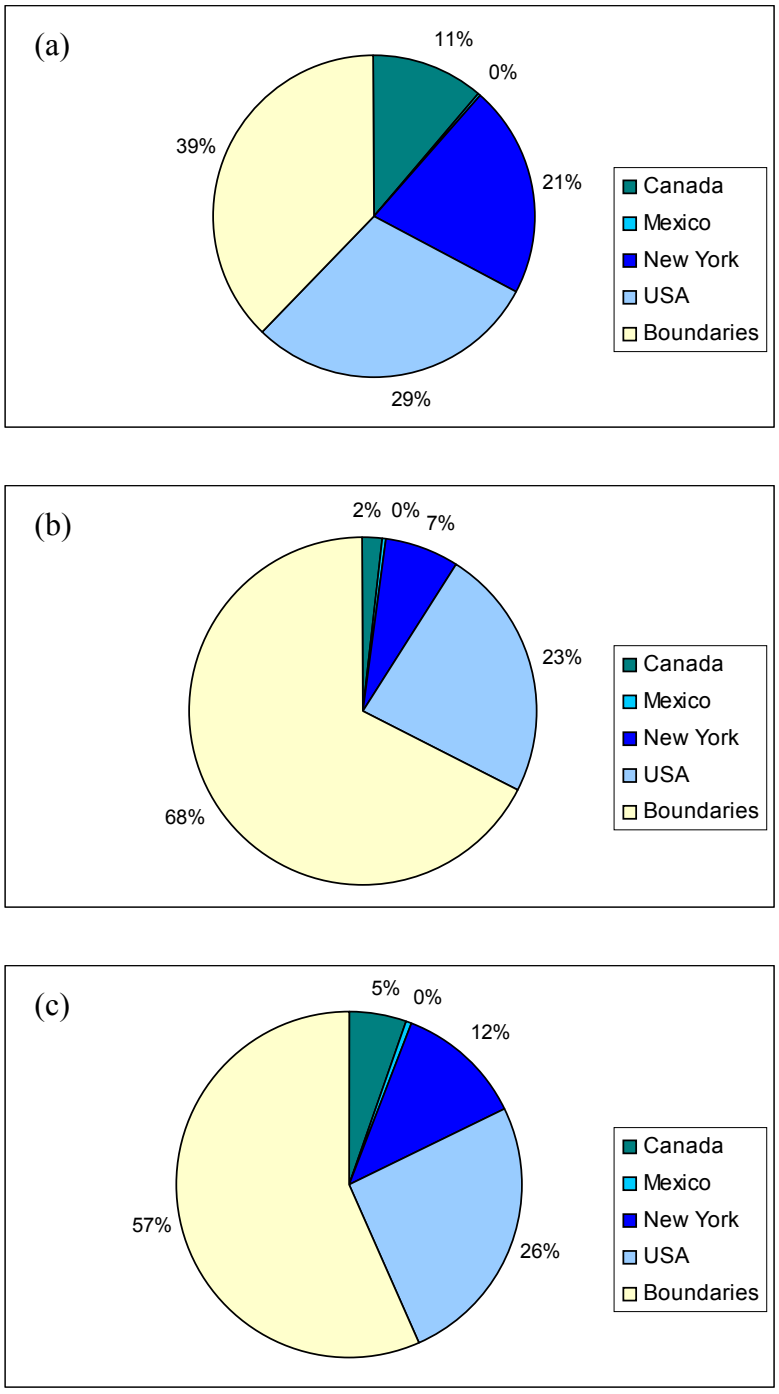

Figure 3-5. Nominal scenario: Regional contributions to Hg deposition at the Adirondacks receptor, (a) dry deposition, (b) wet deposition and (c) total deposition.

non-negligible contribution. This wide distribution among source areas can be explained by the location of the Adirondacks receptor. It is located in the northeastern corner of New York and thus, downwind from most of New York, the U.S., as well as Ontario, Canada. Also, because it is the farthest north of the three receptors, it is closest to the domain boundary and is the most affected by the global contribution. Wet deposition to the Adirondacks receptor is dominated by the contribution due to global sources, because wet deposition is not as influenced by local sources as dry deposition.

The Finger Lakes receptor also receives its largest contribution to total deposition from global and background sources (see Figure 3-6). U.S. emissions (30%) are the next largest contribution source, followed by New York emission sources (21%). Canadian sources have a small impact (4%). The largest contribution to dry deposition at the Finger Lakes receptor is from New York emissions (42%). Emissions from the U.S. are the second largest contribution (33%), followed by global/background sources (19%). The majority of the wet deposition is due to global/background sources. However, at the Finger Lakes receptor, the U.S. and New York emission source contributions to wet deposition are greater than at the Adirondacks receptor, 28 and 13%, respectively. The Finger Lakes receptor is farther from the northern boundary than the Adirondacks receptor, and, consequently, it is less impacted by global/background sources. Also, the Finger Lakes receptor is generally downwind of Lake Erie, which acts as an emission source buffer for nearby U.S. sources. Finally, this receptor is close to several Hg emission sources along the New York shore of Lake Erie, which leads to the large contribution of New York emissions to deposition at the receptor, especially for dry deposition.

The Catskills region of New York is the only receptor for which the largest contribution to total Hg deposition is from U.S. sources rather than global/background sources. Figure 3-7 shows that background sources are the second largest contribution followed by New York sources. Dry deposition is particularly dominated by U.S. sources, which account for 68% of dry deposition at the Catskills receptor. This is due to the location of the receptor, which is in the southern part of New York State, close to the borders of Pennsylvania and New Jersey. There are many Hg emission sources just upwind of those state borders. There are some nearby New York sources as well,

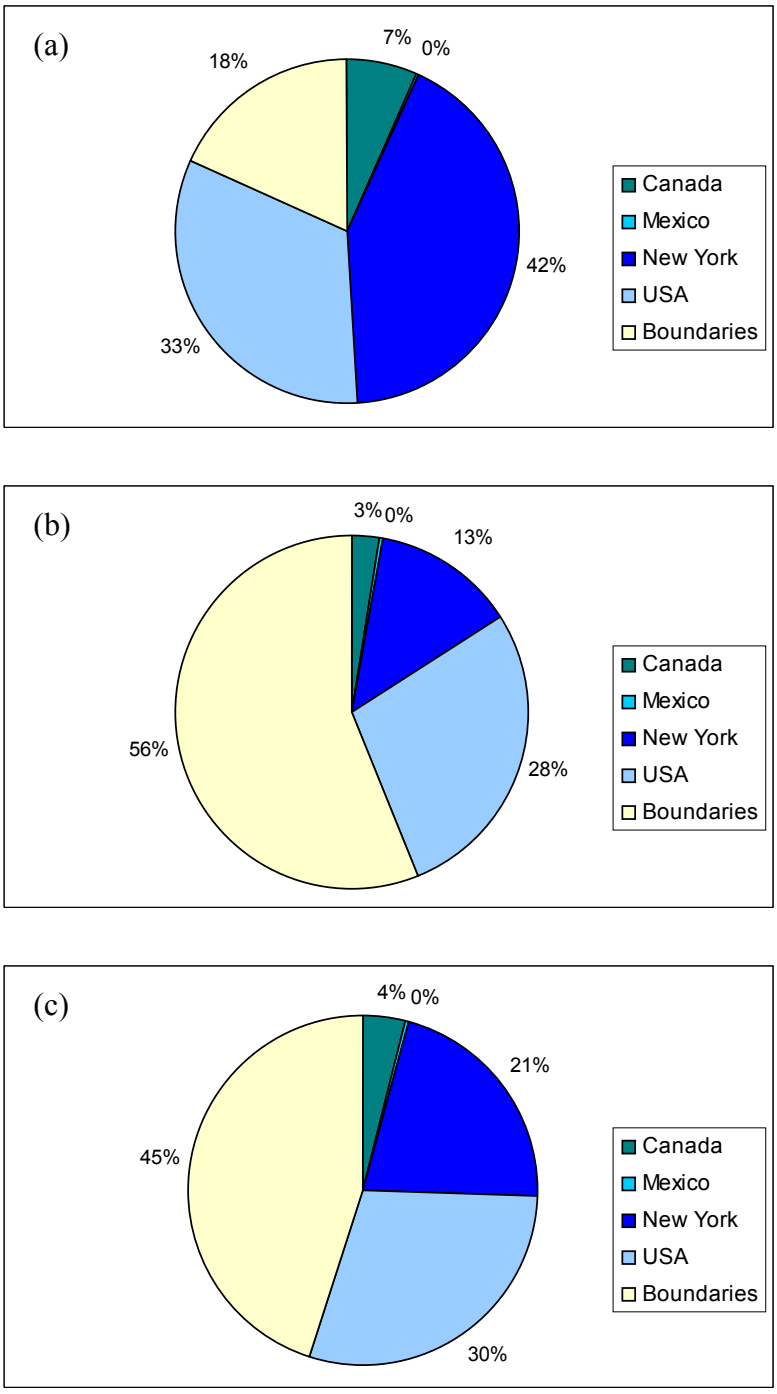

Figure 3-6. Nominal scenario: Regional contributions to Hg deposition at the Finger Lakes receptor, (a) dry deposition, (b) wet deposition and (c) total deposition.

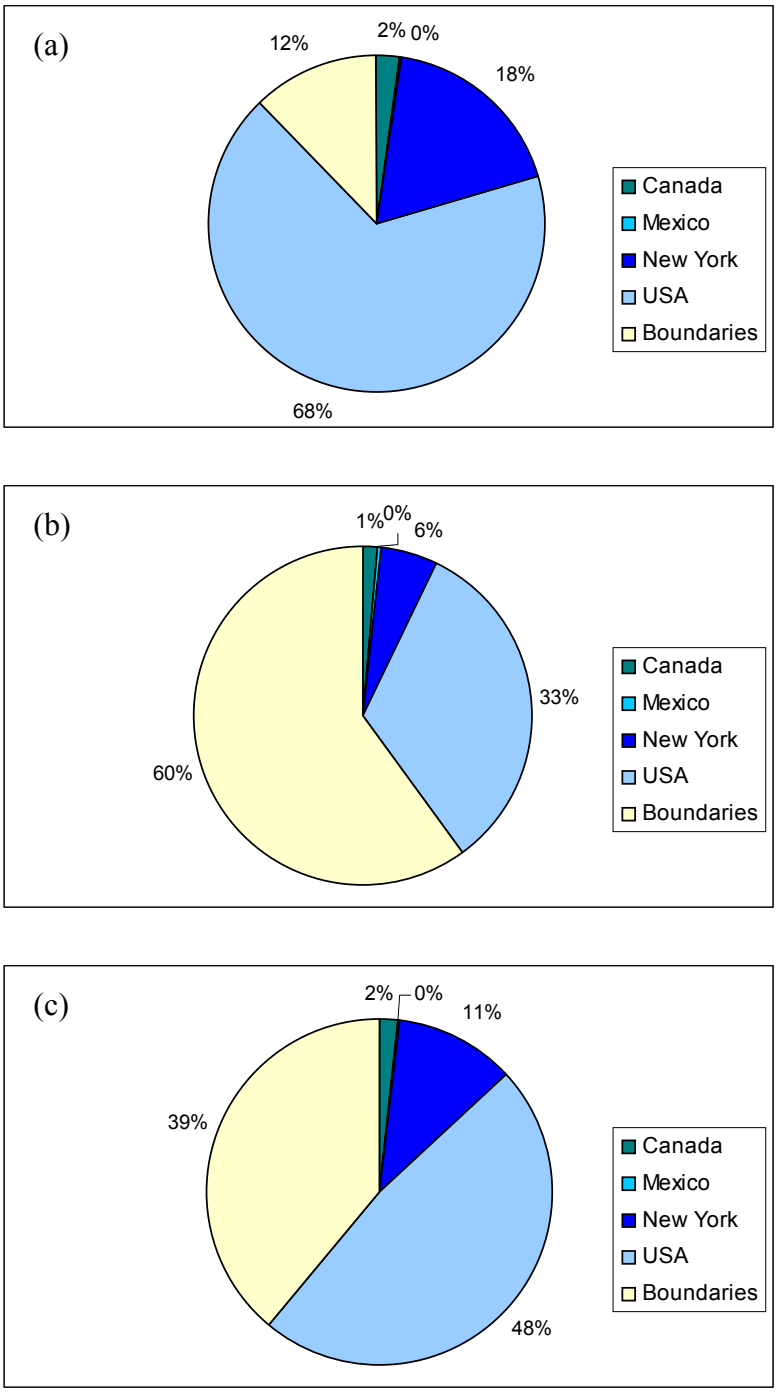

Figure 3-7. Nominal scenario: Regional contributions to Hg deposition at the Catskills receptor, (a) dry deposition, (b) wet deposition and (c) total deposition.

however, they contribute only 18% of dry deposition. Global/background sources only contribute 12% of dry deposition at the Catskills receptor. Wet deposition at the Catskills

receptor, on the other hand, has a pattern very similar to that at the other two receptors. Global/background emission sources contribute 60% of wet deposition, U.S. sources contribute 33% and New York sources contribute only 6%.

3.3.2 Local deposition scenario

When the model parameters were altered to allow for increased local deposition, a common trend emerged. Generally, the deposition contributions due to global/background sources decreased, while the contributions to deposition due to U.S. and New York sources increased. The contribution due to Canadian emissions either remained unchanged or increased slightly, depending on the location of the receptor and the type of deposition. The results for the three receptors are shown in Figures 3-8, 3-9, and 3-10.

3.3.3 Long-range transport scenario

When the model parameters were changed to produce increased long-range transport, most of the trends from the increased local deposition scenario reversed. In general, contributions from global/background sources increased and contributions from New York sources decreased. The contributions due to U.S. and Canadian sources generally decreased slightly or remained unchanged. The results for the long-range transport scenario are shown in Figures 3-11, 3-12, and 3-13.

The exception to this rule of thumb is dry deposition at the Finger Lakes receptor. At this receptor the contribution to dry deposition of Hg due to U.S. sources increased with increased long-range transport. This occurred because some of the Hg emissions that were deposited over Lake Erie in the nominal case, were transported across it and into the Finger Lakes region in the long-range transport scenario.

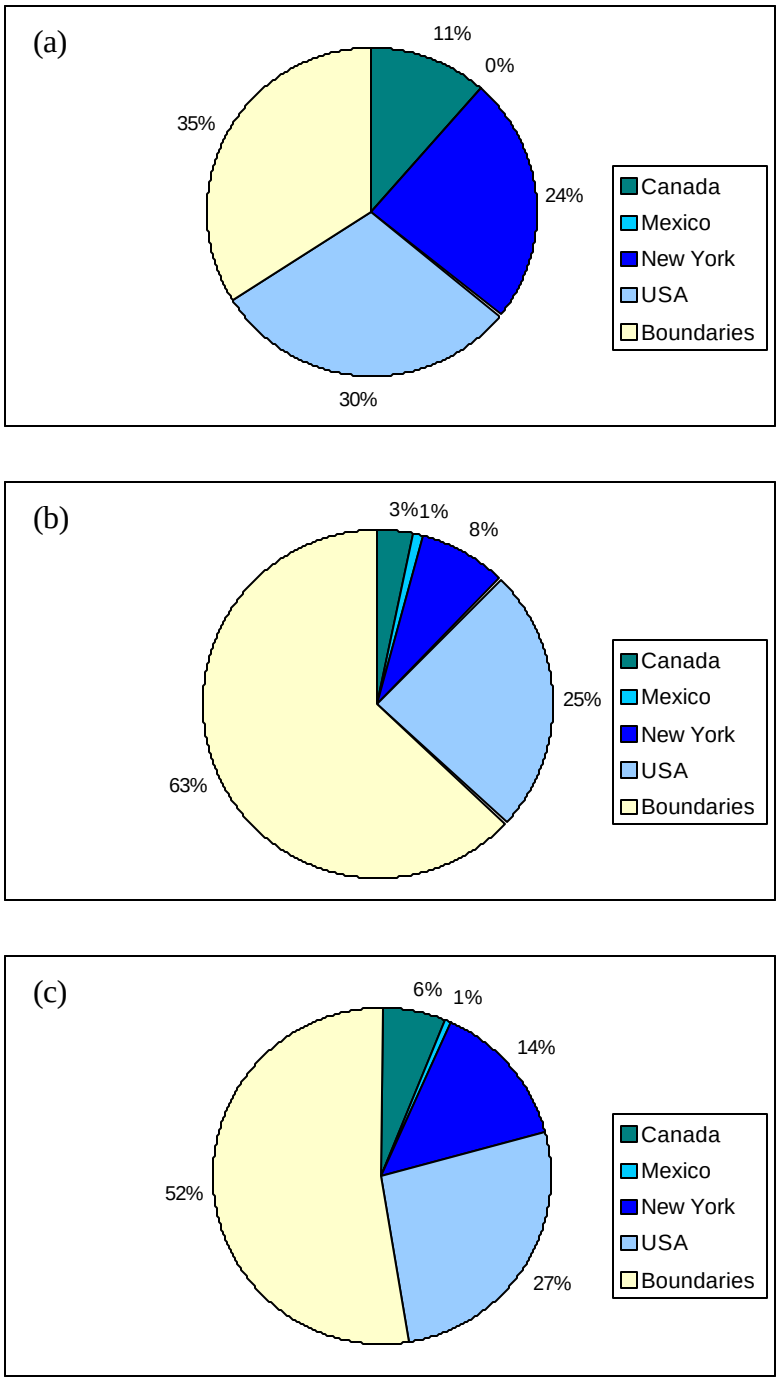

Figure 3-8. Local scenario: Regional contributions to Hg deposition at the Adirondacks receptor, (a) dry deposition, (b) wet deposition, and (c) total deposition.

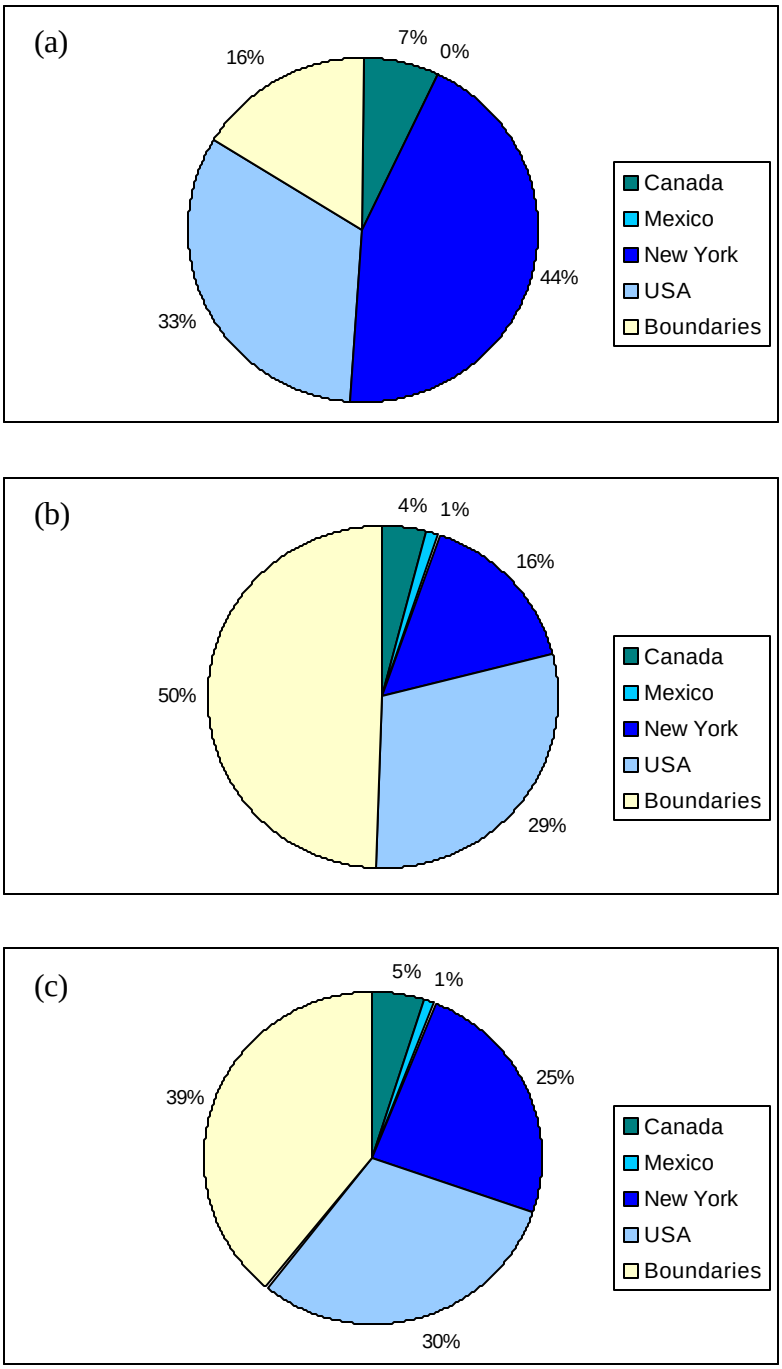

Figure 3-9. Local deposition scenario: Regional contributions to Hg deposition at the Finger Lakes receptor, (a) dry deposition, (b) wet deposition, and (c) total deposition.

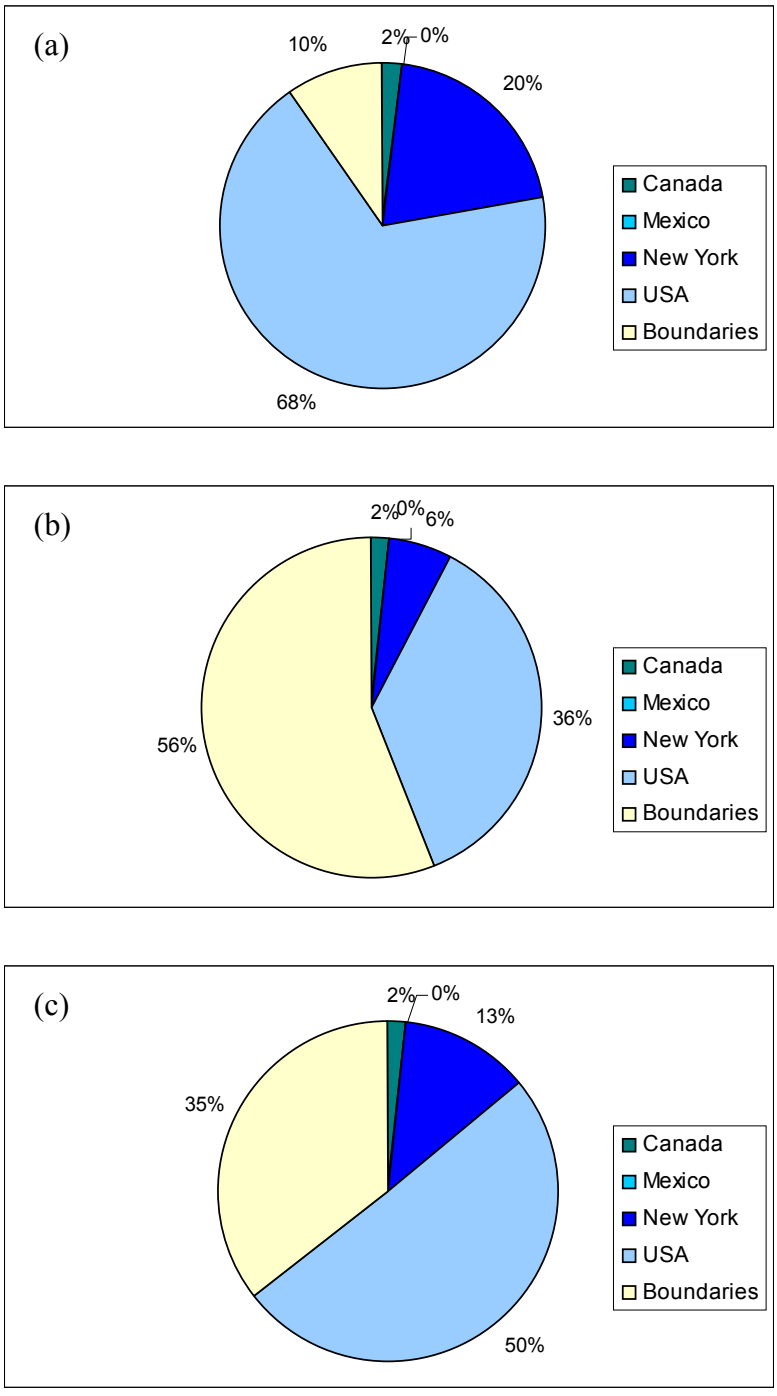

Figure 3-10. Local deposition scenario: Regional contributions to Hg deposition at the Catskills receptor, (a) dry deposition, (b) wet deposition, and (c) total deposition.

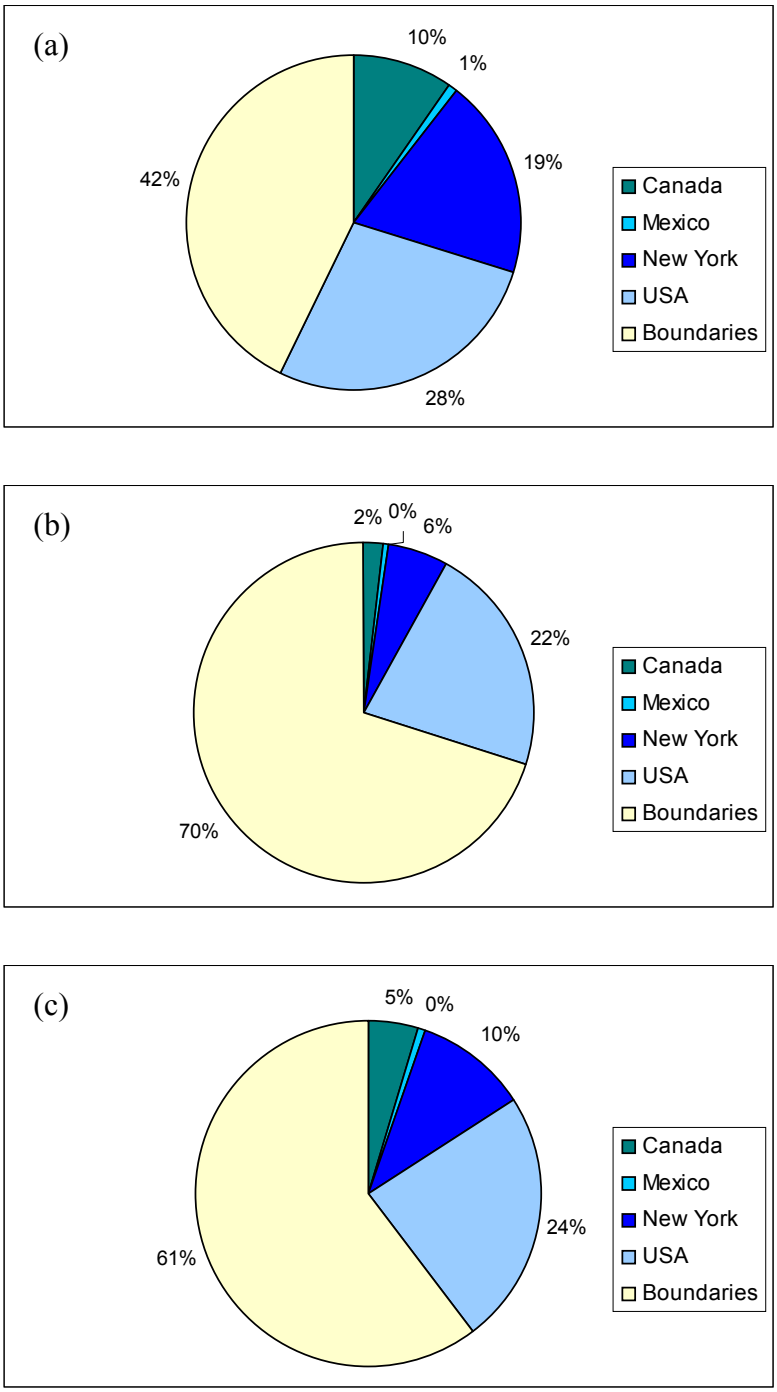

Figure 3-11. Long-range transport scenario: Regional contributions to Hg deposition at the Adirondacks receptor, (a) dry deposition, (b) wet deposition, and (c) total deposition.

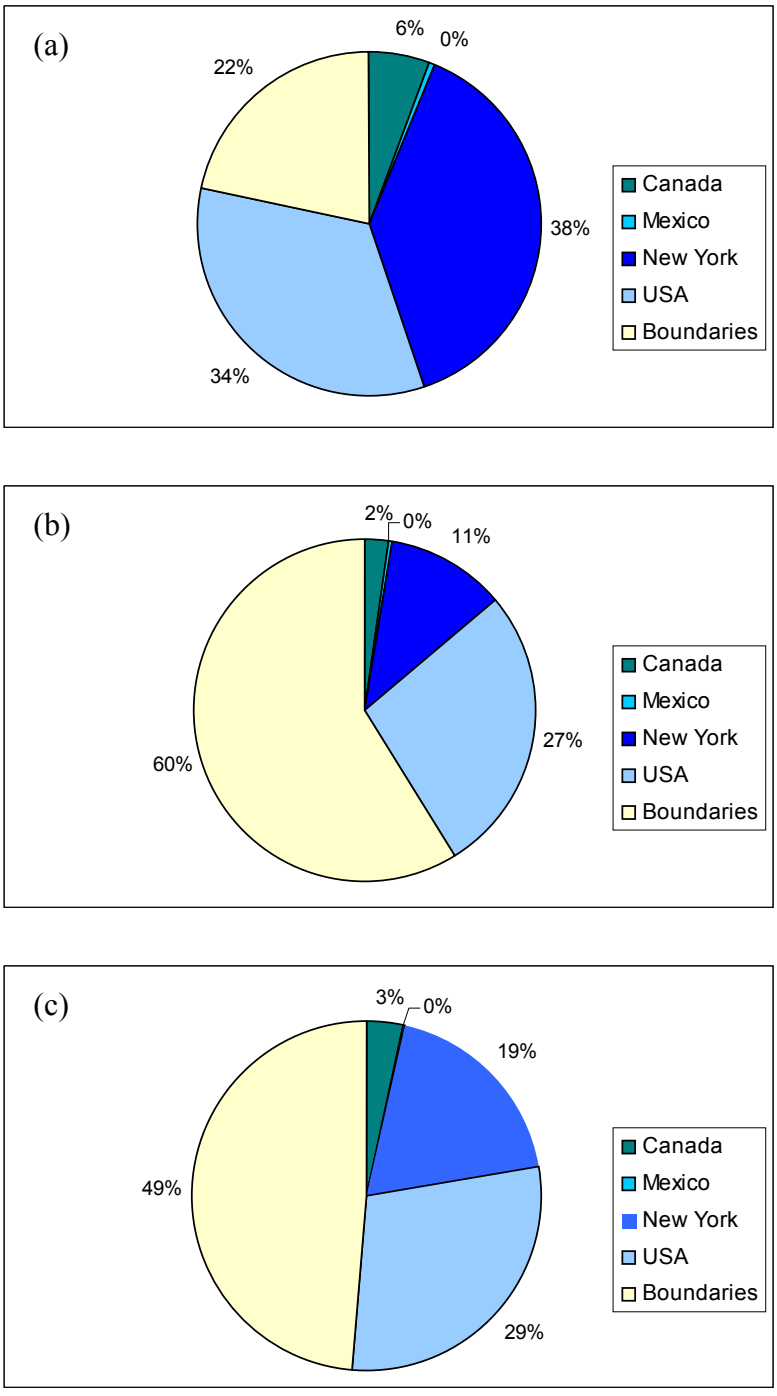

Figure 3-12. Long-range transport scenario: Regional contributions to Hg deposition at the Finger Lakes receptor, (a) dry deposition, (b) wet deposition, and (c) total deposition.

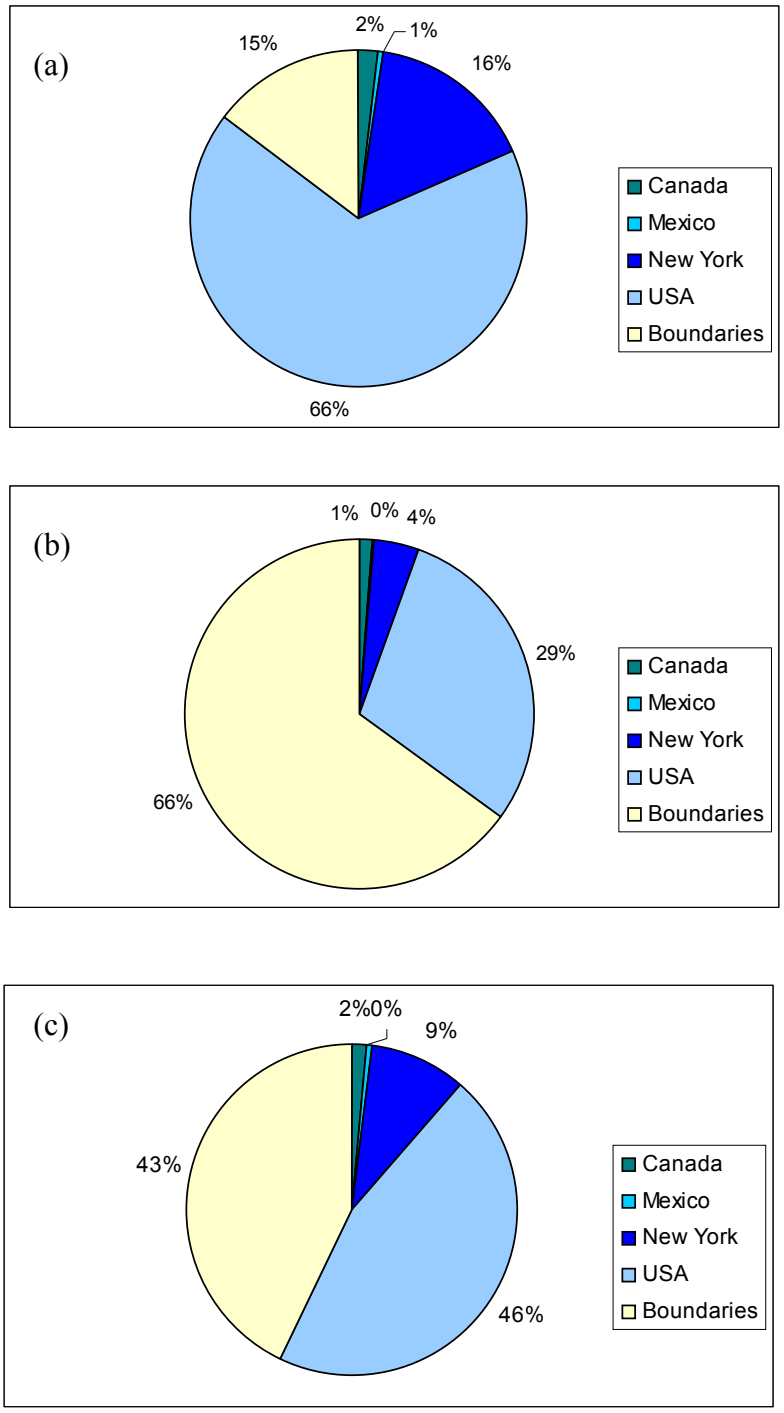

Figure 3-13. Long-range transport scenario: Regional contributions to Hg deposition at the Catskills receptor, (a) dry deposition, (b) wet deposition, (c) total deposition.

3.4 Global and Continental Source Contributions

As discussed in Section 3-3, the global and background source contributions to Hg deposition in New York are significant, ranging from 35% at the Catskills receptor for the local deposition scenario to 61% at the Adirondacks receptor for the long-range transport scenario. It is, therefore, of interest to attribute this component of the continental simulation to the anthropogenic emissions of the other continents and the natural emissions. To that end, we combine the results of the source attributions conducted with the continental and global models. If one compares the source attribution results of the continental and global model simulations, it appears that North American anthropogenic sources have a greater contribution in the continental simulation than in the global simulation. This result is due to the fact that the global model uses a coarse spatial resolution (on the order of 1000 km) that (1) leads to a receptor grid cell that includes part of Quebec, for example, in addition to New York and (2) is conducive to greater dilution (and, therefore, smaller influence) of local emissions. Therefore, to combine the results of the global and continental simulations, we used the contributions of North American sources obtained with the continental simulation and attributed the global/background component of the continental simulation to global and background sources (except North American sources) according to the global simulation results. For example, the boundary conditions (i.e., global and background sources) contributed 57% of total Hg deposition at the Adirondacks receptor for the nominal scenario (see Figure 3-5). This fraction was then attributed to the continents other than North America (i.e., South America, Europe, Africa Asia and Oceania) and background sources according to the results of the global simulation. For example, Asia contributed 25% to Hg deposition in the New York grid cell while all sources besides North America contributed 74% (see Figure 2-2). Thus, Asia, was calculated to contribute to 34% of the boundary conditions in the continental simulation (25% / 74%) and, therefore, to contribute 19% to Hg deposition at the Adirondacks receptor (34% x 57%). The reapportionment of the Hg re-emissions to the various anthropogenic source areas was conducted in the same manner as described in Section 2.

We present below the results of this combined continental/global source attribution for the nominal, local deposition and long-range transport scenarios. Note that U.S. emissions refer to emissions from the 47 contiguous states (i.e., with the exception of New York).

3.4.1 Nominal case

The deposition contributions for the three receptors are shown in Figures 3-14 through 3-16. At all of the receptors, U.S. emissions are the largest sources of total deposition of Hg. New York, natural, and Asian emissions, in varying orders, are the next largest sources. U.S. emissions have the greatest impact (49% of total deposition) at the Catskills receptor, due to its proximity to sources just across the state border. The contribution of natural and Asian emissions is greatest at the Adirondacks receptor (24 and 19%, respectively) because this receptor is the most influenced by sources outside of North America. Emissions from within New York have their greatest impact (21%) at the Finger Lakes receptor.

Dry deposition at the Finger Lakes receptor is dominated by emissions from within New York (42%). U.S. emission sources are responsible for most of the rest of dry deposition at the receptor (33%). At the Catskills receptor, U.S. emissions have by far the largest impact of any source category (67%) and New York emissions contribute most of the rest (18%). Finally, at the Adirondacks receptor the sources are more evenly split with the U.S. contributing 30% of dry deposition, New York contributing 21%, natural emissions contributing 17%, Canadian emissions contributing 11%, and Asian emissions contributing 11%.

Wet deposition at all the receptors has a much larger contribution from sources outside of North America. At the Adirondacks receptor, natural emissions are the largest source of wet deposition (27%), followed by nearly equal contributions from Asia (23%) and the U.S. (24%), respectively. At the Catskills and Finger Lakes receptors, U.S. sources contribute the largest fraction of wet deposition of Hg (33 and 29%, respectively). Natural and Asian emissions are the next largest sources (between 19 and 24%).

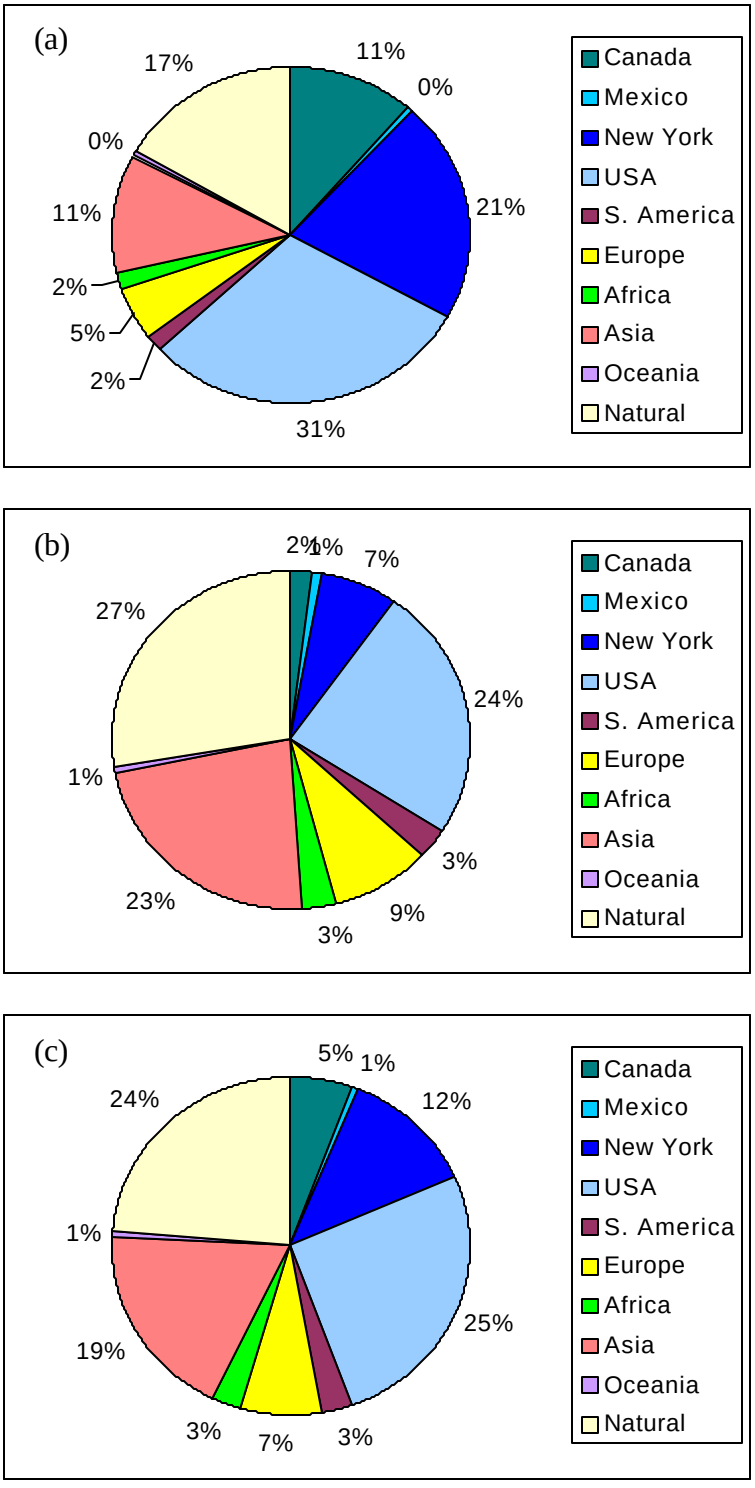

Figure 3-14. Nominal scenario: Regional and global contributions to Hg deposition at the Adirondacks receptor, (a) dry deposition, (b) wet deposition, and (c) total deposition.

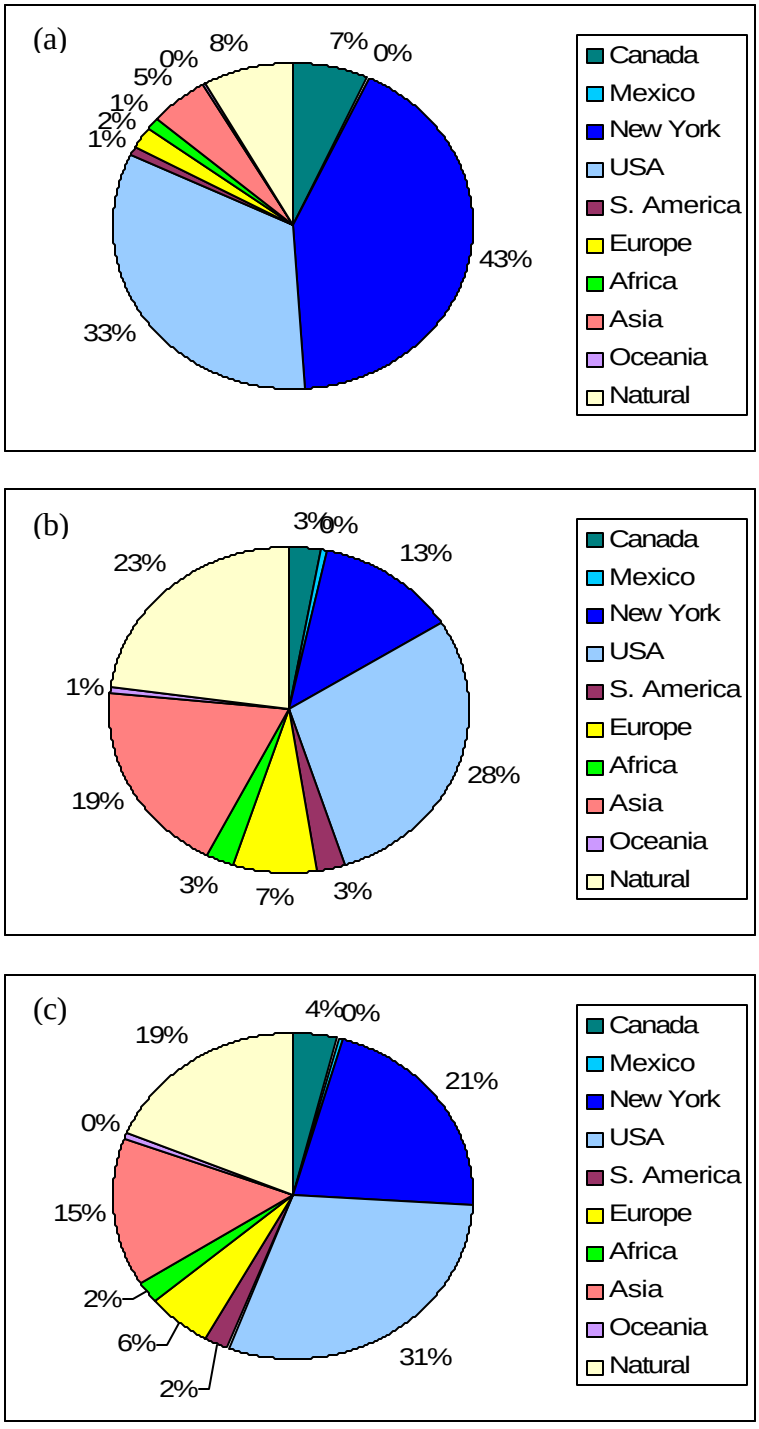

Figure 3-15. Nominal scenario: Regional and global contributions to Hg deposition at the Finger Lakes receptor, (a) dry deposition, (b) wet deposition, and (c) total deposition.

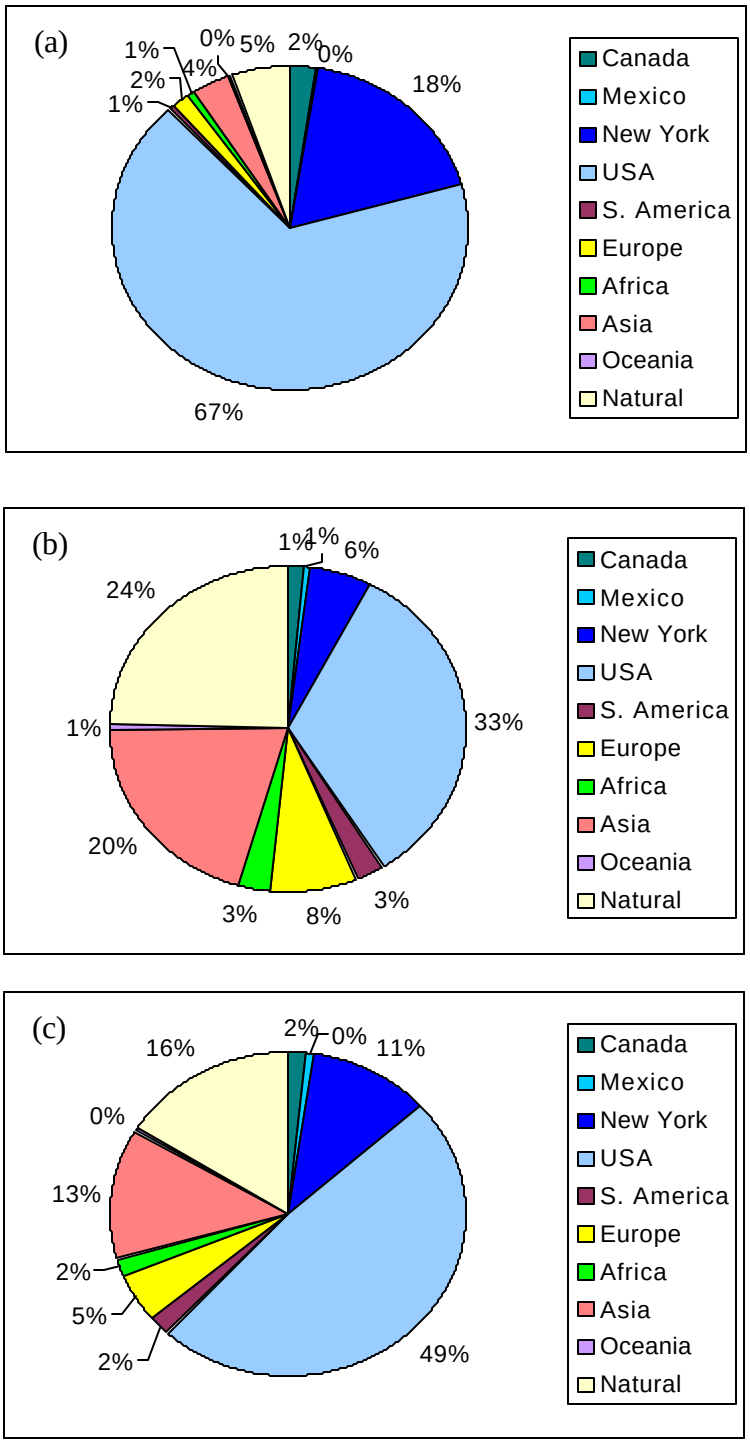

Figure 3-16. Nominal scenario: Regional and global contributions to Hg deposition at the Catskills receptor, (a) dry deposition, (b) wet deposition, and (c) total deposition.

3.4.2 Local deposition scenario

The general trend for total deposition at the three New York receptors from the nominal scenario to the local deposition scenario was an increase in contributions from the U.S. and New York sources and a decrease in contributions from European, African, Asian, and natural sources. The results of the combined continental and global scale modeling for the increased local deposition scenario are shown in Figures 3-17 through 3-19. The impact due to Canadian sources increased slightly for the Finger Lakes scenario but remained the same for the Catskills and Adirondacks receptors. Once again U.S. sources contribute the most to total deposition (from 28% at the Adirondacks receptor to 50% at the Catskills receptor) while New York, Asian, and natural emissions make up most of the rest (from 39% at the Catskills receptor to 55% at the Finger Lakes receptor).

For dry deposition, the impact due to New York and U.S. sources increased while the impact due to natural sources decreased. At the Catskills and Adirondacks receptors, the impacts of Asian and European emissions on dry deposition decreased.

When local deposition was increased, the impact of New York, U.S., and Canadian emissions to wet deposition at the receptors generally increased, while all of the other emission sources decreased.

3.4.3 Long-range transport scenario

As in the other two scenarios, U.S. emissions are the largest source of total deposition at the New York receptors for the increased long-range transport scenario (from 25% at the Adirondacks receptor to 47% at the Catskills receptor), followed by natural (17 to 24%), Asian (14 to 20%), and New York (9 to 19%) emissions. The results for the combined continental and global scale modeling for the increased long-range transport scenario are shown in Figures 3-20 through 3-22. Generally, Canadian and New York emissions contributions to total deposition decreased. The impact due to emission sources outside North America increased. The impact of U.S. emissions on total deposition at the Finger Lakes receptor increased, but remained unchanged at the

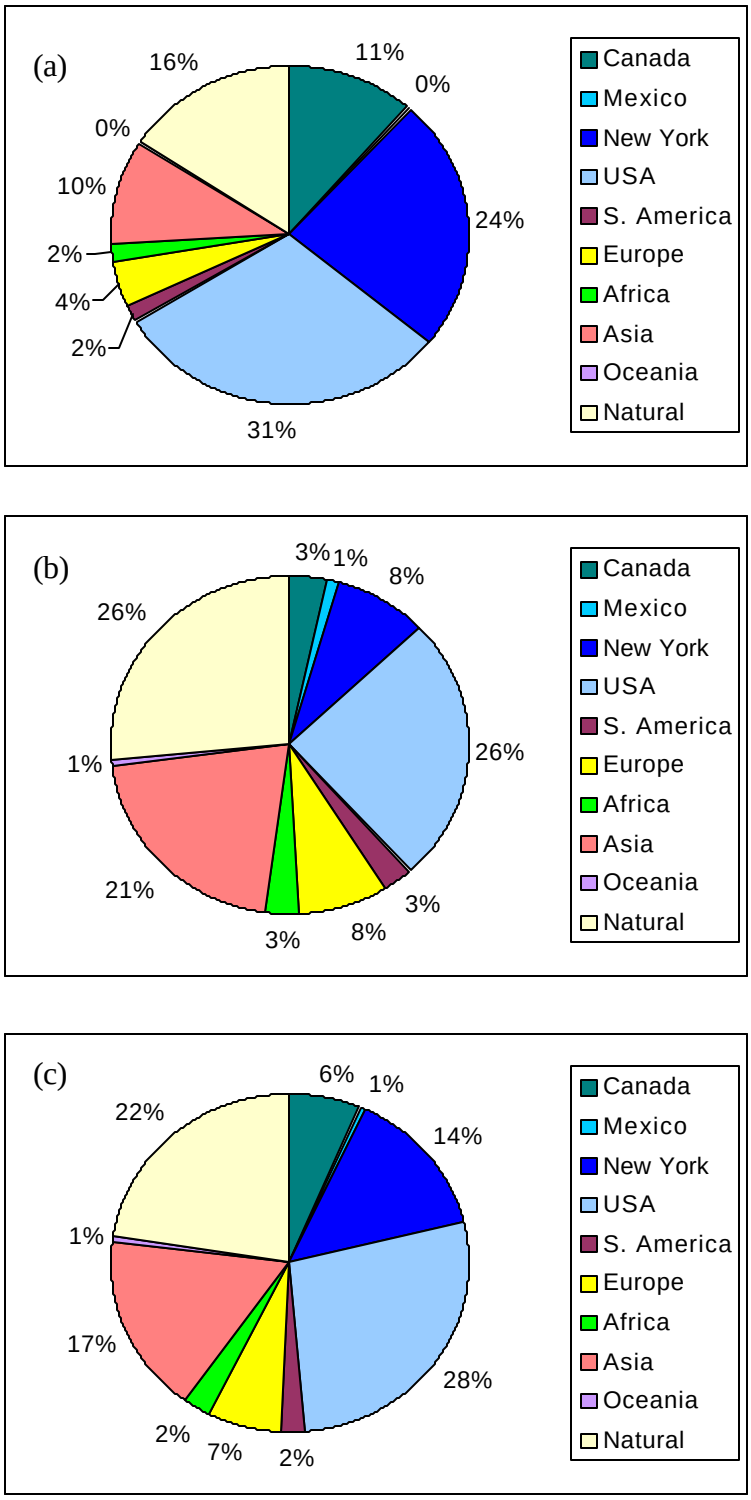

Figure 3-17. Local deposition scenario: Regional and global contributions to Hg deposition at the Adirondacks receptor, (a) dry deposition, (b) wet deposition, and (c) total deposition.

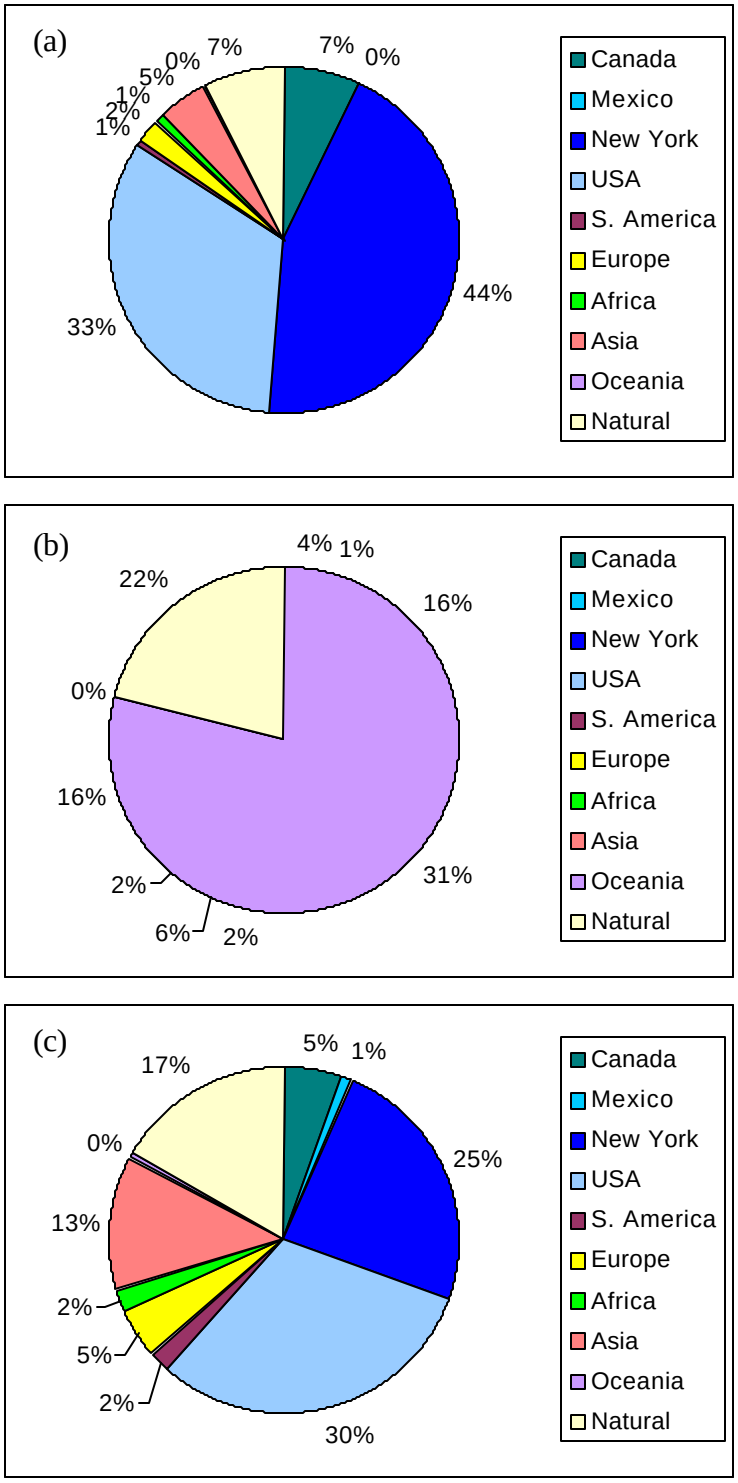

Figure 3-18. Local deposition scenario: Regional and global contributions to Hg deposition at the Finger Lakes receptor, (a) dry deposition, (b) wet deposition, and (c) total deposition.

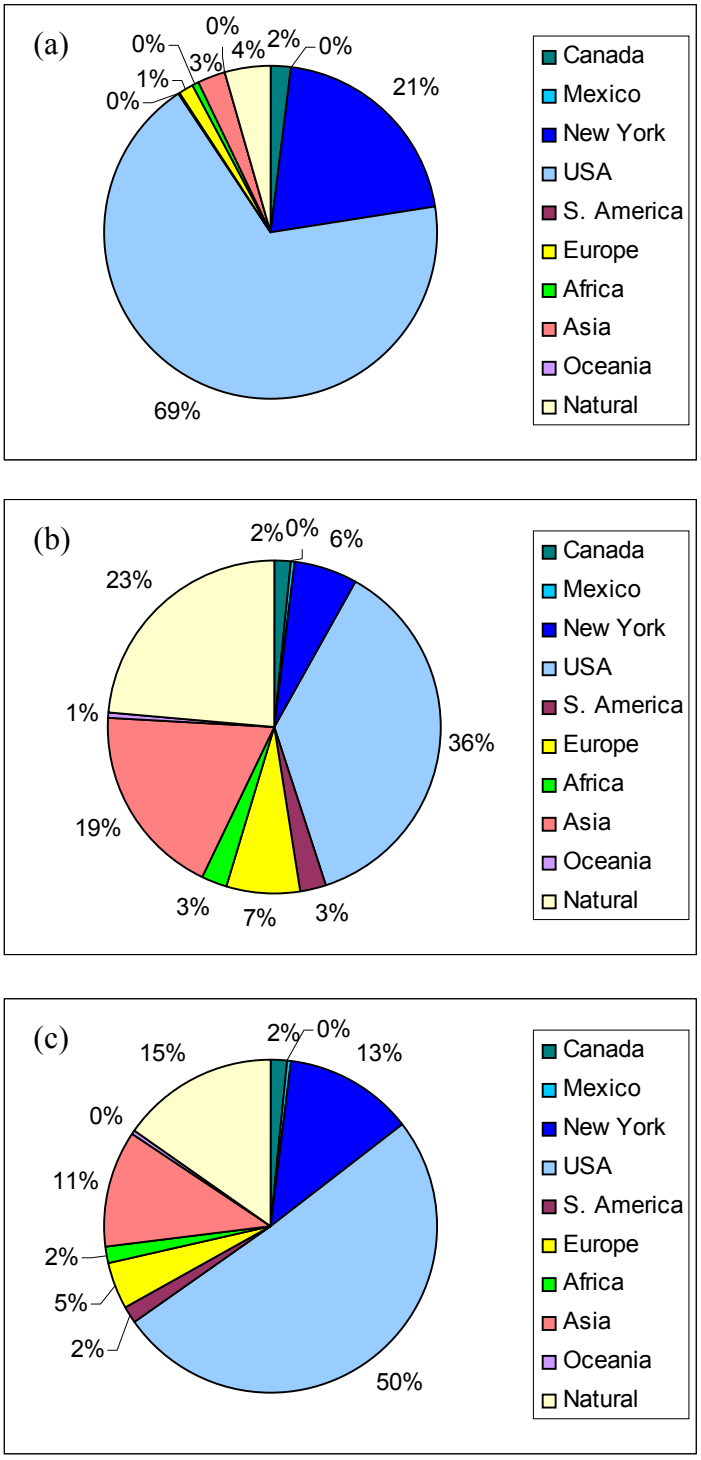

Figure 3-19. Local deposition scenario: Regional and global contributions to Hg deposition at the Catskills receptor, (a) dry deposition, (b) wet deposition, and (c) total deposition.

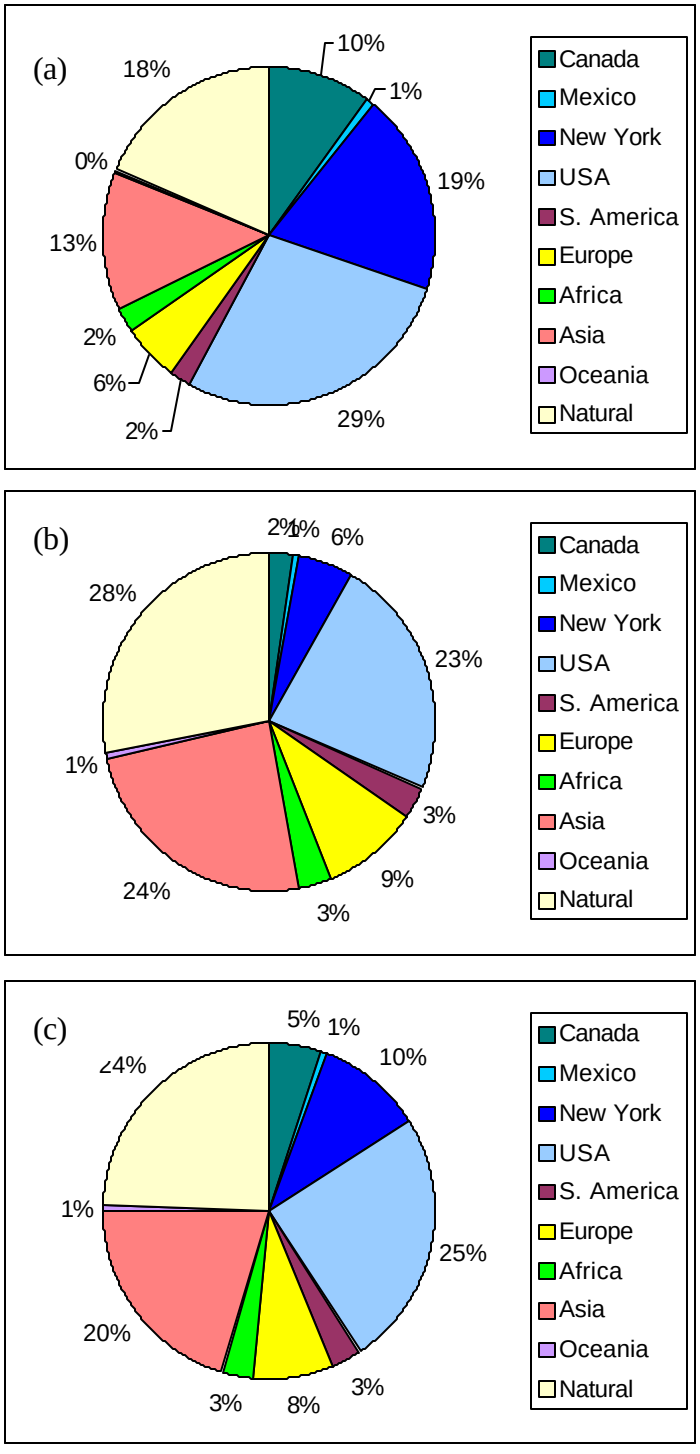

Figure 3-20. Long-range transport scenario: Regional and global contributions to Hg deposition at the Adirondacks receptor, (a) dry deposition, (b) wet deposition, and (c) total deposition.

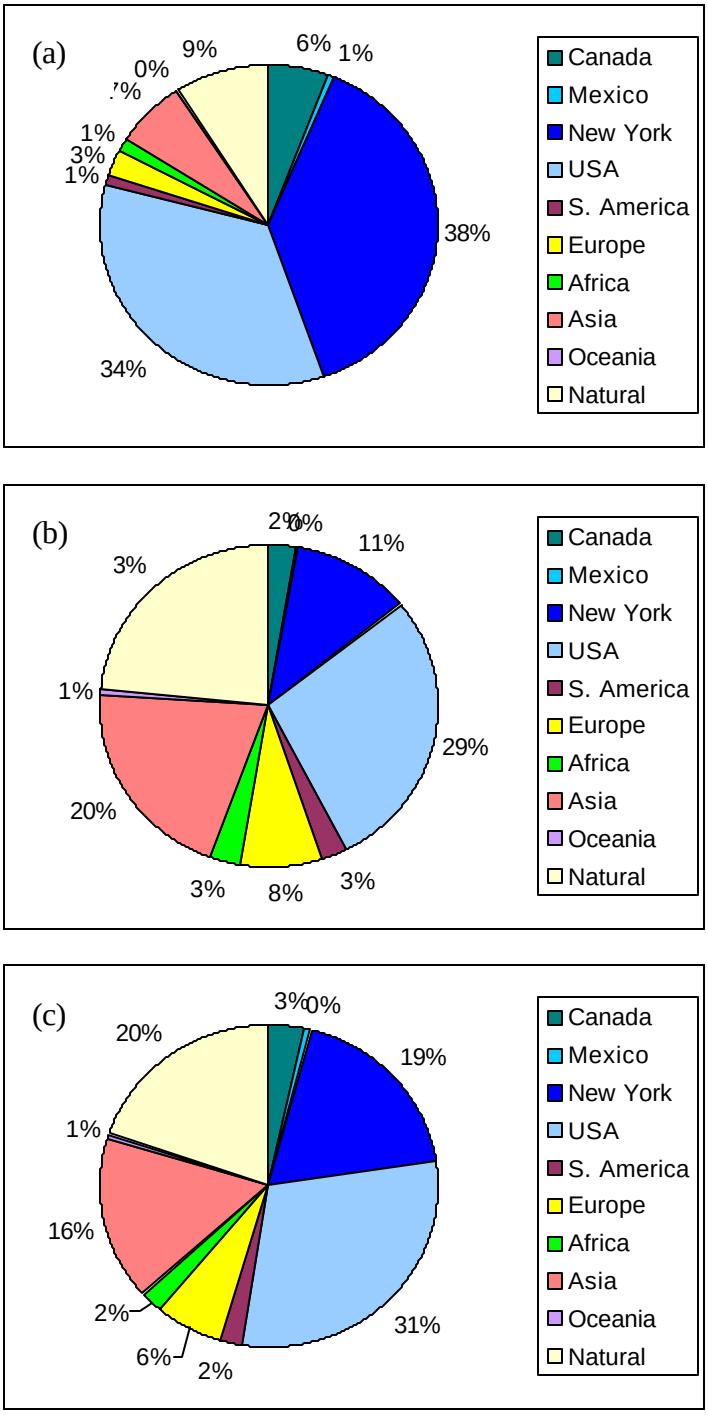

Figure 3-21. Long-range transport scenario: Regional and global contributions to Hg deposition at the Finger Lakes receptor, (a) dry deposition, (b) wet deposition, (c) total deposition.

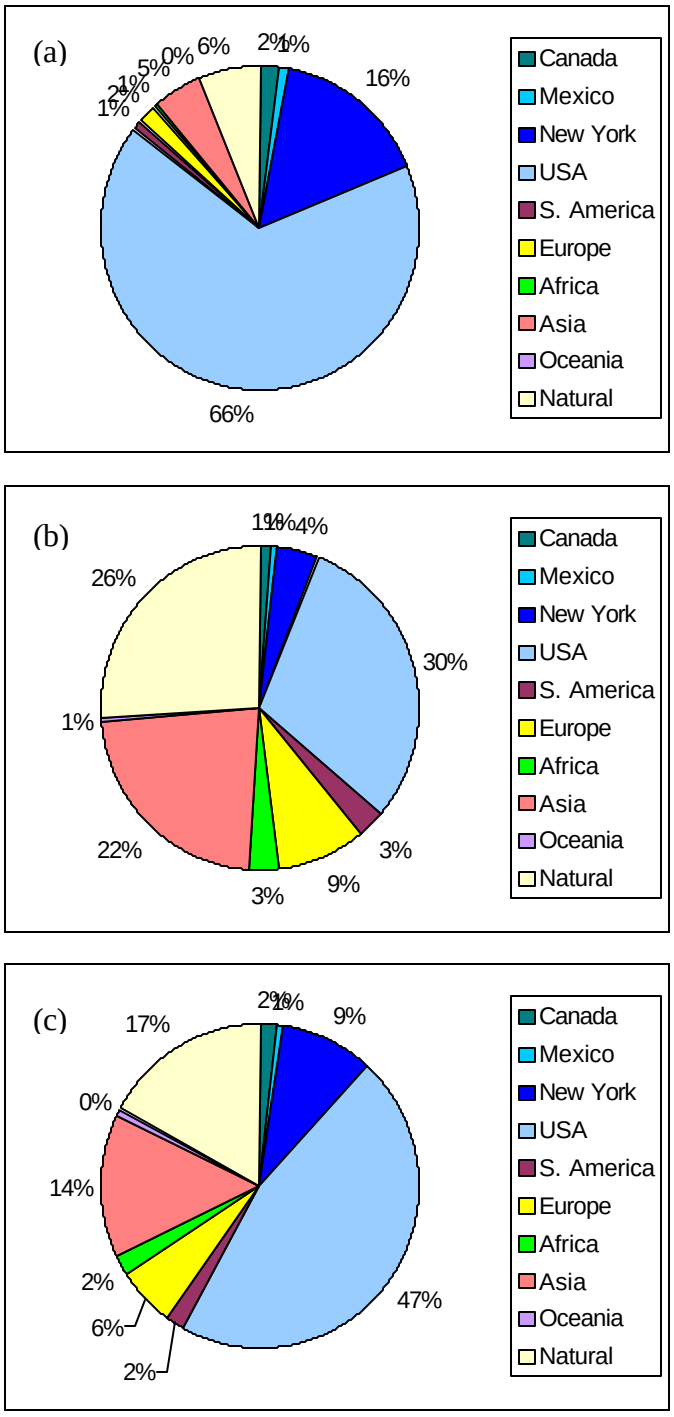

Figure 3-22. Long-range transport scenario: Regional and global contributions to Hg deposition at the Catskills receptor, (a) dry deposition, (b) wet deposition, and (c) total deposition.

Catskills and Adirondacks receptors.

The dry component of the deposition is still dominated by emissions from New York and U.S. sources. However, the impact due to New York sources is less in the long-range transport scenario. The impact of U.S. sources increased at the Finger Lakes receptors but decreased at the Catskills and Adirondacks receptors.

The wet deposition component is still more affected by sources outside North America in the long-range transport scenario. The four largest contributors to wet deposition in New York are U.S. (23 to 30%), natural (23 to 28%), Asian (20 to 24%) and European (8 to 9%) emissions. Changes from the nominal scenario included decreased contributions from U.S., Canada and New York emissions and increased or unchanged contributions from the other source categories.

4. UNCERTAINTIES IN THE FATE AND TRANSPORT MODELING OF MERCURY

There are uncertainties associated with the modeling of the fate and transport of Hg and such uncertainties must be qualified when applying fate and transport models. First, we investigate the sensitivity of the outputs of the atmospheric continental CTM to major input variables. Second, we summarize the results of previous sensitivity analyses of a watershed model, the Regional Mercury Cycling Model (R-MCM). Next, we provide an overview of the existing data bases and discuss the critical data gaps pertinent to the fate and transport of Hg.

4.1 Sensitivity Analysis of the Continental CTM

We conducted a sensitivity analysis of the atmospheric Hg deposition fluxes at the three New York receptors for several of the TEAM input parameters. Nine input variables were modified one at a time, to determine their impact on Hg deposition. The nine parameters included in the study were:

- ambient HO_2 concentrations
- ambient O_3 concentrations
- mercury PM-adsorption coefficient
- Hg(II) dry deposition velocity
- Hg(II) scavenging rate
- Hg(p) dry deposition velocity
- Hg(p) scavenging rate
- boundary conditions
- emission speciation

The sensitivity simulations are listed in Table 4-1.

The first two variables, HO_2 and O_3 concentrations, pertain to the reduction of Hg(II) and the oxidation of Hg(0), respectively. The third variable, adsorption

Table 4-1. Sensitivity scenarios for atmospheric modeling.

Case	Parameter	Variation[(a)]
S1	HO_2 concentrations	x 1.05
S2	O_3 concentrations	x 0.95
S3	Hg PM-adsorption factor	x 0.80
S4	Hg(II) dry deposition velocity	x 0.80
S5	Hg(II) scavenging rate	x 0.80
S6	Hg(p) dry deposition velocity	x 0.80
S7	Hg(p) scavenging rate	x 0.80
S8	Boundary conditions	from long-range scenario
S9	Hg(II) emission speciation	x .95

(a) For internal consistency, the same perturbations were used as for the local deposition and long-range transport scenarios. However, the input variables were changed here one at a time.

coefficient of Hg(II) on PM indirectly affects the reduction of Hg(II). The next four variables affect the removal rate of Hg(II) and Hg(p) by dry deposition and wet scavenging. The last two variables govern the inputs of Hg into the modeling domain, either via inflow into the domain or via emissions within the domain.

In order to quantify the sensitivity of Hg deposition to each input variable, a sensitivity coefficient was calculated for each input variable at each receptor. The sensitivity coefficients, SC, are calculated as follows:

$$SC = \frac{\Delta Y / Y_0}{\Delta X / X_0} \tag{4-1}$$

where Y is the output variable and X is the input variable, Δ is the change in the variable from the base case to the sensitivity case, and Y_0 and X_0 represent the nominal base case output and input variable values, respectively.

The sensitivity coefficients for the wet deposition fluxes of Hg are presented in Figure 4-1. The wet deposition sensitivity for each variable tended to be very similar among the three receptors. Wet deposition is most sensitive to the boundary conditions at the three New York State receptors. This result is consistent with the source contribution presented in Section 3.3 where the boundary conditions were calculated to contribute significantly to Hg in New York State. The wet deposition of Hg is also quite sensitive to the ambient concentration of O_3 (O_3 leads to oxidation of Hg(0) to Hg(II)). This result corresponds to the oxidation of Hg(0) that is advected through the upwind boundaries as well as the oxidation of anthropogenic Hg(0) emitted within the North American domain. Although this oxidation process is slow (Hg(0) half-life of a few months), Hg(0) concentrations are about two orders of magnitude greater than Hg(II) concentrations and, therefore, a change of 1% in the Hg(0) concentrations (which is on the order of the Hg(0) oxidized amount over North America) is commensurate with the Hg(II) concentrations. The wet deposition of Hg is less sensitive to HO_2 concentrations. Since HO_2 radicals affect the reduction of Hg(II), this result suggests that Hg wet deposition may be more sensitive to the long-range transport of oxidized Hg (see sensitivity to O_3 concentrations above) than to local Hg(II) emissions. This is consistent with the results of the source

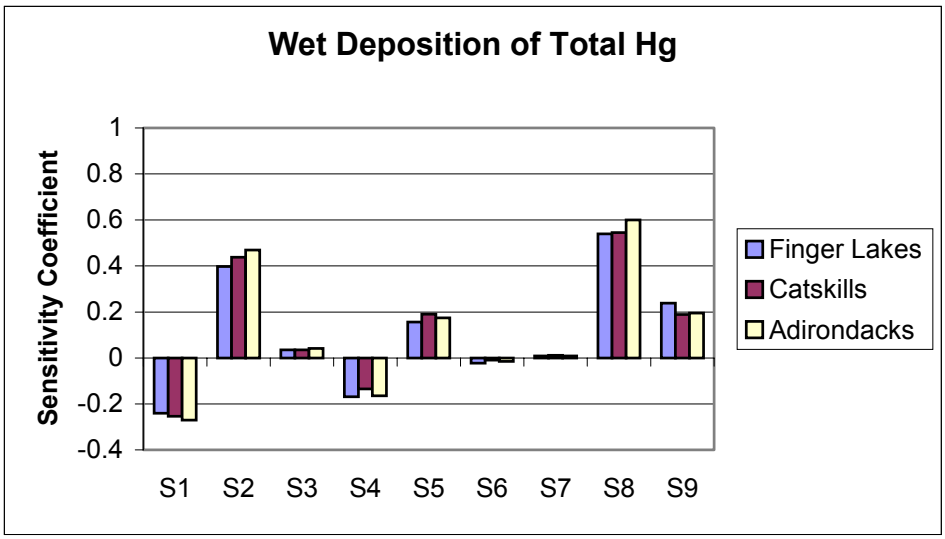

Figure 4-1. Sensitivity coefficients for the wet deposition fluxes of total Hg.

contributions presented in Section 3.3. Wet deposition of Hg(II) is slightly more sensitive to the Hg(II) scavenging rate than to the Hg(II) dry deposition velocity (less dry deposition leaves more Hg(II) available for wet deposition). On the other hand, the wet deposition of Hg(p) is more sensitive to the Hg(p) dry deposition velocity (a decrease in the dry deposition of Hg(p) leaves more Hg(p) available for deposition through wet processes) than to the Hg(p) scavenging rate. In summary, Hg wet deposition in New York State appears to be more sensitive to the boundary conditions and the atmospheric chemical reactants (O_3 and HO_2) than to the local emissions. These results suggest that New York State tends to behave more like a receptor area than a source area (Pai et al., 1999).

The sensitivity coefficients for the dry deposition fluxes of Hg are shown in Figure 4-2. The sensitivity of dry deposition to some variables differed significantly among receptors. Dry deposition of total Hg at all three receptors is most sensitive to the Hg emission speciation. The next most influential variable at the Finger Lakes receptor is the dry deposition velocity of Hg(II). The Catskills and Adirondacks receptors, on the other hand, are not particularly sensitive to the Hg(II) dry deposition velocity. The second most influential variable at the Adirondacks receptor is the boundary condition. The Catskills receptor is the most sensitive to emission speciation of the three receptors, but is not very sensitive to the other variables. The second most influential variable for dry deposition of Hg at the Catskills receptor is the scavenging rate of Hg(II) (less removal of Hg(II) by wet deposition leaves more Hg(II) available for dry deposition).

4.2 Sensitivity Analysis of a Watershed Model

Once Hg has been deposited to a watershed, it will bioaccumulate in the food chain in the form of methyl Hg (MeHg). This bioaccumulation may present some potential health risk to populations who consume large amounts of fish from the impacted watershed.

As described in Sections 2 and 3, Hg deposition to a watershed can be calculated with atmospheric fate and transport models. A watershed fate and transport model can be used to calculate the Hg concentrations in various fish species in a lake located within the

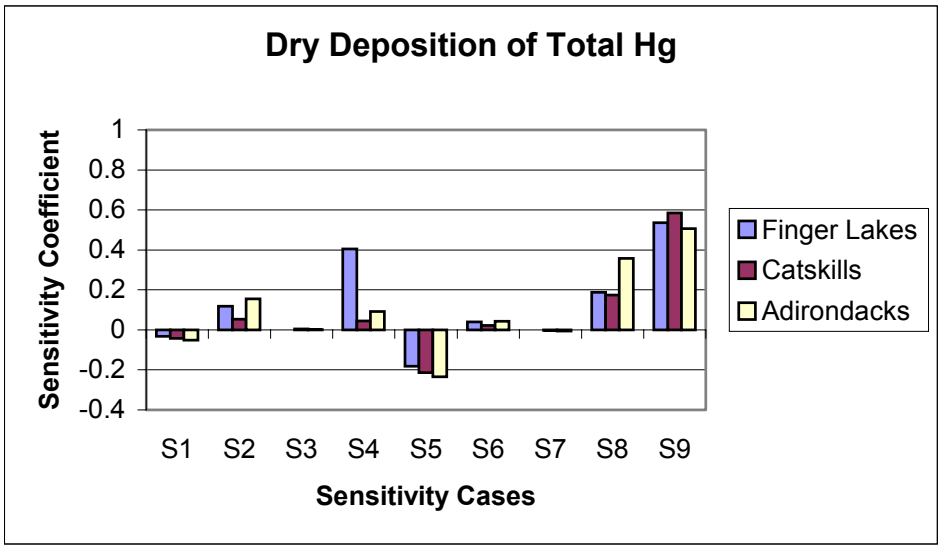

Figure 4-2. Sensitivity coefficients for the dry deposition fluxes of total Hg.

watershed. For example, the Regional Mercury Cycling Model (R-MCM) simulates the transport of Hg from the watershed to the lake, chemical transformations of Hg in the lake water column and sediment layer, bioaccumulation of Hg in the food chain using five trophic levels, and mass transfer of Hg between the lake water column and the atmosphere (Harris et al., 1996). Three Hg species are simulated: Hg(0), inorganic Hg(II), and MeHg.

R-MCM is a steady-state model that uses the annual deposition fluxes calculated by the atmospheric model as input. Although some seasonal variations (e.g., temperature) are taken into account in the model, the calculated Hg concentrations are steady-state values. A sensitivity analysis of R-MCM was conducted by Lohman et al. (2000b). The lake parameters that were included in the sensitivity analysis are: pH, temperature, chloride (Cl^-) concentration, dissolved organic carbon (DOC) concentration, settling velocity of lake particles, and burial rate of sediments (i.e., the rate at which sediments are buried into the benthic layer and removed from contact with the water column).

Three lakes were simulated and used for sensitivity analysis. These three lakes have very different characteristics: one is an acidic oligotrophic lake; another is an alkaline hyper-eutrophic lake and one has characteristics that are generally "average" (Lohman et al., 2000a, 2000b). In all three cases, lake pH and burial rate of sediments were the dominant parameters. In some cases, lake temperature increased in importance. In the case of a lake with a large dissolved organic carbon (DOC) concentration, the DOC parameter becomes influential. Although some variations are expected among lakes, the three most influential parameters identified here (i.e., pH, sediment burial rate, and DOC concentration) can be considered the most influential parameters for a simulation of Hg cycling in a lake.

4.3 Available Data Bases

4.3.1 Databases for atmospheric modeling

Databases needed for atmospheric modeling include emissions of Hg species, concentrations of species reacting with Hg, meteorology, and ambient concentrations and deposition fluxes of Hg for model performance evaluation.

Emissions

Emission databases are available from government agencies such as the U.S. Environmental Protection Agency (EPA) and Environment Canada (e.g., Bullock, 2000). Note that some restrictions may be placed on Canadian emission data for large point sources because of confidentiality issues. An emission database is available from EPRI (e.g., Seigneur et al., 2001a). Coal-fired power plants constitute the best characterized source category, although some uncertainties remain, particularly regarding emission speciation (i.e., the relative fractions of Hg(0), Hg(II) and Hg(p)). Other anthropogenic source categories are typically poorly characterized (e.g., emission speciation is represented by measurements at a single facility) and the resulting uncertainties in Hg emissions directly affect the results of the fate and transport model simulations.

Background sources of Hg are also poorly known. Their speciation is believed to be primarily Hg(0), therefore, uncertainties in these background emissions (both natural emissions and re-emission of previously deposited anthropogenic Hg) are less likely to affect local and regional Hg deposition patterns and will primarily affect the global cycling of Hg.

Meteorology

Atmospheric fate and transport models typically require meteorological fields that are internally consistent and are generally obtained from prognostic meteorological models. For example, the TEAM simulations reported here used wind and temperature fields from the Nested Grid Model (NGM). Simulations conducted under EPA-sponsorship with REMSAD used wind, temperature, cloud and precipitation fields from

either the Rapid Update Cycle model (RUC) or the Mesoscale Meteorological model version 5 (MM5). We selected not to use simulated precipitation fields in the TEAM simulations reported here because of large uncertainties associated with those fields. Instead, we used actual precipitation data (see Section 3.2.1). This allowed better comparison between measured and simulated Hg wet deposition fluxes since the precipitation amount was then identical in the measurement and the simulation. Thus, the model evaluation focused solely on Hg concentrations in precipitation.

The treatment of clouds and precipitation is critical for Hg modeling because of the importance of chemical transformations within cloud droplets for the removal of Hg from the atmosphere. In particular, the simulation of deep convective clouds is difficult and will lead to uncertainties in simulated wet deposition. We anticipate that such uncertainties will be larger for regions such as Florida where precipitation is dominated by subtropical convective storms than for other regions such as New York State.

Concentrations of atmospheric species

There are three main possibilities for preparing the 3-D concentration fields of the atmospheric species that react with Hg.

- Simulate these concentrations together with the Hg concentrations. This approach is used for most species in REMSAD and Models-3/CMAQ.
- Use the results of an earlier model simulation since Hg concentrations are sufficiently low that they do not affect concentrations of other species. This approach is used for most species in the global Hg CTM and TEAM simulations presented here.
- Use ambient data. The major limitation of this approach is that ambient data are typically available at the surface but not aloft. Nevertheless, this approach is used for atmospheric species that are not simulated or are simulated with insufficient spatial resolution.

Ambient concentrations of Hg

Ambient concentrations of Hg are useful to evaluate model performance. In New York State, a few databases are available (Olmez et al., 1994; Hopke et al., 2001). Speciated Hg data, however, are rare but are needed to test the model for Hg speciation. We recommend that such measurements be made, for example, in the three receptor regions considered here (i.e., Adirondacks, Finger Lakes and Catskills areas).

Deposition fluxes of Hg

Wet deposition of Hg is measured routinely in the Mercury Deposition Network. One station, at the Huntington Wildlife Refuge, started to operate recently.

Dry deposition fluxes can be measured, for example, using gradient measurement techniques (e.g., Lindberg and Stratton, 1998). Through-fall measurements could also be used to corroborate model simulation results.

Additional Hg deposition measurements are needed. For example, Hg wet deposition measurements could be conducted in the Finger Lakes region and in the Catskills mountains in addition to those currently made in the Adirondacks. We also recommend that dry deposition measurements be made in these three receptor areas.

4.3.2 Databases for limnological information

In order to run the Regional Mercury Cycling Model (R-MCM), data about the physical, chemical, sediment, and biological characteristics of the lake(s) to be studied must be gathered. Some of these data are available in large national, state, or regional databases while others must be gathered from other sources. For the data not available from databases, the next alternative is to perform a literature search for the particular lake. If some characteristics are still not found, then they must be estimated based on what is known about the lakes or about other lakes in the area.

The parameters that must be gathered include:

Physical parameters: mean depth, surface area, inflow rate, outflow rate, mean annual precipitation, residence time, thermocline area, watershed area, the amount of the

watershed covered by wetlands and lakes, seston concentration and composition, groundwater velocity, and the peak temperatures in the epilimnion and hypolimnion.

Chemical parameters: pH, dissolved organic carbon (DOC), chloride, calcium, sulfate, particulate organic carbon (POC), chlorophyll a, and the peak hypolimnetic sulfide concentration.

Sediment parameters: particulate settling velocity, sediment deposition, sediment burial velocity, sediment porosity, and sediment mineralization rate.

Biological parameters: amount of fishing relative to the fish population, phytoplankton growth rate, phytoplankton cell volume, and size, life cycle, and dietary information on prey and predatory fish species.

Available Databases

Four limnological databases for New York lakes are available. The databases are (1) the Adirondack Lakes Survey, (2) STORET, (3) EMAP, and the (4) National Water Information System. Table 4-2 summarizes some of the data available in these surveys.

The Adirondack Lakes Survey Corporation (ALSC) is a nonprofit corporation supported by NYSERDA, EPA, and NYSDEC. The ALSC has two databases. The first is called the Adirondack Lakes Survey (1984-1987) which consists of one-time samples of 1469 lakes. The second is the Long-Term Monitoring Study (1992-2000) which tested 52 lakes once each year. As the name suggests, the ALSC databases only contain information for lakes in the Adirondacks region.

STORET is operated by EPA. It contains information on lakes from all over the United States. It contains biological, chemical, and physical data from the beginning of the 20th century to present day. Because the STORET data come from many different state, federal, local, tribal, and academic sources, there is a lot of variability in the consistency of reported data.

EMAP is the Environmental Monitoring and Assessment Program. One portion of the EMAP program was a survey of lakes by EPA in the northeastern United States from 1991 to1994. There was also an earlier EPA lake survey called the National Surface Water Study – Eastern Lake Study. It was conducted from 1984 to 1986 and collected the same types of data as the EMAP survey.

Table 4-2. Summary of data available in limnological databases for New York State.

	Adirondack Lakes Surveys	STORET	EMAP	USGS
Latitude & longitude	✓	✓	✓	✓
Outflow rate		✓		
Annual precipitation		✓	✓	
Residence time	✓	✓	✓	
Mean depth	✓	✓	✓	
Lake surface area	✓	✓	✓	
Watershed area	✓	✓	✓	✓
pH	✓	✓	✓	✓
DOC	✓	✓	✓	
Chloride	✓	✓	✓	✓
Calcium	✓	✓	✓	✓
Sulfate	✓	✓	✓	✓
Chlorophyll a		✓	✓	

Finally, the USGS National Water Information System has water quality information on five New York lakes.

AER also has information from a fish database on species, length, weight, and age of fish caught in U.S. lakes. There are 44 New York lakes and reservoirs in the database.

Other Sources

For those parameters for which a value is not available in a database, there are several other options. One option is to contact a state or local agency. For example, the state fish and wildlife bureau may have information on the biological parameters required. Also the state natural resources or department of environmental conservation may have had a study performed on a particular lake of interest which would provide most of the physical and chemical parameters. Additionally, parameters not available in a database may be found by performing a literature search. This will locate information published on a particular lake or region.

Estimates and Calculations

Some parameters may not be available and will have to be calculated or estimated based on the information that is known about the lake. For example, the inflow rate and the groundwater velocity can be calculated based on the hydrologic budget, residence time, and lake dimensions. The percentage of the watershed covered by lakes and wetlands can be determined using land cover maps. Seston concentrations and components may need to be estimated from suspended solids measurements or organic carbon measurements along with information on the lake trophic status (Seston is a collective term for suspended mineral matter, living and dead animals and other organic debris).

4.4 Summary of Data Gaps

4.4.1 Input data

The sensitivity analyses conducted with the continental CTM, TEAM, and with the regional watershed model, R-MCM have pointed out which input variables are the most influential for the fate and transport modeling of Hg. For atmospheric modeling, the boundary conditions, the O_3 concentrations, the speciation of the Hg emissions and the dry deposition velocity of Hg(II) were the most influential variables. For lake modeling, the lake pH, the rate of burial of sediments and the DOC concentrations were the most influential variables. Among those variables, the atmospheric O_3 concentrations, the lake pH and the DOC concentrations are generally available with reasonable accuracy. However, data gaps are associated with the other input variables.

The boundary concentrations of atmospheric Hg are generally poorly characterized because there is a paucity of speciated ambient measurements of Hg, both at the surface and aloft. Therefore, the most reliable approach at this time is to use a global model to provide boundary conditions for continental models.

The speciation of the emissions is a key input variable because it affects whether Hg will be deposited locally as Hg(II) or enter the global background as Hg(0). Two comprehensive programs that have provided Hg emission speciation data are the EPRI-sponsored PISCES program and the Information Collection Request (ICR) mandated by EPA. Thus, a reasonable database exists for coal-fired power plants. However, there is a paucity of data for other source categories.

The dry deposition velocity of Hg(II) is typically assumed to be similar to that of HNO_3, because the two chemical species have similar solubilities. There is a dire need for a better assessment of the dry deposition velocity of Hg(II) over a variety of surfaces and under a variety of meteorological conditions.

The rate of sediment burial is typically unknown and a default value is assumed in the lake simulations. Although the outputs of R-MCM simulations have shown good performance (Lohman et al., 2000a, 2000b) using this default value, one must be aware that it will also affect the response of the model to changes in Hg loading (e.g., resulting

from a change in Hg atmospheric emissions). Therefore, this variable needs to be estimated more precisely in future lake studies.

4.4.2 Data for model evaluation

Data needed for the evaluation of an atmospheric CTM include speciated ambient concentrations, wet deposition flux and dry deposition flux of Hg. Of those data, the wet deposition flux is the most readily available (e.g., MDN). There is a lack of Hg ambient data with chemical speciation in existing databases although such measurements are starting to be more common. There is also a need for dry deposition flux data since dry deposition is commensurate with wet deposition and is, therefore, a major contributor to Hg loading to watersheds.

4.4.3 Other issues

There are still some gaps in our understanding of the fate and transport of Hg in the environment. The poor performance of continental CTMs for predicting Hg wet deposition in Pennsylvania suggests that some chemical reactions that reduce Hg(II) to Hg(0) may be missing in existing chemical kinetic mechanisms (Seigneur et al., 2001b). As new laboratory data become available, they should be incorporated into Hg CTMs to assess their effect on model simulation results and model performance.

5. CONCLUSION

A modeling system that includes a global CTM and a nested continental CTM (TEAM) was used to simulate the atmospheric transport, transformations and deposition of Hg. We considered three scenarios:

(1) a nominal scenario
(2) a scenario conducive to local deposition
(3) a scenario conducive to long-range transport

The two latter scenarios were designed to provide plausible Hg concentrations and deposition fluxes when compared to observations. Variations in the model inputs were, therefore, constrained accordingly. Consequently, these scenarios do not constitute a rigorous uncertainty analysis of the CTMs but simply reflect the sensitivity of the CTMs to some changes in model inputs.

5.1 Model Performance

Model performance was evaluated by comparing model outputs to measurements of ambient Hg species concentrations and wet deposition fluxes of Hg. Overall, the model performance suggests that the model captures most of the processes that govern the atmospheric fate and transport of Hg. For example, for the nominal simulation, comparison of model simulation results with data from the Mercury Deposition Network (MDN) by sites gave a coefficient of determination (r^2) of 0.45, an average bias of -7% and an average error of 28%. However, some weaknesses in model performance were also apparent. For example, the model predicts about 70% more Hg wet deposition in Pennsylvania than in Minnesota, whereas MDN data show similar values in both states. This result implies that the model overestimates Hg deposition in the northeast, possibly because of an overestimation of the impact of local/regional emission sources.

Model predictions at three receptor sites in New York State are summarized in Table 5-1 for the nominal simulation (results for the local-deposition and long-range transport simulations differed from those of the nominal simulation by less than 6%).

Total Hg deposition ranges from 13.2 $\mu g/m^2$-yr in the Finger Lakes area, to 19.2 $\mu g/m^2$-yr in the Adirondacks and 22.9 $\mu g/m^2$-yr in the Catskills. Dry deposition ranges from 3.9 $\mu g/m^2$-yr in the Finger Lakes area to 10.2 $\mu g/m^2$-yr in the Catskills. Wet deposition shows less spatial variation; it ranges from 9.3 $\mu g/m^2$-yr in the Finger Lakes area to 12.7 $\mu g/m^2$-yr in the Catskills. In the Finger Lakes area, dry deposition accounts for 30% of total deposition. It accounts for 36% and 45% of total deposition in the Adirondacks and the Catskills, respectively. These values suggest that the Catskills are more impacted by local sources than the Adirondacks or the Finger Lakes area since Hg(II) and Hg(p) contribute to dry deposition more near their emission sources. The local deposition scenario leads to greater Hg deposition at all three sites; the increase in total deposition varies from 0.5% in the Adirondacks to 1% in the Catskills and 5% in the Finger Lakes area. The long-range transport scenario leads to less Hg deposition at all three sites; the decrease in total deposition varies from 2% in the Adirondacks and the Catskills to 6% in the Finger Lakes area.

5.2 Contributions of Global and Regional Sources

The modeling system was then used to conduct a source attribution using the results of the global and continental CTMs. In this analysis, re-emission of anthropogenic Hg previously deposited was reallocated to anthropogenic source regions. The anthropogenic source regions include New York State, the other contiguous United States, Canada, Mexico, South America, Europe, Asia, Africa and Oceania. Natural emissions from the oceans and land were also taken into account.

We present below the results of this combined continental/global source attribution for the nominal, local deposition and long-range transport scenarios. The calculated deposition contributions for the three New York State receptors (Adirondacks, Finger Lakes and Catskills) are shown in Tables 5-2 through 5-4.

Table 5-1. Simulated deposition fluxes of Hg(II) and Hg(p) at three receptors in New York State.

Site and Deposition Process	Deposition Flux ($\mu g/m^2$-yr)
Adirondacks	
Dry deposition	7.0
Wet deposition	12.2
Total deposition	19.2
Finger Lakes	
Dry deposition	3.9
Wet deposition	9.3
Total deposition	13.2
Catskills	
Dry deposition	10.2
Wet deposition	12.7
Total deposition	22.9

Table 5-2. Contributions of regional and global sources to Hg deposition at the Adirondacks receptor (%).

	New York	Other U.S.	Canada	Mexico	South America	Europe	Asia	Africa	Oceania	Natural
Nominal scenario										
Dry deposition	21	31	11	0	2	5	11	2	0	17
Wet deposition	7	24	2	1	3	9	23	3	1	27
Total deposition	12	25	5	1	3	7	19	3	1	24
Local deposition scenario										
Dry deposition	24	31	11	0	2	4	10	2	0	16
Wet deposition	8	26	3	1	3	8	21	3	1	26
Total deposition	14	28	6	1	2	7	17	2	1	22
Long-range transport scenario										
Dry deposition	19	29	10	1	2	6	13	2	0	18
Wet deposition	6	23	2	1	3	9	24	3	1	28
Total deposition	10	25	5	1	3	8	20	3	1	24

Table 5-3. Contributions of regional and global sources to Hg deposition at the Finger Lakes receptor (%).

	New York	Other U.S.	Canada	Mexico	South America	Europe	Asia	Africa	Oceania	Natural
Nominal scenario										
Dry deposition	43	33	7	0	1	2	5	1	0	8
Wet deposition	13	28	3	0	3	7	19	3	1	23
Total deposition	21	31	4	0	2	6	15	2	0	19
Local deposition scenario										
Dry deposition	44	33	7	0	1	2	5	1	0	7
Wet deposition	16	31	4	1	2	6	16	2	0	22
Total deposition	25	30	5	1	2	5	13	2	0	17
Long-range transport scenario										
Dry deposition	38	34	6	1	1	3	7	1	0	9
Wet deposition	11	29	2	0	3	8	20	3	1	23
Total deposition	19	31	3	0	2	6	16	2	1	20

Table 5-4. Contributions of regional and global sources to Hg deposition at the Catskill Mountains receptor (%).

	New York	Other U.S.	Canada	Mexico	South America	Europe	Asia	Africa	Oceania	Natural
Nominal scenario										
Dry deposition	18	67	2	0	1	2	4	1	0	5
Wet deposition	6	33	1	1	3	8	20	3	1	24
Total deposition	11	49	2	0	2	5	13	2	0	16
Local deposition scenario										
Dry deposition	21	69	2	0	0	1	3	0	0	4
Wet deposition	6	36	2	0	3	7	19	3	1	23
Total deposition	13	50	2	0	2	5	11	2	0	15
Long-range transport scenario										
Dry deposition	16	66	2	1	1	2	5	1	0	6
Wet deposition	4	30	1	0	3	9	22	3	1	28
Total deposition	9	47	2	1	2	6	14	2	0	17

5.2.1 Nominal case

At all three receptors, U.S. emissions are the largest source of total deposition of Hg. New York, natural, and Asian emissions, in varying orders, are the next largest sources. U.S. emissions have the greatest impact (49% of total deposition) at the Catskills receptor, due to its proximity to sources just across the state border. The contribution of natural and Asian emissions is greatest at the Adirondacks receptor (24 and 19%, respectively) because this receptor is the most influenced by sources outside of North America. Emissions from within New York have their greatest impact (21%) at the Finger Lakes receptor.

Dry deposition at the Finger Lakes receptor is dominated by emissions from within New York (43%). U.S. emission sources are responsible for most of the rest of dry deposition at the receptor (33%). At the Catskills receptor, U.S. emissions have by far the largest impact of any source category (67%) and New York emissions contribute most of the rest (18%). Finally, at the Adirondacks receptor, the sources are more evenly split with the U.S. contributing 31% of dry deposition, New York contributing 21%, natural emissions contributing 17%, Canadian emissions contributing 11%, and Asian emissions contributing 11%.

Wet deposition at all the receptors has a much larger contribution from sources outside of North America. At the Adirondacks receptor, natural emissions are the largest source of wet deposition (27%), followed by nearly equal contributions from Asia (23%) and the U.S. (24%), respectively. At the Catskills and Finger Lakes receptors, U.S. sources contribute the largest fraction of wet deposition of Hg (33 and 28%, respectively). Natural and Asian emissions are the next largest sources (between 19 and 24%).

5.2.2 Local deposition scenario

The general trend for total deposition at the three New York receptors from the nominal scenario to the local deposition scenario was an increase in contributions from the U.S. and New York sources and a decrease in contributions from European, African,

Asian, and natural sources. The impact due to Canadian sources increased slightly for the Finger Lakes scenario but remained the same for the Catskills and Adirondacks receptors. Once again U.S. sources contribute the most to total deposition (from 28% at the Adirondacks receptor to 50% at the Catskills receptor) while New York, Asian, and natural emissions make up most of the rest (from 39% at the Catskills receptor to 55% at the Finger Lakes receptor).

For dry deposition, the impact due to New York and U.S. sources increased while the impact due to natural sources decreased. At the Catskills and Adirondacks receptors, the impacts of Asian and European emissions on dry deposition decreased.

When local deposition was increased, the impact of New York, U.S., and Canadian emissions to wet deposition at the receptors generally increased, while all of the other emission sources decreased.

5.2.3 Long-range transport scenario

As in the other two scenarios, U.S. emissions are the largest source of total deposition at the New York receptors for the increased long-range transport scenario (from 25% at the Adirondacks receptor to 47% at the Catskills receptor), followed by natural (17 to 24%), Asian (14 to 20%), and New York (9 to 19%) emissions. Generally, Canadian and New York emissions contributions to total deposition decreased. The impact due to emission sources outside North America increased. The impact of U.S. emissions on total deposition at the Finger Lakes receptor increased, but remained unchanged at the Catskills and Adirondacks receptors.

The dry component of the deposition is still dominated by emissions from New York and U.S. sources. However, the impact due to New York sources is less in the long-range transport scenario. The impact of U.S. sources increased at the Finger Lakes receptors but decreased at the Catskills and Adirondacks receptors.

The wet deposition component is still more affected by sources outside North America in the long-range transport scenario. The four largest contributors to wet deposition in New York are U.S. (23 to 30%), natural (23 to 28%), Asian (20 to 24%) and European (8 to 9%) emissions. Changes from the nominal scenario included

decreased contributions from U.S., Canada and New York emissions and increased or unchanged contributions from the other source categories.

5.3 Uncertainties and Data Gaps

The source attribution results presented above should be seen as preliminary because, as pointed out in Section 5.1, there are still some significant uncertainties in our knowledge of the environmental fate and transport of Hg.

A sensitivity analysis of the atmospheric CTM identified the boundary Hg concentrations, Hg emission speciation, O_3 ambient concentrations and Hg(II) dry deposition velocity as the most influential variables. We still have significant uncertainties in the Hg emission speciation and the Hg(II) dry deposition velocity. In addition, our knowledge of the atmospheric chemistry of Hg is probably not complete since model performance for some MDN sites in the Northeast was poor.

An earlier sensitivity analysis conducted with a lake Hg cycling model (R-MCM) identified the lake pH, sediment burial rate and dissolved organic carbon (DOC) concentration as the most influential variables. Typically, no data are available for the sediment burial rate and a default value must be assumed.

Data gaps fall into three major categories: (1) data gaps for model inputs, (2) data gaps for model formulation and (3) data gaps for model evaluation.

For inputs to atmospheric CTMs, speciation of Hg emissions and the dry deposition of Hg(II) are the most significant data gaps. Currently, Hg emissions are reasonably well characterized for coal-fired power plants but there are few data for other source categories. There is also a paucity of data on Hg(II) dry deposition fluxes. Such data, over a variety of surfaces and under various meteorological conditions, are needed.

For inputs to lake cycling models, the sediment burial rate can be a critical variable, as it may significantly affect the model response to a change in Hg loading.

As mentioned above, there are still some considerable uncertainties in the formulation of Hg CTMs. For example, we anticipate that our knowledge of Hg atmospheric chemistry is still incomplete and laboratory experiments are needed to characterize the thermodynamics and kinetics of important Hg transformations.

Finally, data are critically needed to evaluate atmospheric CTMs. Data needs include speciated ambient measurements (Hg(0), Hg(II) and Hg(p)), wet deposition fluxes and dry deposition fluxes. Clearly, it is essential to ensure that CTMs have satisfactory performance against data before they can be used to develop effective emission control strategies.

6. REFERENCES

Bullock, O.R., 2000. Modeling assessment of transport and deposition patterns of anthropogenic mercury air emissions in the United States and Canada, *Sci. Total Environ.*, **259**, 145-157.

Calhoun, J.A. and E. Prestbo, Kinetic Study of the Gas Phase Oxidation of Elemental Mercury by Molecular Chlorine (Cl_2), Frontier Geosciences, Inc., Seattle, WA, unpublished manuscript, 1998.

Chin, M., D. J. Jacob, G. M., Gardner, M. S. Forman-Fowler, P. A. Spiro, and D. L. Savoie, 1996. A global three-dimensional model of tropospheric sulfate, *J. Geophys. Res.,* **101***,* 18,667-18,690.

Clever, H., S.A. Johnson and E.M. Derrick, 1985. The solubility of mercury and some sparingly soluble mercury salts in water and aqueous solutions, *J. Phys. Chem. Ref. Data*, **14**, 631-680.

Ebinghaus, R., S.G. Jennings, W.H. Schroeder, T. Berg, T. Donaghy, J. Guentzel, C. Kenny, H.H. Kock, K. Kvietkus, W. Landing, T. Muhleck, J. Munthe, E.M. Prestbo, D. Schneeberger, F. Slemr, J. Sommar, A. Urba, D. Wasllschlager, and Z. Xiao, 1999. International field intercomparison measurements of atmospheric mercury species at Mace Head, Ireland, *Atmos. Env.*, **33**, 3063-3073.

Graedel, T.E., and W.C. Keene, 1995. Tropospheric budget of reactive chlorine, *Global Biogeochem. Cycles,* **9***,* 47-77.

Hall, B. and N. Bloom, 1993. Report to EPRI, Palo Alto, California, U.S.A.

Hall, B., 1995. The gas-phase oxidation of elemental mercury by ozone, *Water Air Soil Pollut.*, **80**, 301-315.

Harris, R., S. Gherini and R. Hudson, 1996. Regional mercury cycling model: a model for mercury cycling in lakes, R-MCM Version I.V User's guide and technical reference; EPRI, Palo Alto and Wisconsin Department of Natural Resources, Madison, Wisconsin.

Hopke, P.K., W. Lin, Y.-J. Han, S.-M. Yi, T.M. Holsen, S. Cybart and M. Milligan, 2001. Measured summertime concentrations of particulate components, Hg^0, and speciated polycyclic aromatic hydrocarbons, *Environ. Pollut.*, submitted.

Jacob, D. J. and M. Prather, 1990. Radon-222 as a test of convective transport in a general circulation model, *Tellus, Ser. B.*, **42**, 118-134.

Jacob, D. J., M. Prather, S. Wofsy and M. McElroy, 1987. Atmospheric distribution of ^{85}Kr simulated with a general circulation model, *J. Geophys. Res.*, **92**, 6614-6626.

Jacob, D.J., 2000. Heterogeneous chemistry and tropospheric ozone, *Atmos. Environ.*, **34**, 2131-2159.

Jacob, D.J., J.A. Logan, and P. Murti, 1999. Effects of rising Asian emissions on surface ozone in the United States, *Geophys. Res. Lett.*, **26**, 2175-2178.

Jacobson, M., 1999. Fundamental of Atmospheric Modeling, Cambridge University Press, Cambridge, UK.

Jaeglé, L., D.J. Jacob, W.H. Brune and P.O. Wennberg, 2001. Chemistry of HO_x radicals in the upper troposphere, *Atmos. Environ.*, **35**, 469-489.

Kosak-Channing, L.F. and G.R. Helz, 1983. Solubility of ozone in aqueous solutions of 0-0.6 M ionic strength at 5-30°C, *Environ. Sci. Technol.*, **17**, 581-591.

Kotamarthi, V. R., J. M. Rodriguez, M. K. W. Ko, T. K. Tromp and N. D. Sze, Trifluoroacetic acid (TFA) from degradation of HCFCs and HFCs: a three-dimensional modeling study, *J. Geophys. Res.*, **103**, 5747-5758, 1998.

Lin, C.-J. and S.O. Pehkonen, 1997. Aqueous free radical chemistry of mercury in the presence of iron oxides and ambient aerosol, *Atmos. Environ.*, **31**, 4125-4137.

Lin, C.J. and S.O. Pehkonen, Oxidation of elemental mercury by aqueous chlorine ($HOCl/OCl^-$): Implications for tropospheric mercury chemistry, *J. Geophys. Res.*, **103**, 28093-28102, 1998.

Lind, J.A. and G.L. Kok, 1986. Henry's law determinations for aqueous solutions of hydrogen peroxide, methylhydroperoxide, and peroxyacetic acid, *J. Geophys. Res.*, **91**, 7889-7895.

Lindberg, S.E. and W.J. Stratton, 1998. Atmospheric mercury speciation: Concentrations and behavior of reactive gaseous mercury in ambient air, *Environ. Sci. Technol.*, **32**, 49-57.

Lindqvist, O. and H. Rodhe, 1985. Atmospheric mercury – a review, *Tellus*, **37**, 136-159.

Liu, X.G., G. Mauersberger and D. Moller, 1997. The effects of the cloud processes on the tropospheric photochemistry: An improvement of the EURAD model with a coupled gaseous and aqueous chemical mechanism, *Atmos. Environ*., **31**, 3119-3135.

Lohman, K., P. Pai, C. Seigneur, D. Mitchell, K. Heim, K. Wandland and L. Levin, 2000a. A probabilistic analysis of regional mercury impacts on wildlife, *Hum. Ecol. Risk Assess.*, **6**, 103-130.

Lohman, K., P. Pai, and C. Seigneur, 2000b. Sensitivity analysis of mercury human

exposure, *Sci. Total Environ.*, **259**, 3-11.

van Loon, L., E. Mader and S.L. Scott, 2000. Reduction of the aqueous mercuric ion by sulfite: UV spectrum of $HgSO_3$ and its intramolecular redox reactions, *J. Phys. Chem.*, **104**, 1621-1626.

Marsh, A.R.W. and W.J. McElroy, 1985. The dissociation constant and Henry's Law constant of HCl in aqueous solution, *Atmos. Environ.*, **19**, 1075-1080.

McArdle, J.V. and M.R. Hoffman, 1983. Kinetics and mechanism of the oxidation of aquated sulphur dioxide by hydrogen peroxide at low pH, *J. Phys. Chem.*, **87**, 5425-5429.

Munthe, J., Z.F. Xiao and O. Lindqvist, 1991. The aqueous reduction of divalent mercury by sulfite, *Water Air Soil Pollut.*, **56**, 621-630.

Munthe, J., 1992. The aqueous oxidation of elemental mercury by ozone, *Atmos. Environ.*, **26**, 1461-1468.

NCAR, Archives supplied by the Techniques Development Laboratory, OSD, NWS, NOAA, available from the Data Support Section, Scientific Computing Division, National Center for Atmospheric Research, Boulder, CO, 2000.

Olmez, I., G.J. Keeler and P.K. Hopke, 1994. Interim data interpretation report of the MIT/ALSC data set. MIT Report No. MITNRL-060, Massachusetts Institute of Technology, MA.

Pai, P., P. Karamchandani and C. Seigneur, 1997. Simulation of the regional atmospheric transport and fate of mercury using a comprehensive Eulerian model, *Atmos. Environ*., **31**, 2717-2732.

Pai, P., P. Karamchandani, C. Seigneur and M.A. Allan, 1999. Sensitivity of simulated atmospheric mercury concentrations and deposition to model input parameters, *J. Geophys. Res.*, **104**, 13855-13868.

Pai, P., D. Niemi, and B. Powers, 2000. A North American inventory of anthropogenic mercury emissions, *Fuel Processing Technol.,* **65-66**, 101-115.

Pehkonen, S.O. and C.J. Lin, 1998. Aqueous photochemistry of divalent mercury with organic acids, *J. Air Waste Manage. Assoc.*, **48**, 144-150.

Prather, M. J., M. McElroy, S. Wofsy, G. Russell and D. Rind, 1987. Chemistry of global troposphere: Fluorocarbons as tracers of air motion, *J. Geophys. Res.*, **92**, 579-6613.

Sanemasa, I., 1975. The solubility of elemental mercury vapor in water, *Bull. Chem. Soc. Jpn.*, **48**, 1795-1798.

Seigneur, C. and P. Saxena, 1988. A theoretical investigation of sulfate formation in clouds, *Atmos. Environ*., **22**, 101-115.

Seigneur, C., H. Abeck, G. Chia, M. Reinhard, N. Bloom, E. Prestbo, and P. Saxena, 1998. Mercury adsorption to elemental carbon (soot) particles and atmospheric particulate matter, *Atmos. Environ*., **32**, 2649-2657.

Seigneur, C., P. Karamchandani, K. Lohman, K. Vijayaraghavan and R.-L. Shia, 2001a. Multiscale modeling of the atmospheric fate and transport of mercury, *J. Geophys. Res*., **106**, 27795-27809.

Seigneur, C., P. Karamchandani, K. Vijayaraghavan, K. Lohman, R.-L. Shia and L. Levin, 2001b. On the effect of spatial resolution on atmospheric mercury modeling, *Sci. Total Environ.*, submitted.

Shia, R.L., C. Seigneur, P. Pai, M. Ko and N.D. Sze, 1999. Global simulation of atmospheric mercury concentrations and deposition fluxes, *J. Geophys. Res.*, **104**, 23747-23760.

Sillen, G.L. and A.E. Martell, 1964. Stability Constants of Metal Ion Complexes; Special Publication of the Chemical Society: London, p. 17.

Smith, R.M. and A.E. Martell, 1976. Critical Stability Constants, Vol. 4, Inorganic Complexes, Plenum Press, New York.

Spicer, C.W., E.G. Chapman, B.J. Finlayson-Pitts, R.A. Plastridge, J.M. Hubbe, J.D. Fast, and C.M. Berkowitz, 1998. Unexpectedly high concentrations of molecular chlorine in coastal air**,** *Nature***,** 394, 353-356.

Spivakovsky, C. M., J.A. Logan, S.A. Montzka, Y.J. Balkanski, M. Foreman-Fowler, D.B.A. Jones, L.W. Horowitz, A.C. Fusco, C.A.M. Brenninkmeijer, M.J. Prather, S.C. Wofsy, M.B. McElroy, 2000. Three-dimensional climatological distribution of tropospheric OH: Update and evaluation*, J. Geophys. Res.*, **105**, 8931-8980.

Spivakovsky, C.R., R. Yevich, J. Logan, S. Wofsy, M. McElroy, and M. Prather, 1990. Tropospheric OH in the three-dimensional chemical tracer model: an assessment based on the observations of CH_3CCl_3**,** *J. Geophys. Res*., **95,** 433-439.

Spivakovsky, C.M., 2001, private communication, Department of Earth and Planetary Sciences, Harvard University, Cambridge, MA.

Tokos, J.J.S., B. Hall, J.A. Calhoun and E.M. Prestbo, 1998. Homogenous gas-phase reaction of Hg^0 with H_2O_2, O_3, CH_3I, and $(CH_3)_2S$: Implications for atmospheric Hg cycling, *Atmos. Environ.*, **32**, 823-827.

Wang, Y., J.A. Logan, and D. J. Jacob, 1998. Global simulation of tropospheric O_3-NO_x-hydrocarbon chemistry 2. Model evaluation and global ozone budget, *J. Geophys. Res.,* **103***,* 10,727-10,755.

Zannetti, P., Air Pollution Modeling – Theories, Computational Methods and Available Software, 444 pp., Van Nostrand Reinhold, New York, NY, 1990.

Contributions of Global and Regional Sources to Mercury Deposition in New York State

Final Report 02-09

State of New York
George E. Pataki, Governor

New York State Energy Research and Development Authority
Vincent A. DeIorio, Esq., Chairman
William M. Flynn, President

NYSERDA